Effects of oestrogen on prolactin transcription patterns in living pituitary tissue

A thesis submitted to the University of Manchester for the degree of Doctor of Philosophy in the Faculty of Medical and Human Sciences

2013

Amanda Louise Patist

Centre for Endocrinology and Diabetes

Institute of Human Development

School of Medicine

Contents

Chapter 1: Introduction 18

1.1. The pituitary 19

1.1.1. Structure and function of the anterior pituitary 19

1.1.2. Development of the anterior pituitary 20

1.1.3. Hormone specific cell networks 21

1.2. Prolactin 22

1.2.1. Functions of prolactin 22

1.2.1.1. Reproductive cycles, pregnancy and lactation 22

1.2.2. The prolactin gene 24

1.2.2.1. The pituitary prolactin promoter 24

1.2.2.2. The human pituitary prolactin promoter and extrapituitary prolactin promoter 25

1.2.3. Prolactin secretion 26

1.2.4. Prolactin associated pathologies 27

1.2.4.1. Pituitary adenomas 27

1.2.4.2. Hyperprolactinaemia 27

1.3. Pit-1 28

1.4. Oestrogen 29

1.4.1. Oestrogen: function and synthesis 29

1.4.2. Oestrogen and prolactin 32

1.4.3. The oestrogen receptor 32

1.4.4. The oestrogen response element (ERE) 34

1.4.5. Oestrogen mediated prolactin transcription 36

1.4.6. Gene regulation through chromatin structure and the histone code 37

1.4.7. The oestrous cycle and prolactin 38

1.5. Dopamine 40

1.6. Real-time transcription dynamics of prolactin 41

1.6.1. Evidence for stochastic transcription 41

1.6.2. Reporter genes 42

1.6.3. Models for studying prolactin transcription 43

1.6.3.1. In Vitro 44

1.6.3.2. In Vivo: The development of a model to enable the real-time visualisation of prolactin gene expression in individual cells 45

1.6.4. Mathematical modelling of transcription 48

1.7. Aims 54

Chapter 2: Materials and methods 55

2.1. Flow cytometry 56

2.2. Immunohistochemistry 56

2.2.1. Fixing and sectioning tissue 56

2.2.2. H&E 57

2.2.3. Immunofluoresence staining 57

2.3. Basic cell culture 57

2.3.1. Cell stock maintenance 58

2.3.2. Splitting cells 58

2.3.3. Cryogenic freezing and thawing 59

2.4. The luciferase assay 59

2.5. Live cell luminometry 60

2.6. Animal husbandry 61

2.6.1. Genotyping 62

2.6.1.1. DNA isolation 62

2.6.1.2. PCR 62

2.7. Cycle stage synchronisation and staging 63

2.7.1. Oestrous cycle staging 63

2.7.2. Synchronisation of the oestrous cycle 64

2.7.3. Blood collection and serum analysis 65

2.8. qPCR 65

2.8.1. Genomic RNA extraction 65

2.8.2. Conversion of RNA to cDNA 66

2.8.3. qPCR 66

2.8.4. Primers 66

2.9. Implantation of E_2 pump 67

2.9.1. Pump preparation 67

2.9.2. Implantation 67

2.9.3 Postoperative care 68

2.10. Live cell imaging 68

2.10.1. Fluorescence 68

2.10.1.1. Tissue culture and preparation 68

2.10.1.2. Microscopy 69

2.10.1.3. Cell tracking 70

2.10.2. Luminescence microscopy protocol 70

2.11. Statistical analysis 70

2.11.1. Basic analysis and plotting of data 70

2.11.2. Mathematical modelling 71

Chapter 3: Results: Establishment of experimental models: the oestrous cycle and male E_2 implants 72

3.1. Introduction 73

3.1.1. Prolactin and oestrogen 73

3.1.2. Transgenic rat model 73

3.2. Aim 74

3.3. Results 75

3.3.1. Validation of the oestrous cycle as a model for the effects of circulating oestrogens on prolactin transcription 75

3.3.2. Validation of subcutaneous oestradiol implant in males 79

3.4. Discussion 81

3.4.1. Validation of *in vivo* model 81

3.4.2. Heterogeneity and lactotroph localisation 84

3.4.3. *In vitro* model of prolactin transcription 85

3.4.4. Effects of oestrogen on prolactin transcription patterns 85

Chapter 4: Results: Effects of oestrogen on prolactin transcription cycles 87

4.1. Introduction 88

4.1.1. Fluorescence microscopy 88

4.1.2. Confocal microscopy and optical imaging 90

4.1.3. Our systems 90

4.2. Optimisation of tissue culture for live cell imaging 94

4.3. hPRL-d2eGFP transgene expression across the oestrous cycle 95

4.4. hPRL-d2eGFP transgene expression in males treated with chronic E2 101

4.5. Discussion 106

4.5.1. High vs low oestrogen state does not alter patterns in prolactin gene expression reporter activity 106

4.5.2. Dopamine 108

4.5.3. Imaging 109

4.5.4. Cell tracking 111

4.5.5. Determination of fluorescence cycles 112

Chapter 5: Results: Mathematical modelling of prolactin transcription dynamics .. 114

5.1. Introduction 115

5.1.1. Prolactin transcription cycles 115

5.1.2. The hierarchical model 116

5.1.3. Effects of oestrogen on patterns in prolactin transcription rates 117

5.2. Prolactin transcription rates across the oestrous cycle 118

5.3. Prolactin transcription rates in male high and low oestrogen sates 122

5.4. Discussion 122

5.4.1. Patterns in prolactin transcription cycles and the effects of oestrogen 122

5.4.2. Development of the transcription rate switch model 126

5.4.3. Further analysis 127

Chapter 6: Discussion 130

6.1. Stochastic gene expression 131

6.2. Oestrogen *in vivo* promotes the transcription of prolactin 131

6.3. Origins of cyclical activity 133

6.4. Future work 137

6.5. Conclusion 140

References 141

Appendix A 155

Appendix B 161

Appendix C 164

Appendix D 167

Total word count: 41,052

List of figures

Figure 1.1. Development of the rodent pituitary 20

Figure 1.2. Schematic of regulatory regions of the human prolactin gene 25

Figure 1.3. Biosynthesis of oestrogen from cholesterol 30

Figure 1.4. E_2 treatment of GH3 cells induces prolactin transcription through oestrogen response elements 35

Figure 1.5. Serum hormone concentrations during female reproductive cycles 39

Figure 1.6. Structure of the BAC reporter gene constructs 45

Figure 1.7. Luminescence and fluorescence activity of the human prolactin gene transcriptional reporters from the Fischer 344 (luc/d2eGFP-hPRL 455) rats 47

Figure 1.8. A binary model of prolactin transcription dynamics 50

Figure 1.9. A refractory period introduces cyclicity into transcriptional cycles 51

Figure 1.10. Model for the generation of transcription cycles 53

Figure 2.1. Live cell luminometry re-stimulation experimental design 61

Figure 2.2. Cellular make up of vaginal lining at proestrus, oestrus and diestrus 64

Figure 2.3. Positioning of ALZET® micro-osmotic E_2 pump 68

Figure 2.4. Experimental set up of pituitary slice tissue for fluorescence confocal live cell imaging 69

Figure 3.1. Serum prolactin across the oestrous cycle 76

Figure 3.2. Sample of flow cytometry data 77

Figure 3.3. Flow cyctometry and qPCR validation of oestrous cycle model 78

Figure 3.4. Immunofluorescent staining of Fischer 344 (d2eGFP-hPRL 455) anterior pituitaries at different stages of the oestrous cycle 79

Figure 3.5. Validation of ALZET® micro-osmotic pump function 80

Figure 3.6. Flow cytometry and qPCR identify a significant increase in prolactin transcription in males subjected to chronic oestradiol stimulation 81

Figure 3.7. Male rats subjected to chronic oestradiol administration show an increase in prolactin gene transcription 82

Figure 4.1. The basic concept of fluorescence microscopy 89

Figure 4.2. Concept of confocal microscopy based on the Zeiss Pascal Scanning Laser Microscope 91

Figure 4.3. The LSM 780 confocal microscope at the Systems Microscopy Centre at the University of Manchester 92

Figure 4.4. LSM 780 and LSM 5 Pascal inverted tissue imaging setup 93

Figure 4.5. Comparison of cell viability in tissue pituitary slice kept in an incubator and in a perfusion chamber 94

Figure 4.6. Composite image of 250 µm coronal pituitary slice at 0h of a 48 hour imaging series 97

Figure 4.7. Time-lapse imaging of 250 µm coronal sections of Fischer 455 (d2eGFP-hPRL 344) female rats at oestrus and diestrus, selected for cell tracking 98

Figure 4.8. Single cell fluorescence patterns from diestrus and oestrus 99

Figure 4.9. Distribution of fluorescence peaks across the oestrous cycle 100

Figure 4.10. Imaging position of E_2 treated male 102

Figure 4.11. Time-lapse imaging of 250µm coronal sections of Fischer 344 (d2eGFP-hPRL 455) males treated with E_2 and controls 103

Figure 4.12. Single cell fluorescence patterns from control and E_2 treated males 104

Figure 4.13. Distribution of fluorescence peaks in E_2 treated and control males 105

Figure 4.14. Detector sensitivity 110

Figure 4.15. Single cell fluorescence tracking using CellTracker 112

Figure 5.1. Switch rate model algorithm outputs for females in oestrus and diestrus 119

Figure 5.2. Summary of prolactin transcription rate switch model algorithm output for females at diestrus and oestrus 121

Figure 5.3. Switch rate model outputs from males with and without E_2 treatment 123

Figure 5.4. Summary of prolactin transcription rate model outputs for E_2 treated and control males 125

Figure 5.5. Statistical analysis of transcription rate data 128

Figure 6.1. Model for the mechanism of single cell prolactin transcription cycles in high and low prolactin producing states 136

Figure 6.2. Light sheet microscopy 139

List of tables

Table 2.1. Optimised antibody concentrations 58

Table 2.2. Genotyping primers 62

Table 2.3. Oestrous cycles induction scheme 64

Table 2.4. qPCR primers 67

Table 3.1. Comparison of the timing of prolactin transcription and prolactin secretion 84

Table 4.1. Distribution of fluorescence peaks across the oestrous cycle 100

Table 4.2. Distribution of fluorescence peaks in E_2 treated and control males 105

Table 5.1. Frequency of estimated switches in transcription rate per cell across the oestrous cycle 120

Table 5.2. Frequency of estimated switches in transcription rate per cell, in males with E_2 implants and controls 124

Table 6.1. Changes in relative levels of prolactin, oestrogen and dopamine and their receptors, through the oestrous cycle 135

Abstract

Effects of oestrogen on prolactin transcription patterns in living pituitary tissue *Amanda Louise Patist*
PhD in the Faculty of Medical and Human Sciences**,** September 2013**,**
The University of Manchester

Oestrogen is a well-known modulator of the transcription and secretion of prolactin as well as having a role in the physiological proliferation and possibly also in pathological hyperplasia of lactotrophs. Our group has studied prolactin gene promoter regulation in single living pituitary cells in Fischer 344 (d2eGFP-hPRL 455) rats, that express a destabilised eGFP reporter gene under the control of a human prolactin genomic fragment, and identified prolactin transcription cycles that occur in a non-circadian and non-synchronised fashion. Pulsatile transcription has been identified in fetal tissue, stabilising during development.

Here we assess the effects of physiological and supraphysiological oestrogen exposure *in vivo* on prolactin transcription in the adult rat. We have established and validated models of both states by evaluating the expression of the hPRL-d2eGFP transgene during the oestrous cycle and in males with long-term oestradiol-releasing implants, respectively.

The oestrous cycles of adult female rats were synchronised by IP LHRH injection. A 1.8-fold increase in the number of cells expressing the prolactin transgene at oestrus (n=7) as compared to diestrus (n=5) and a 10.6 fold increase in mean fluorescence per cell was identified by flow cytometry. In males, chronic oestrogen stimulation induced a 2.5-fold increase in pituitary weight, a 5.2-fold increase in number of cells expressing the transgene and 4.4-fold increase in fluorescence per cell, as indicated by flow cytometry (n=3). Immunofluorescence, qPCR and serum analysis confirmed the high-production state of lactotroph cells in both female and male models.

250µm pituitary slices were imaged for 48 hours using time-lapse confocal microscopy and pulsatile fluorescent reporter activity was evident in both female and male models. Interestingly, no significant difference was seen between transcription cycle patterns (timing or amplitude of transcriptional pulses) in individual cells between high and low oestrogen states. Using a novel mathematical model, that calculates transcription rate from fluorescence data, we have been able to study the transcription rates displayed by single cells and the estimated points at which a cell switches from one rate to another. Patterns in switches in transcription rates were similar between high and low oestrogen states, suggesting that individual pituitary cells within the context of tissue, continue to display cyclical patterns of gene expression, in states of both high and low prolactin production. This implies that cyclical transcription is a fundamental property of prolactin gene expression that persists in different physiological states, and that modulation of cycle characteristics is not the mechanism for increased prolactin synthesis in these circumstances.

Declaration

No portion of the work referred to in the thesis has been submitted in support of an application for another degree or qualification of this or any other university or other institute of learning.

Copyright statement

Acknowledgments

First and foremost I would like to thank Prof. Julian Davis and Dr. Karen Featherstone. Julian, thank you for giving me the opportunity to do this PhD and for all of your help and support through the past four years. Karen, you have been my rock in all things science. Thank you to the past and present members of the group, Dr. Adam Giles, Dr. Frederic Madec and Lee Dunham and to my advisor Dr. Karen Piper Hanley.

A large part of the success of this project is down to a network of collaborators who have provided valuable scientific input and support. I would like to thank the Liverpool group, in particular my co-supervisor Prof. Mike White, Dr. David Spiller, Dr. Anne McNamara, Dr. Antony Adamson, Dr. Raheela Awais and Dr. Claire Harper. Thank you to the Warwick Systems Biology Centre in particular Kirsty Hey for development of the switch model, Dr. Hiroshi Momiji, Dr. Bärbel Finkenstädt and Prof. David Rand. I'd like to thank everyone else at the Lake District meetings Prof. Alan McNeilly, Judy McNeilly, Prof. John Mullins, Dr. Sabrina Semprini and Dr. Paul LeTissier. I'd also like to thank the BSF staff, for their expertise and their help in the care for my rats.

Thank you to the AV Hill 3rd floor Endocrine Sciences group, for support and useful discussion and in particular Dr. Suzanne Meredith and Jennifer Bryant for playing a big part in making Manchester a home away from home, and of course, the rest of the White group.

I couldn't have done any of this without the support of my family, my parents who have always believed in me and Mike, Karina and Leon. A big thank you to Jason Gough, who especially in the last few months of writing, has kept me sane.

Finally I would like to thank the funding bodies, the BBSRC and the Centre for Integrative Mammalian Biology for my studentship and the Wellcome Trust for program grant funding.

Abbreviations

ACTH adrenocorticotropic hormone

AMP adenosine monophosphate

APC allophycocyanin

ATP adenosine triphosphate

AUC area under the curve

BAC bacterial artificial chromosome

BMP bone morphogenic protein

bp base pair

cAMP cyclic adenosine monophosphate

CCD charged coupled device

CREB cAMP response element

ChIP chromatin immunoprecipitation

DCT dextran-charcoal treated

DES diethylstilbestrol

DS data set

D2R dopamine receptor D2

E_1 oestrone

E_2 17β-oestradiol

E_3 oestriol

EGF epidermal growth factor

EMSA electrophoretic mobility shift assay

ER oestrogen receptor

ER α oestrogen receptor α

ER β oestrogen receptor β

ERE oestrogen response element

FACS fluorescence-activated cell sorting

FBS fetal bovine serum

FGF fibroblast growth factor

FSK forskolin

GFP green fluorescent protein

GH growth hormone

HAT histone acetylase

HDR high dynamic range

hPRL human prolactin gene

HPRT hypoxanthine-guanine phosphoribosyltransferase

IMS industrial methylated spirit

IP intraperitoneal

qPCR quantitative polymerase chain reaction

kpb kilo base pair

LH luteinising hormone

LPS lipopolysaccharide

LSFM light sheet fluorescence microscope

LSM laser scanning microscope

MCMC Markov Chain Monte Carlo (algorithm)

MSH melanocyte-stimulating hormone

NF-κB nuclear factor κB

PCR polymerase chain reaction

PBS phosphate buffered saline

PEG polyethylene glycol

PFA	paraformaldehyde
PI	propidium iodide
Pit-1	pituitary transcription factor 1
Pol II	RNA polymerase II
PMT	photomultiplier tube
PRL	prolactin gene
RER	rough endoplasmic reticulum
SC	subcutaneous
SDE	stochastic differential equation
Shh	Sonic Hedgehog
TA	transcription apparatus
TIC	transcription initiation complex
TNFα	tumour necrosis factor alpha
TRH	thryrotropin-releasing hormone
TSA	trichostatin A
TSH	thyrotropin stimulating hormone

Chapter 1

Introduction

Introduction

1.1. The pituitary

1.1.1. Structure and function of the anterior pituitary

The anterior pituitary is a structure common to all vertebrates, and has key functions in homeostasis, metabolism, reproduction, growth and lactation. The gland consists of three lobes, the posterior, which holds nerve ending from the hypothalamus, an intermediate and the anterior lobe, which consists of five distinct endocrine cell types. The cell types and the hormones they produce are as follows: Somatotrophs; growth hormone (GH), thyrotrophs; thyrotropin stimulating hormone (TSH), corticotrophs; adrenocorticotropic hormone (ACTH), gonadotrophs; follicle stimulating hormone (FSH) and luteinising hormone (LH) and our endocrine cell of interest, the lactotroph, which produces prolactin (Scully & Rosenfeld, 2002). These distinct cell types are spread throughout the structure of the pituitary, organised as interdigitated networks, functioning to coordinate hormone secretion (Harper *et al.*, 2010, Hodson *et al.*, 2010).

Lactotrophs can be subdivided into three groups according to their function and morphology (Nogami *et al.*, 1985). Type I cells contain large irregularly shaped granules with a diameter of 300-700/500-900nm (DePaul *et al.*, 1997, Takahashi & Miyatake, 1991), type II contain round secretory granules with a diameter of between 150 and 250nm and the third subtype contains small round granules of ≥ 100nm. An additional intermediate lactotroph has since been discovered, that has a large number of granules (>300 nm diameter) and do not coexpress GH (Huerta-Ocampo *et al.*, 2005). The proportions of these cell subtypes differentiates between the sexes at an age of 30 days in rats, with females having 90% and males having 35% type I lactotrophs (Takahashi & Miyatake, 1991).

1.1.2. Development of the anterior pituitary

Organogenesis of the anterior pituitary begins at embryonic day 8.5 (E8.5). Growth of the forebrain displaces the anterior neural ridge (ANR). Cells of the anterior pituitary placode in the oral ectoderm thicken and invaginate to form the nascent pituitary, in a structure referred to as Rathke's pouch. The distinct endocrine cell types emerge in a spatially and temporally specific manner, starting with the corticotrophs and rostral tip thyrotrophs at E12.5 and from E15.5 to E17.5, the somatotrophs, thyrotrophs, gonadotrophs, melanotrophs (intermediate lobe) and lactotrophs emerge (Reviewed by Ben-Jonathan *et al.*, 2008, Scully & Rosenfeld, 2002).

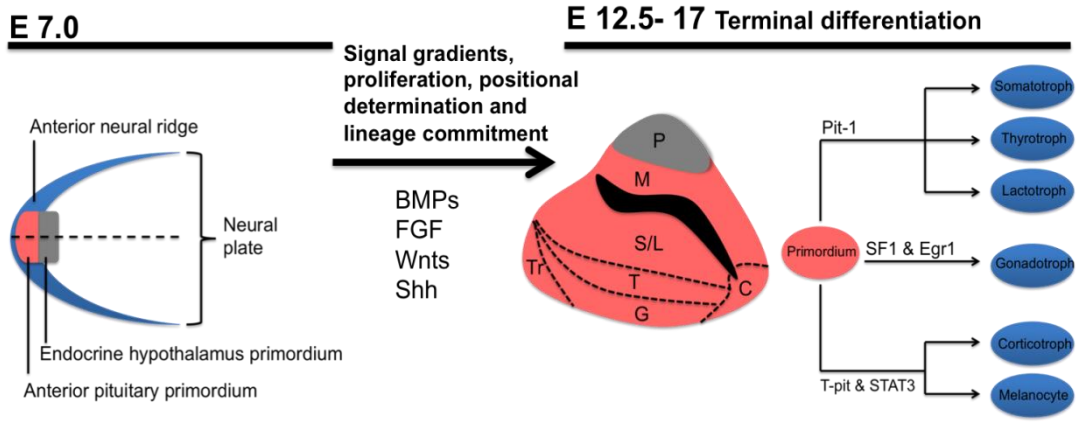

Figure 1.1. Development of the rodent pituitary

The anterior pituitary is formed from the anterior pituitary primordium after displacement from the anterior neural ridge of the neural plate. Signalling gradients (mid panel) induce the spatial organisation and differentiation of pituitary cells from a primordial cell from days E12.5 to E17.0 and the organisation of transcription factors involved in this process. P: posterior lobe Tr: rostral tip thyrtropes, S: somatotropes, L :lactotropes, G: gonadotropes, M: melanocytes, C: corticotropes. ***Adapted from Scully and Rosenfeld. 2002***

A combination of both exogenous (eg. bone morphogenic protein (BMP), fibroblast growth factor (FGF), members of the *Wnt* gene family and Sonic Hedgehog (Shh) (Reviewed by Cadigan & Nusse, 1997, Scully & Rosenfeld, 2002) and endogenous signalling (eg. BMP2 and Wnt4) are responsible for the formation of the nascent pituitary and proliferation of pituitary cells (Scully & Rosenfeld, 2002, Zhu *et al.*, 2007).

After the proliferation of cells and patterning by spatial organisation, the six specific endocrine cell types differentiate from a common primoridum. For this lineage commitment, the induction of additional transcription factors is required. SF1 and Egr-1 are required for the differentiation of gonadotrophs, the transcription factor Pit-1 is required for the differentiation of the thyrotrophs, somatotrophs, and lactotrophs (GonzalezParra *et al.*, 1996), and T-pit and STAT3 for corticotrophs and melanotrophs (As reviewed by Scully & Rosenfeld, 2002), which appear to be determined in a ventral-to-dorsal gradient, respectively (Treier *et al.*, 1998).

1.1.3. Hormone specific cell networks

In the adult pituitary, hormone producing cells exist as homotypic, interdigitated cell networks (Hodson *et al.*, 2010). By using whole pituitary scale 3D imaging, Budry *et al.* (2011) determined that during development, newly differentiated corticotrophs appear (E13.5) on the ventral surface of the gland, after which they quickly form homotypic strands of cells that extend from the lateral tips of the anterior pituitary along the ventral surface and into the medial regions of the gland. Gonadotrophs were found to differentiate later and position themselves in close proximity to both corticotrophs and capillaries. The corticotrophs are likely to form the scaffold of the 3D structure, as the GH cell network is only established later, beginning at E15.5/E16.5. Somatotrophs exist as a continuum connected by adherens junctions, with a robustness that is maintained throughout life (Bonnefont *et al.*, 2005).

Positional organization continues after birth (Budry *et al.*, 2011). Further evidence for a hormone cell network is seen in the experience dependent plasticity displayed by lactotrophs in response to repeated activation by sequential lactation (Hodson *et al.*, 2012) and in the reorganisation of growth hormone cell networks after ovariectomy in rats (Schaeffer *et al.*, 2011).

1.2. Prolactin

1.2.1. Functions of prolactin

Originally named for its function to promote lactation in response to the suckling of young mammals, prolactin is a multifunctional polypeptide, with an array of over 300 functions (Bole-Feysot *et al.*, 1998, Teilum *et al.*, 2005). Classical roles of prolactin are related to reproduction, while non-classic roles include numerous processes including metabolism, osmoregulation, immunology and behaviour (Ben-Jonathan *et al.*, 2008). Prolactin has also been seen to play a role in the pathology of breast cancer (Llovera *et al.*, 2000).

1.2.1.1. Reproductive cycles, pregnancy and lactation

The classical roles of prolactin are related to the reproductive cycle of females, pregnancy and lactation. The significance of the role of prolactin during pregnancy is evident from the increase in the proportion of (type II) lactotrophs as compared to other cell types, within the pituitary at this time (El-Kasti *et al.*, 2008). The functions of prolactin in the rodent oestrous cycle (see section 1.5.6 for more detail on the oestrous cycle) include the luteolysis of the corpus luteum (Gaytan *et al.*, 2001) involvement in follicular growth and oocyte maturation and ovulation (Ben-Jonathan *et al.*, 2008). In addition to this, the prolactin receptor plays a crucial role in physiology, with receptor deficient mice showing normal ovulation and fertilisation, but infertility due to failure of embryo implantation (Grosdemouge *et al.*, 2003). During pregnancy in rodents, prolactin has luteotropic actions, and is essential for the support of the corpus luteum, promoting progesterone production and the maintenance of gestation (Ben-Jonathan *et al.*, 2008).

During the 28 day menstrual cycle in humans, a preovulatory rise in oestrogen and progesterone is seen. The circulating levels of prolactin, however, remain relatively low (Ben-Jonathan *et al.*, 2008). In addition to pituitary prolactin, the human ovaries express their own prolactin (at a higher level in pre- as opposed to postmenopausal women) (Schwarzler *et al.*, 1997) and it is also found in several locations throughout the reproductive organs. Prolactin throughout the cycle may have a role as a survival factor in granulosa cells and may have potential autocrine/paracrine roles within the ovary (Ben-Jonathan *et al.*, 2008).

The onset and maintenance of pregnancy is characterised by a coordinated release and overlapping functions of prolactin and placental lactogens, which again, differs between the species. In the rodent, the first 10 to 12 days of pregnancy are dominated by prolactin surges, essential for the maintenance of the corpus luteum (Reviewed by Soares, 2004). An oestrogen and progesterone induced surge of PRL directly before parturition participates in the final maturation of the mammary gland in preparation for lactation and brings the onset of maternal behaviour (Andrews, 2005, Mann & Bridges, 2001). The most well established role for prolactin in rodent pregnancy is its function, in conjunction with placental lactogen, to prevent progesterone catabolism via the suppression of 20α-hydroxysteroid dehydrogenase (20αHSD) (Ben-Jonathan *et al.*, 2008).

The role of prolactin in human pregnancy is entirely different, and significantly more complicated, involving maternal, fetal and decidual contributions (Ben-Jonathan *et al.*, 2008). Both prolactin and the prolactin receptor have been found to be expressed in luteinized human ovary tissue (Schwarzler *et al.*, 1997, Vlahos *et al.*, 2001) and the protein hormone has been suggested to contribute significantly to early corpus luteum formation and survival, by acting as a potent antiapoptotic factor for human granulosa cells (Perks *et al.*, 2003).

In the fetal, neonatal and pubertal development of the mammary gland, prolactin plays a limited role. However, the hormone is heavily involved with mammogenesis (lobuloaveolar branching and differentiation), lactogenesis (acquisition of the ability to produce milk), galactopoiesis (the maintenance of milk secretion), and involution (the return to non-lactating state). Prolactin and placental lactogens are key controllers in the transition from a proliferative to a secretory state in the gland (Reviewed by Ben-Jonathan *et al.*, 2008). Furthermore, prolactin stimulates the production of the major constituents of milk: proteins (including those responsible for glucose uptake), lactose and lipids (Neville *et al.*, 2002, Peters & Rillema, 1992). The release of prolactin from the anterior pituitary increases many fold within minutes of suckling, in a well-established neuroendocrine reflex that also causes releases of oxytocin from the posterior pituitary (Freeman *et al.*, 2000).

1.2.2. The prolactin gene

In rodents, prolactin is predominantly expressed in the pituitary. Further expression can be found in the decidua of the uterus, placenta and lactating mammary gland. Contrastingly, in primates, prolactin expression is more wide spread and can be found in, amongst other sites, the endometrium, decidua, myometrium, T lymphocytes, leukocytes, brain, breast, prostate, skin and adipose tissues, where it is under tissue-specific control (Ben-Jonathan *et al.*, 2008, Gerlo *et al.*, 2006, Semprini *et al.*, 2009).

Despite a 90% sequence homology between the human and rat genes (Dimattia *et al.*, 1990), the structure and expression patterns of the two genes vary. The human prolactin gene exists in a gene poor region and consists of a single gene containing five coding exons with two independent promoter regions, a pituitary specific and a non-pituitary start site. In contrast to the human gene, the rodent prolactin locus consists of a large family of prolactin related genes, resulting from gene duplication (Gerlo *et al.*, 2006).

The expression of prolactin is influenced by numerous molecules, including steroids, hormones and cytokines produced throughout the body. The level of expression is a delicate balance between inhibitory and stimulatory signals from numerous organ systems (reviewed by Featherstone *et al.*, 2012). Of these, oestrogen, dopamine and Pit-1 regulation are of particular interest and are further discussed in sections 1.5, 1.6. and 1.4, respectively. The response to regulators of prolactin expression varies between the two species. Oestrogen for example, has a much more subtle effect on prolactin expression in humans than in rats, having to do with a synergy between oestrogen and Pit-1 (which works in conjunction with cAMP) in rodents (Day *et al.*, 1990).

1.2.2.1. The pituitary prolactin promoter

Both rat and human prolactin gene loci contain a proximal and a distal enhancer, within a 5000 bp region (Berwaer *et al.*, 1991). The proximal promoter, located between -250 and -20 bp, contains four Pit-1 binding sites and the distal enhancer, located between -1800 and -1500 bp relative to the transcription start site, hold an

additional four Pit-1 binding sites (Ben-Jonathan *et al.*, 2008, Gourdji & Laverriere, 1994).

1.2.2.2. The human pituitary prolactin promoter and extrapituitary prolactin promoter

Cell specific and Pit-1 independent (Gellersen *et al.*, 1994) extrapituitary prolactin expression originates from a distal promoter region located 5.8 kbp upstream of the pituitary start site (Berwaer *et al.*, 1994). This sequence contains a proximal promoter at -250 to +1bp from the transcriptional start site (Van de Weerdt *et al.*, 2000) and both a distal enhancer at -1968 to -1064 and two super-distal enhancers at -5100 to -4430 and -3473 to -2600. Within these regions, are an additional 13 Pit-1 binding sites: three in the proximal region, eight in the distal enhancer and two in the super-distal region (Ben-Jonathan *et al.*, 2008, Peers *et al.*, 1990).

Functional chromosome looping has been seen between the proximal and distal promoter regions (Gothard *et al.*, 1996). Additionally, enhancer RNAs may promote both *cis* and *trans* chromosome looping (Li *et al.*, 2013).

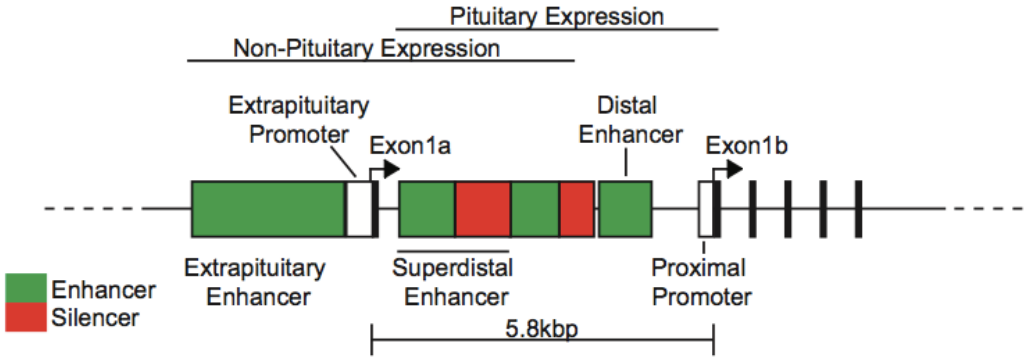

Figure 1.2. Schematic of regulatory regions of the human prolactin gene

Schematic diagram of the regulatory elements of the human prolactin gene locus. Exons are shown as black boxes, promoters are shown as white boxes and green and red boxes represent transcriptional enhancers and silencers, respectively. ***Taken from Featherstone et al., 2012.***

Transcription of the 1a exon at the extrapituitary start site results in the production of prolactin mRNA (Berwaer *et al.*, 1994, Gellersen *et al.*, 1994), which is 150bp longer than pituitary prolactin from exon 1b, as determined by northern blot analysis (Dimattia *et al.*, 1988, Gellersen *et al.*, 1989).

1.2.3. Prolactin secretion

Prolactin is produced as a prohormone with an N-terminal signalling peptide of 28 to 30 residues, which is proteolytically cleaved to the mature 197 and 199 residue proteins of the rodent and human, respectively. Further post-translational modifications including polymerization, proteolytic cleavage, glycosylation and phosphorylation are responsible for the allocation of the biological characteristics of prolactin, such as its half-life, stability and receptor binding. The mature protein hormone is then stored within the lactotrophs and is released by calcium-dependent exocytosis (Ben-Jonathan & Hnasko, 2001).

Without a single defined target organ, the regulation of prolactin secretion is a complex process, in which dopamine and oestrogen play major roles. In addition to classical genomic pathways (Freeman *et al.*, 2000), oestradiol can exert non-genomic effects on prolactin secretion, in normal pituitary tissue, by inducing the release of stored protein from type II lactotrophs (Christian & Morris, 2002). Oestradiol can also modulate prolactin secretion by thyrotropin-releasing hormone (TRH) through membrane oestrogen receptors via PI3K/Akt (Sosa *et al.*, 2012).

Anterior pituitary prolactin is under tonic inhibition by dopamine from the hypothalamus, which can in itself be counteracted by many neuropeptides, steroids and growth factors (Ben-Jonathan & Hnasko, 2001). The inhibitory effects of dopamine are seen in all three subtypes of lactotrophs in basal conditions. The treatment of lactating rats with a dopamine D2 receptor antagonist, significantly increased prolactin granule exocytosis from types I and III and the proportion of type I and II cells undergoing exocytosis (Christian *et al.*, 2007). Further distant releasing and inhibiting factors include endocrine, paracrine, juxtacrine and autocrine signals (Ben-Jonathan & Hnasko, 2001).

1.2.4. Prolactin associated pathologies

In healthy individuals, the secretion of prolactin from the anterior pituitary is under the inhibitory control of dopamine produced by the hypothalamus. Additional control is provided by hormones including oestrogens, TRH, oxytocin and vasopressin. An interruption in the regular functioning of any of the above will cause alterations in the levels of circulating prolactin (Demssie & Davis, 2008). However, apart from the use of dopamine antagonist drugs, pituitary tumours are the primary pathological cause of major increases in serum prolactin levels.

1.2.4.1. Pituitary adenomas

Pituitary tumours constitute 10% of all intracranial tumours, making them the most common type of intracranial neoplasm (Asa & Ezzat, 1998). More often than not, these tumours are indolent and benign, with slow growth rates. While MRI studies have indicated pituitary abnormalities in 10% of the asymptomatic population (Hall *et al.*, 1994), the clinical problems arising from pituitary tumours are cell type dependent, giving rise to diverse endocrine and reproductive effects (Davis *et al.*, 2001).

Clonal expansion of lactotroph cells results in the development of a prolactinoma. Little is known about the aetiology of this pathology, or of the mechanisms by which some become more aggressive while others remain small and non-invasive. Studies into tumour suppressor genes and oncogenic mutations have lead to the identification of the Multiple Endocrine Neoplasia type 1 (MEN1) genes, that may be involved in the development of some of these tumours (Davis *et al.*, 2001, Farrell & Clayton, 1998).

1.2.4.2. Hyperprolactinaemia

Hyperprolactinaemia, characterised by an excess of prolactin in the circulation, is most often caused by a prolactinoma. Non-tumoural causes of hyperprolactinaemia can raise prolactin levels to over 2,000mu/l, micoprolactinomas can reach up to 5,000 mu/l, while macroprolactinomas can reach prolactin levels of over 10,000 mu/l. Consequences of such elevations include effects on the mammary gland, which may cause galactorrhoea, and gonadal dysfunction, which can manifest in menstrual disturbances in the form of either oligomenorrhoea or amenorrhoea,

sexual dysfunction including low libido or erectile dysfunction in men, or anovulatory infertility (Demssie & Davis, 2008).

1.3. Pit-1

The pituitary transcription factor-1 (Pit-1) is a member of the POU domain family of transcription factors and is essential for the regulation of growth hormone and prolactin as well as the proliferation of both somatotrophs and lactotrophs (Bodner *et al.*, 1988, GonzalezParra *et al.*, 1996, Ingraham *et al.*, 1988). Pit-1 dependent sexual dimorphism occurs at puberty, increasing lactotroph proportions in females and somatotrophs in male (GonzalezParra *et al.*, 1996). Furthermore, mutations in Pit-1 have been shown to cause combined pituitary hormone deficiency in both mice and humans (Quentien *et al.*, 2006).

Pit-1 has been shown to play an essential role in the transcription of prolactin, by interacting with the nuclear hormone receptor, its response element and a host of co-regulators (Andersen & Rosenfeld, 2001). Pit-1 binding sites located proximally and distally from the transcription start site contribute differentially to the oestrogen responsiveness of the prolactin gene (Nowakowski & Maurer, 1994). The modifications of chromatin induced by the binding of Pit-1 are complicated, multifactorial and depending on the different intracellular signalling pathways activated, results in the recruitment of different histone acteylases (HATs). The activity of Pit-1 is determined by a regulated balance of both a co-repressor complex (containing N-CoR/SMRT, mSin3A/B and HDACs) and a co-activator complex (including CREB-binding protein and p/CAF) (Xu *et al.*, 1998). Further to this, while Pit-1 enhances the Ras signalling pathway to the prolactin promoter, the Pit-1β isoform represses basal prolactin promoter activity as well as Ras signalling to the prolactin promoter in pituitary cells, despite both having identical DNA binding domains (Diamond & Gutierrez-Hartmann, 2000).

Pit-1 has been shown to alter nucleosome positioning on prolactin constructs reconstituted into chromatin *in vivo*, independently from its function in transcriptional activation (Kievit & Maurer, 2005). It has been suggested that this may play a role in the regulation of transcription dynamics by competing with other DNA binding factors for nucleosome occupation.

1.4. Oestrogen

1.4.1. Oestrogen: function and synthesis

Oestrogens are a group of hormones named for their importance in the menstrual and oestrous reproductive cycles of females. They play many additional roles in mammalian physiology (Gruber *et al.*, 2002, Nelson & Bulun, 2001, Simoncini *et al.*, 2000), including influencing mood, reducing intraocular pressure, ameliorating the signs of skin aging and having neuroprotective properties. Oestrogen has been shown to play a role in the maintenance of bone density, vasodilation, cardioprotection, the increased production of liver proteins such as coagulation factors and hepatic lipoprotein receptors and may putatively reduce the risk of colon cancer. In the breast tissue, oestrogen stimulates the growth of mammary ducts and is also a risk factor for cancer. In the ovary and uterus, the hormone stimulates growth and differentiation and controls water retention and also acts as a risk factor for endometrial cancer (Reviewed by (Gruber *et al.*, 2002). A balance between androgens and oestrogens is essential for normal sexual development and reproduction in both sexes (Carreau *et al.*, 2010). In males, oestrogen has been found to be essential for the fusion of epiphyses and the maintenance of bone mass in young adult men (Nelson & Bulun, 2001, Smith *et al.*, 1994).

Oestrogens are derived from cholesterol. Cholesterol is bound to lipoprotein receptors and moved into the inner membrane of the mitochondria of steroidogenic cells, where the number of carbon atoms is reduced from 27 to 18 (Gruber *et al.*, 2002). Members of the cytochrome P450 family of enzymes, cholesterol monooxygenase (CYP11A), 17 α-hydroxylase (CYP17), and aromatase (CYP19) and the hydroxysteroid dehydrogenase family, 3β-HSD and 17β-HSD are of particular importance in the biosynthesis of oestrogens. (Reviewed by Gruber *et al.*, 2002, Mitrunen & Hirvonen, 2003). This process is summarised in Figure 1.3.

Naturally occurring oestrogens within the body are oestrone (E_1), 17β-oestradiol (E_2) and oestriol (E_3). E_1 and E_2 are most abundant in circulation. All three are C_{18} steroids, with an aromatic A ring, a phenolinic hydroxyl group at C-3 and a methyl group at position C-13. E_2, with a hydroxyl group at C-17 and E_1 with a keto-group

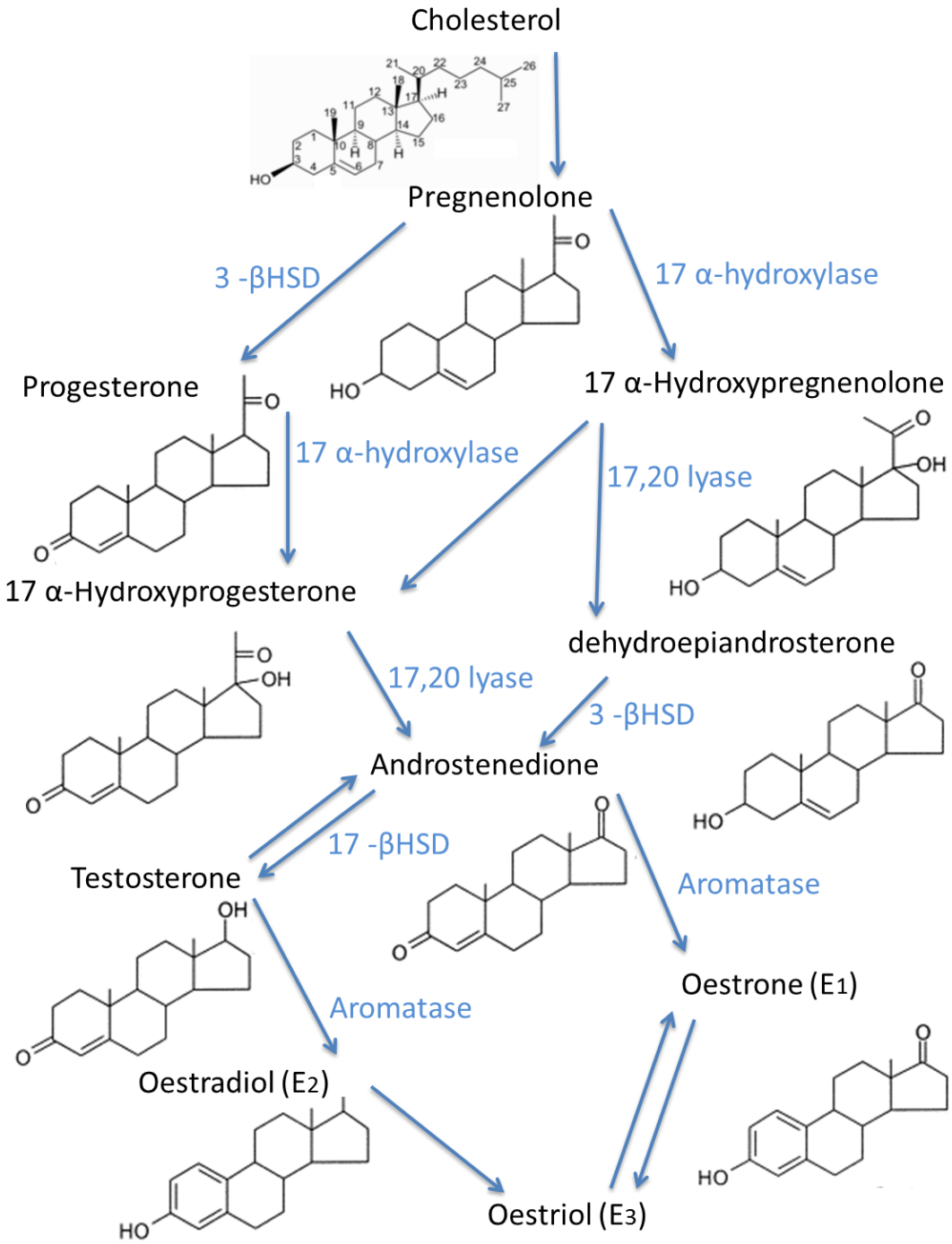

Figure 1.3. Biosynthesis of oestrogen from cholesterol

Names of hormones are indicated above the chemical structures in black and enzymes are indicated in blue. ***Adapted from Mitrunen & Hirvonen, 2003 and Rang* et al.*, 2005.***

at C-17, are the major oestrogens in the blood (Reviewed by Mitrunen and Hirvonen, 2003).

In women, oestradiol is nearly all of ovarian origin. During the menstrual cycle, the production of oestradiol varies, with the highest serum concentrations in the preovulatory phase and the lowest premenstrually. Oestrone and oestriol are primarily formed in the liver, from oestradiol. During pregnancy, oestriol is synthesized in the syncytiotrophoblast (part of the embryonic placental villi) by aromatization of 16a-hydroxyandrostenedione. Post-menopause, the majority of oestrogens are formed by the aromatization of androstenedione to oestrone in peripheral adipose tissue (Reviewed by Gruber *et al.*, 2002, Nelson & Bulun, 2001).

Oestradiol is known to regulate both the transcription (Maurer, 1982) and the secretion of prolactin in the pituitary (Zyzek *et al.*, 1981). Oestrogen can stimulate the expression of target genes via a classical, ligand-dependent and an alternative, ligand-independent pathway (Acconcia & Kumar, 2006). In regard to the ligand independent pathway, most nuclear receptors are phosophoproteins and as such, their function can be altered by changes in phosphorylation state, regardless of ligand binding. The majority of phosphorylation occurs at specific tyrosine or serine residues and is catalysed by enzymes such as mitogen-activated protein kinases and receptor tyrosine kinase. Cross-talk between the signalling pathways of dopamine, epidermal growth factor, transforming growth factor α, insulin or insulin-like growth factor-1, heregulin and cAMP, have been shown to activate the oestrogen receptor in this way. Furthermore, cell surface receptors act without nuclear interaction, as is the case in rapid onset actions such as the short-term vasodilation of coronary arteries, insulinotropic effect of oestradiol on the pancreatic beta cells and rapid activation of growth-factor related signalling pathways in neurons (Reviewed by Gruber *et al.*, 2002, Shupnik, 2002). The cytokine tumour necrosis factor α (TNFα), mediated by nuclear factor κB (NF-κB) (Friedrichsen *et al.*, 2006), has been shown to work synergistically with E_2 to activate human prolactin transcription (Adamson *et al.*, 2008). The ligand dependent pathway will be further discussed in section 1.5.5.

1.4.2. Oestrogen and prolactin

Oestrogen is a well-established modulator of prolactin, having been shown to increase expression, secretion and induce lactotroph proliferation, *in vitro,* in *in vivo* models and in humans (Amara *et al.*, 1987, Freeman *et al.*, 2000, Kansra *et al.*, 2005, Shupnik *et al.*, 1979). The effects of oestrogens on prolactin gene expression within the pituitary, varies between species. In the rat, oestrogen induces a 60-fold increase in the level of prolactin mRNA, while for the human gene only 2-fold increase is seen (Gellersen *et al.*, 1995). Furthermore, oestrogens have been implicated in the pathophysiology of hyperprolactinaemia as well as prolactinomas (Heaney & Melmed, 1999).

Despite a lack of human cell lines to investigate the effects of oestrogen on the expression of prolactin by lactotrophs, the following five points have served as evidence for the effects of oestrogen on prolactin expression in humans: 1. females have a higher basal level of serum prolactin than men; 2. serum prolactin is increased during pregnancy; 3. the incidence of prolactinomas is higher in young females than males; 4. the prolactin release response is increased in oestradiol treated hypogonadal women and transsexuals; and 5. the mean level of serum prolactin is higher in cycling women than in postmenopausal women or in men (Ben-Jonathan *et al.*, 2008).

1.4.3. The oestrogen receptor

The oestrogen receptor (ER) belongs to a nuclear hormone-receptor superfamily with approximately 150 members (Gruber *et al.*, 2002). Oestrogen receptors consist of five functional domains. The highly conserved DNA binding domain (C) contains two zinc fingers that are involved in DNA binding and dimerization. The ligand-binding domain (E) is less highly conserved, contains a set of amino acids important for ligand binding, receptor dimerization, and interactions with coactivators and corepressors. The N-terminal A/B domain is highly variable in sequence and in length and usually contains a transactivation function, activating target genes by direct interaction with component of the core transcriptional machinery or with coactivators responsible for mediating signals to downstream proteins. The hinge domain (D) provides flexibility to the DNA and ligand binding domain and has been shown to influence receptor DNA binding properties as well as serve as an anchor

for corepressor proteins. The C-terminal domain (F) has been shown to contribute to the transactivation capacity of the receptor (Enmark & Gustafsson, 1999, Gruber *et al.*, 2002).

Two ER subtypes exist, ER α and ER β, each with various isoforms and splice variants, expressed differentially throughout the body. Whilst some ligands bind both receptors, the degree of affinity may differ between them. E_2 for example, has a higher affinity for ER β (Gruber *et al.*, 2002). ER α was first discovered in 1985 (Enmark & Gustafsson, 1999) and cloned from the uterus in 1986 (Green *et al.*, 1986). ER β was discovered more recently (Kuiper *et al.*, 1996, Mosselman *et al.*, 1996). The ER α gene has been mapped to the long arm of chromosome 6 and the ER β gene to band q22-24 of chromosome 24 (Gruber *et al.*, 2002).

The ERα and ERβ are structurally different, with dissimilar ligand-independent transactivation domains (AF-1), but a highly conserver ligand binding domain (55% sequence homology) (Gruber *et al.*, 2002). The human ERβ shows c. 89% homology to the rat receptor, 88% to the mouse receptor and 47% to the human ERα (Enmark & Gustafsson, 1999). Both receptors have been shown to bind similar oestrogen response element sequences and show a similar response pattern to E_2.

The distribution of ERα and ERβ differs between species, reflecting their functional roles. In the rat, ERα expression is highest in the uterus, testis, pituitary, kidney, epididymis and adrenal, whereas ERβ is found in the brain, prostate, ovary, lung, bladder and epididymis (Enmark & Gustafsson, 1999). The mouse pituitary expresses ERα only, while the rat and human pituitaries express predominantly ERβ. All three receptors are found on GH3 cells (Ben-Jonathan *et al.*, 2008). ERα knock out studies have shown that the receptor subtype has a profound effect on the expression and secretion of prolactin (Klinge, 2001).

The oestrogen receptor can modulate target gene transcription in three ways. In the first, the oestrogen binds to the ER in the nucleus and activates the transcriptional domain directly. In the second mechanism, the ER binds to an oestrogen response element (ERE) and in the last, protein-protein interactions are formed with other DNA biding transcription factors (O'Lone *et al.*, 2004). Ligand free ER is loosely bound to its cytoplasmic or nuclear location via receptor associated proteins, which

serve as chaperones, to stabilise the receptor and masking the DNA binding domain.

1.4.4. The oestrogen response element (ERE)

The oestrogen response element (ERE) is a sequence of DNA on the target gene locus recognised and bound by the activated oestrogen receptor. The 13 bp inverted repeat consensus sequence of the ERE is 5'GGTCAnnnTGACC3' (n denotes random nucleotide) and was defined in the *Xenopus laevis* vitellogenin gene (Walker *et al.*, 1984).

The rat prolactin gene contains two non-classical sequences that have been proposed to act as EREs. The first ERE (PrlERE1) is located -1582 bp upstream of the prolactin transcriptional start site. This deviates from the consensus AGGTCA by two bases in the 5' half-site and by one base on the 3' half-site. The second ERE (PrlERE2) is located at -1722 and has a perfect 5' but a 3' half-site that differs in four out of six base pairs. The ER was seen to bind to the PrlERE1 with a 10-fold higher affinity than with PrlERE2. The ER has been seen to bind to the ERE with a stoichiometry of 1:1 (Murdoch *et al.*, 1995), but also 2:1 (Klinge, 2001). The ER and ERE have also been seen to interact with Pit-1 binding sites (Ben-Jonathan *et al.*, 2008). Furthermore, variant oestrogen response elements or even partial EREs, often separated by many base pairs can confer oestrogen responsiveness and are termed oestrogen response units (Gruber *et al.*, 2002).

In the human prolactin gene locus, Adamson *et al.,* (2008), found that E_2 induced a 1.8-fold increase in transcription, using GH3 cells stably transfected with a 5000 bp human prolactin promoter fragment linked to a luciferase reporter gene (D44 cell line) (Figure 1.4 a. and c.). By means of mutagenesis and promoter deletion experiments, the group found that ERα mediated activation of the human pituitary prolactin promoter by E_2 is dependent on an ERE sequence located 1189 bp upstream from the prolactin start site. The ERE described here differs from the consensus ERE by one base pair per half-site. Further to this, when a larger fragment of the gene locus is incorporated into the cell by means of bacterial artificial chromosome (BAC), a much larger transcriptional response is seen (Figure 4 c.), suggesting the inclusion of multiple EREs.

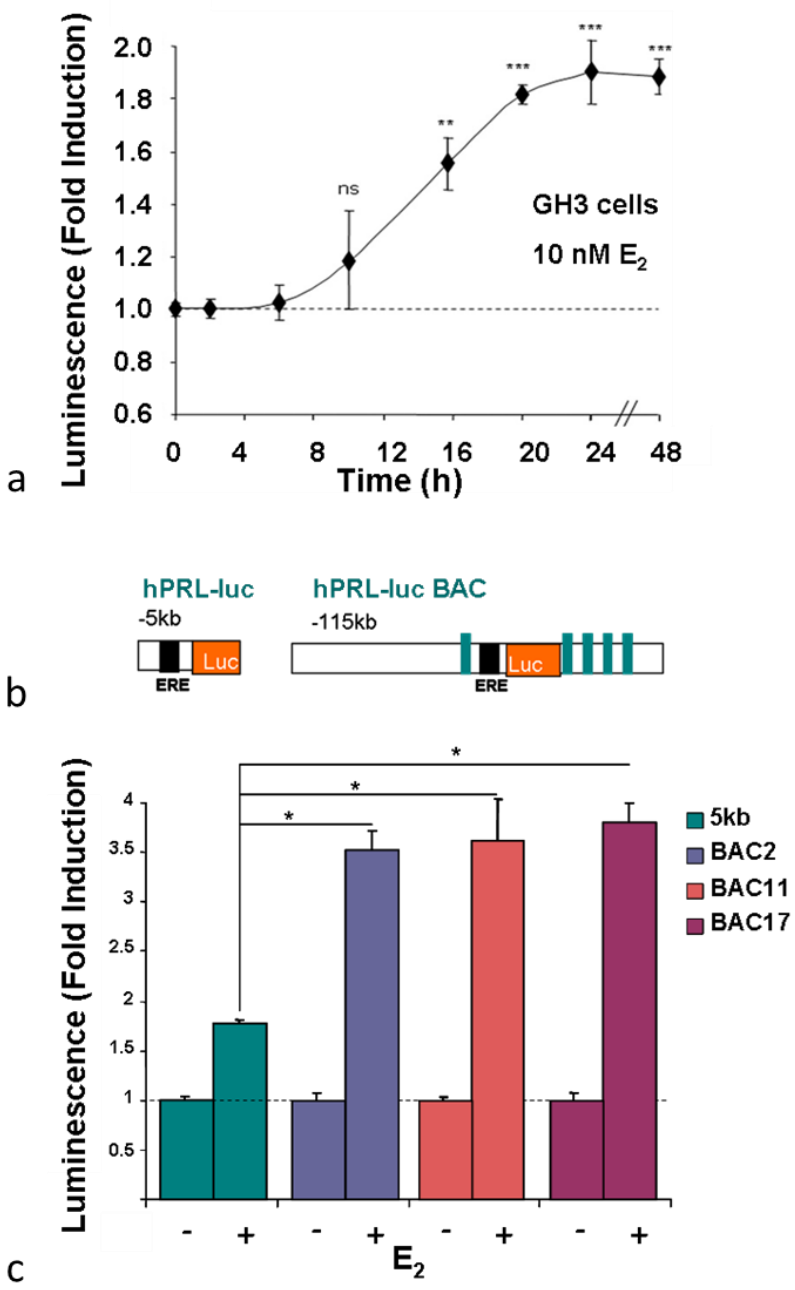

Figure 1.4. E_2 treatment of GH3 cells induces prolactin transcription through oestrogen response elements

*24 hours of 10nm E_2 treatment induces a 1.8-fold increase in prolactin reporter transcription (**a.** and **c.** turquoise histogram) in GH3 cells expressing luciferase under the control of a 5 kpb fragment of the human prolactin promoter (**b.** left hand construct). Inclusion of the entire human prolactin locus (**b.** right hand construct) within the GH3 cells, as is the case in the BAC2, 11 and 17 lines, elicits a much larger change in reporter gene activity (**c.**).* ***Partially adapted from Adamson* et al., *2008 and unpublished data.***

1.4.5. Oestrogen mediated prolactin transcription

Oestradiol mediates its effects on pituitary prolactin by binding to the oestrogen receptor, a steroid hormone nuclear receptor that functions as a ligand-activated transcription factor (Fullwood *et al.*, 2009). Oestrogen binds to the ligand binding domain, and receptor phosphorylation of Ser-118, Ser-104 and Ser-106 of the N-terminal domain (Duplessis *et al.*, 2011, Lannigan, 2003), induces an activating conformational change, dissociating the ER from the chaperones (eg. Hsp 70 and hsp 90 (Klinge, 2001)) and the E_2-ER complex diffuses into the nucleus where it binds the ERE as either a hetero- or homo-dimer (Pettersson *et al.*, 1997) and in the case of E_2, recruits RNA polymerase II (Pol II) transcription initiation complex and further nuclear-receptor coactivators and repressors (Gruber *et al.*, 2002, Klinge, 2001). The SWI/SNF ATP dependent chromatin remodelling complex, is recruited to oestrogen target genes by means of BAF57, enabling the p160 coactivator to potentiate transcriptional activity by ER (Belandia *et al.*, 2002). p160 transmits an activating signal via the C-terminal activation domains AD1 and AD2. AD1 acts as a binding site and plays a role in cAMP pathway activation and AD2 binds p300 (Chen *et al.*, 2000).

At the ERE, the ER receptor works with chromatin to modify its local structure as to allow access and interaction with transcription factors necessary for the initiation of gene transcription (Malayer & Gorski, 1995). While extensive research has gone into the coactivators recruited by ER and the chromatin binding landscape in breast tissue (Zwart *et al.*, 2011), less is known about that of oestrogen in the pituitary.

The ER has been shown to possess large-scale chromatin unfolding activity whether tethered or recruited to the DNA of the target gene (Nye *et al.*, 2002). At the prolactin locus, real-time imaging of a prolactin enhancer/promoter array, visualized by GFP-ER interactions in PRL-HeLa cell line, showed large scale chromatin decondensation and recondensation with differing temporal dynamics upon induction and removal of epidermal growth factor (EGF) and oestrogen. While both EGF and E_2 induced an equal amount of chromatin decondensation, the decondensation rate was doubled in E_2 treated cells (15 as opposed to 30 minutes). Furthermore, EGF treated chromatin recondensed to basal level within a few hours, whereas, E_2 induced chromatin modification persisted for at least 24 hours. Differences in molecular mechanisms are not yet known, but the differential

regulation is speculated to be of particular importance for endocrine tissues that require rapid and short responses to growth factors in addition to the strong and sustained E_2 dependent transcriptional responses (Berno *et al.*, 2008).

E_2 has been seen to stimulate histone H4 acetylation, in the rat prolactin promoter region of GH4 cells, by 2- to 3-fold in 30 minutes (Liu & Bagchi, 2004). It has been suggested that the DNA binding domain of the ER alone is not sufficient for the receptor to access ER-response elements in the chromosomal environment, but rather that the helix-12 is required for this function. Presumably, the helical domain fosters productive ER-protein interactions and decondensation of the chromatin (Sharp *et al.*, 2006).

Oestrogen induced changes in chromatin structure and may be rate-limiting for the prolactin transcriptional response (Murdoch *et al.*, 1995). Oestrogen-induced changes in prolactin chromatin, have been seen, support a looping model (Malayer & Gorski, 1995). The topology of the prolactin EREs may play a role in regulating the timing and strength of the transcriptional response affecting ER binding (Murdoch *et al.*, 1995).

1.4.6. Gene regulation through chromatin structure and the histone code

The major influence of chromatin on nuclear processes such as transcription and replication is well established. Chromatin is the ensemble of genomic DNA and the large number of proteins and RNA that are associated with it. DNA is wrapped around nucleosome comprised of eight histone proteins H2A, H2B, H3 and H4 (Reviewed by Zlatanova *et al.*, 2009). Linker DNA binds nucleosomes together aiding in the folding and stabilisation of the chromatin and forming a ‘beads on a string’ conformation (Featherstone *et al.*, 2012).

The structure of chromatin is plastic and can be modified post-translationally to accommodate the activity of transcription or to silence it (Eberharter & Becker, 2002). On the macromolecular scale, biochemical mechanisms that contribute to the folding of chromatin exist in three main types, local compaction, long-range interactions and anchoring to nuclear scaffolds. Such modifications affect interactions with DNA, generating binding motifs enabling the recruitment of transcriptional regulatory proteins (van Steensel, 2011). Canonical histones can be

replaced and nucleosomes can be remodelled by ATP-dependent chromatin remodelling complexes (Featherstone *et al.*, 2012, van Steensel, 2011).

On the molecular scale, at least eight different classes of chromatin modifications have been identified (Reviewed by Kouzarides, 2007). These small covalent modifications include acetylation, methylation and phosphorylation. Acetylation (by acetyltransferases) is almost invariably associated with the activation of transcription, by the unfolding chromatin by neutralising the basic charge of lysine (Eberharter & Becker, 2002, Grunstein *et al.*, 1997). Methylation (by methyltransferases) is more specific than acetylation and generally serves to 'open' chromatin. Phosphorylation also has been seen to activate transcription and all three are reversible by deacetylation, demethylation and dephosphorylation, respectively, bringing chromatin back to a 'closed' state. Further modifications include ubiquitylation and sumoylation (both larger modifications, associated with transcriptional repression), ADP ribosylation, deamination and proline isomerization. These distinct histone amino-terminal modifications work synergistically or antagonistically to alter and dictate transitions between transcriptionally active or silent states, in what is referred to as the 'histone code' (Jenuwein & Allis, 2001).

The chromatin modifying functions of Pit-1, oestrogen and dopamine are further discussed in section 1.4. and 1.5. and 1.6., respectively.

1.4.7. The oestrous cycle and prolactin

In the reproductive cycle of the female mammal, ovulation occurs after the development and enrichment of the endometrium. In most mammals, if fertilisation does not occur, this endometrial lining is reabsorbed (oestrous cycle), while in some, such as humans, the lining is shed (menstrual cycle) (Campbell & Reece, 2005). The human menstrual cycle lasts 28 days and consists of a follicular phase, a short ovulatory phase and a luteal phase. The oestrous cycle of the rat lasts 4-5 days and can be divided into three stages: proestrus, oestrus, and diestrus. The latter can be further split into metestrus and anoestrus (Shaikh, 1971).

The stages are characterised by temporal changes in the release of pituitary hormones luteinising hormone (LH), follicle stimulating hormone (FSH) and PRL and two ovarian hormones oestrogen and progesterone. Serum prolactin remains

low during the majority of the cycle, peaks at the afternoon of proestrus, driven by a peak in oestrogen secretion. This rise in prolactin coincides with the preovulatory LH surge and consists of three phases: a sharp peak, a plateau and a termination phase (Figure 1.5.). Oestrogen actions are circadian and involve interactions with dopaminergic systems as well as requiring input form the hypothalamus and posterior pituitary (Reviewed by Ben-Jonathan *et al.*, 2008).

Ovulation is triggered by an oestrogen-mediated LH surge which is accompanied by a surge in FSH. The corpus luteum will continue to secrete progesterone autonomously for up to 48 hours. In order for the corpus luteum to remain functional, continued prolactin secretion is required. In the case of copulation, prolactin is released twice daily by the lactotrophs into the adenophysis (Neill, 1988).

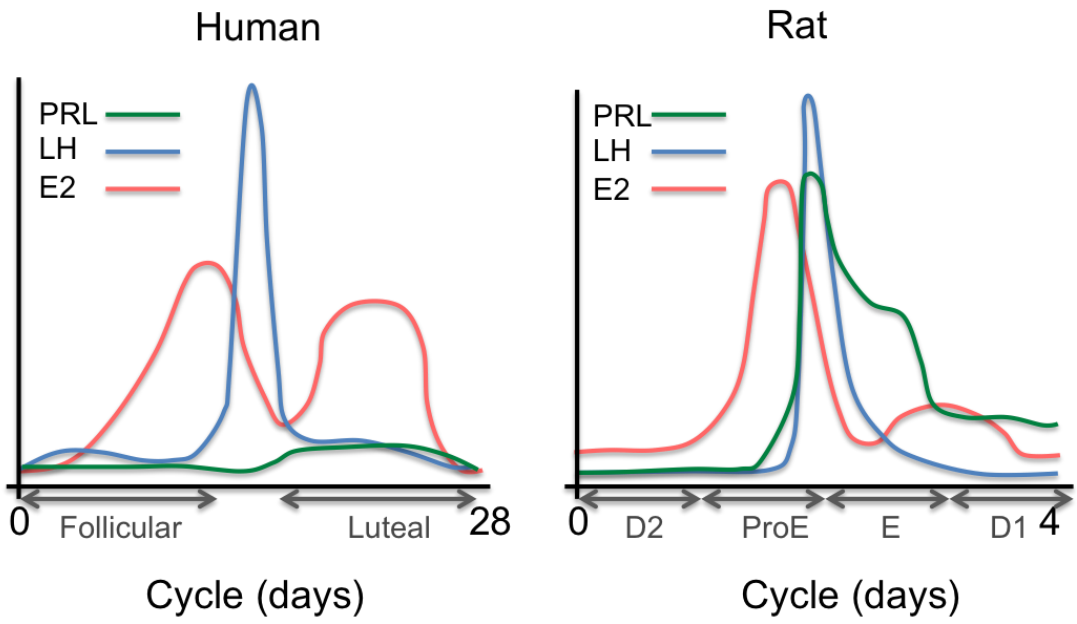

Figure 1.5. Serum hormone concentrations during female reproductive cycles

Serum levels of prolactin (PRL), luteinizing hormone (LH) and oestradiol (E_2) in the human menstrual and rat oestrous cycles. Phases of cycle indicated on x-axis. ***Figure adapted from Ben-Jonathan 2008.***

1.5. Dopamine

The modulatory effects of dopamine on prolactin are well documented. Dopamine has been shown to inhibit prolactin gene transcription, secretion and lactotroph mitotic activity. This tonic inhibition of the anterior pituitary is exerted by the hypothalamus, whose nerve endings are located within the posterior pituitary (Ben-Jonathan *et al.*, 2008). Dopamine has been shown to inhibit the secretion of prolactin from all three subtypes of lactotrophs. Treatment of lactating females with a dopamine D2 receptor antagonist significantly increased granule exocytosis from types I and II (Christian *et al.*, 2007).

Dopamine is synthesised in the tuberoinfundibular hypothalamic neurons (Zabavnik *et al.*, 1993). Three key hypothalamic dopaminergic systems deliver dopaminergic control to the pituitary via the infundibular stalk. These are the tuberoinfundibular (TIDA), tuberohypophysial (THDA) and the periventricular (PHDA) systems (Ben-Jonathan & Hnasko, 2001). The cell bodies of the TIDA neurons stem from the arcuate nucleus and terminate in the median eminence, but have not been seen to form functional synapses. Instead, dopamine is transported to the anterior pituitary via the long portal vessels. THDA neurons from the rostral arcuate nucleus terminate in the posterior or neural lobe and intermediate lobe of the pituitary. PHDA neuron perikarya are found in the periventricular nucleus and terminals are found in the intermediate lobe. The posterior and anterior pituitary are connected by the short portal vessels and this enables the transport of dopamine to the lactotrophs (Ben-Jonathan *et al.*, 2008).

Dopamine binds to either of two isoforms of the dopamine receptor. Dopamine receptor D2 (D2R) is a G-protein coupled receptor, existing in both a long and short isoform. It is the long D2R that is predominantly found in the pituitary. In a matter of seconds after ligand binding, potassium conductance is increased, inactivating voltage sensitive calcium channels, hyperpolarizing the cell membrane, depleting calcium and thus inhibiting prolactin release. Adenylyl cyclase and inositol phosphate metabolism are suppressed resulting in the down-regulation of prolactin gene expression, in a matter of minutes. Lactotroph proliferation is visibly inhibited within the span of a few day (Ben-Jonathan & Hnasko, 2001).

Dopamine is capable of exerting epigenetic control over the chromatin structure of the prolactin gene. D2 receptor activation and subsequent inhibition of MAPK (ERK1/2) signalling leads to rapid deactylation. Dopamine was shown to inhibited histone H4 acetylation by 2-fold in 30 minutes. HDAC2 and the corepressor mSin3A were rapidly recruited to the promoter and association was sustained for over an hour (Liu & Bagchi, 2004).

The expression of the D2 receptor has been shown to vary throughout the oestrous cycle as well as during pregnancy and lactation. The lowest concentrations of D2 mRNA in the anterior pituitary are found at oestrus. The reporter mRNA increases at the beginning of diestrus and peaks at late diestrus and begins to decline again at proestrus. Interestingly, the expression of the dopamine receptor is lowest when the circulating levels of dopamine are the highest. In addition to this, D2 mRNA was found to be reduced during pregnancy as compared to lactation in rat (Zabavnik *et al.*, 1993).

1.6. Real-time transcription dynamics of prolactin

The temporal dynamics of biological systems is a key component of tissue and organism function. In endocrine systems, frequency encoding of information via pulsatile hormone secretion has long been appreciated to be important in the regulation of target systems (Featherstone *et al.*, 2012, Walker *et al.*, 2010). Evidence has been seen for the pulsatile nature of transcription and here I discuss evidence for stochastic transcription seen by other groups and the methods used by our group to analyse the stochasticity of prolactin gene expression.

1.6.1. Evidence for stochastic transcription

Over the past few decades, a surge in interest has been seen in the temporal patterns of gene expression and regulation. It has become evident that transcription is stochastic and heterogeneous in otherwise identical cells and is subject to, and must be distinguished from, both intrinsic and extrinsic noise (Elowitz *et al.*, 2002, Raj & van Oudenaarden, 2009). This phenomenon has been seen in simple systems such as bacteria and yeast, but also in more complex mammalian cells.

Mammalian gene transcription occurs in cycles of transient pulses, or 'transcriptional bursts' in tissues ranging from muscle fibres (Newlands *et al.*, 1998) to fibroblasts (Suter *et al.*, 2011a) to hematopoietic cells (Hume, 2000). By means of transcript counting technologies, including RNA fluorescent *in situ hybridisation* and single cell quantitative reverse transcriptase-polymerase chain reaction, snapshots of transcriptional activity of populations of cells can be captured (Featherstone *et al.*, 2012). Such studies have shown mammalian genes to be expressed in highly variable transcriptional bursting patterns, with pulses, which in most cases have gene specific kinetics (Raj *et al.*, 2006, Raj & van Oudenaarden, 2008, Suter *et al.*, 2011b). Real time imaging of individual lactotrophs has shown the prolactin gene to undergo non-circadian cycles of expression, with up to a 40-fold fluctuation from hour to hour (Shorte *et al.*, 2002, Stirland *et al.*, 2003, Takasuka *et al.*, 1998).

1.6.2. Reporter genes

Reporter genes have been widely used in the study of gene regulation in both cultured cells and *in vivo*, with its most recent applications allowing real-time visualisation of gene transcription (Craig *et al.*, 1991, Spiller *et al.*, 2010, White *et al.*, 1990, White *et al.*, 1996).

The enzyme luciferase, catalyses the conversation of the substrate luciferin, oxygen and adenosine triphosphate (ATP) to oxyluciferin, carbon dioxide, adenosine monophosphate (AMP) and light. The use of the firefly *Photinus pyralis* gene in mammalian expression vectors was pioneered by, (Dewet *et al.*, 1987) and has since been the most commonly used luciferase in molecular biology. Recently, the firefly luciferase gene has been used as a reporter enabling the visualisation of the temporal dynamics of gene activity. The use of experiments of this type has grown extensively, owing to its convenience, sensitivity and temporal resolution. The development of ultra-low-light imaging cameras, has enabled the quantitative imaging of luminescence. Charged coupled device (CCD) photon-counting cameras work by integrating a light signal over a period of time. Digital images are then used for spatial and quantitative analysis. Using this system, we can study the mechanisms of dynamic changes in gene expression in living cells (Takasuka *et al.*, 1998).

The luciferase assay provides a quantitative indication of the stochastic gene expression over time (Takasuka *et al.*, 1998). Typically a luminometer is used to analyse bulk cell lysates incubated with luciferin and ATP, with the drawback of losing information about single cell activity as well as causing the death and disruption of cells. The development and incorporation of the CCD camera allows the measurement of bioluminescence from viable living mammalian cells, transiently expressing luciferase under the control of the promoter of choice (White *et al.*, 1990).

The green fluorescent protein (GFP) was first extracted and purified by Shimomura in 1962 (Shimomura, 2009, Shimomura *et al.*, 1962) and developed as a fluorescent tag by Tsien during the 1990s (Heim *et al.*, 1995). Since then, its use as a protein tag has become well established (Magoulas *et al.*, 2000). GFP was first destabilised, by fusing amino acids 422-461 of the degradation domain of a mouse ornithine de-carboxylase to the C-terminal of an enhanced variant for GFP, giving the protein a half-life of c. 2 hours (Li *et al.*, 1998) as opposed to the 26 hour half-life of stable GFP (Corish & Tyler-Smith, 1999), providing a platform to study spatial and temporal dynamics. The d2eGFP used in our studies has a half-life of 2.5 hours, in cell lines and *in vivo* (Semprini *et al.*, 2009) and in combination with confocal time-lapse microscopy, has become a very powerful tool in the study of human prolactin gene transcription patterns (Featherstone *et al.*, 2012).

1.6.3. Models for studying prolactin transcription

Transcriptional regulation has been studied in a wide variety of models, including sheep, hamsters, rats, mice, zebrafish and a host of cell lines. A wide variety of immortal cell lines have been derived from rat pituitary tumours, for example GH3 cells, and the less widely used MMQ and PR1 (Ben-Jonathan *et al.*, 2008). As a result, the majority of our knowledge on the expression of prolactin is based on the rat genes.

The lack of availability of human pituitary tissue and human derived cell lines for experimental study has necessitated the use of experimental animal models for studies of prolactin function and gene regulation, with the rat often being the animal model of choice for endocrinologists (Featherstone *et al.*, 2012).

1.6.3.1. In Vitro

Over time, various members of our research group have used cell lines based on the GH3 cells, originally derived from a radiation induced mammosomatotroph tumour in the pituitary of a Wistar-Furth rat (Tashjian *et al.*, 1968). These cells, producing both GH and PRL, are immortalised and have a doubling time of 42 to 48 hours (Bancroft & Tashjian, 1971).

The temporal dynamics of prolactin transcription have been studied for over a decade, using derivatives of the GH3 cells, via indirect measurement of transcript abundance using luciferase or d2eGFP reporter genes. Constructs containing 5 kbp of the human prolactin gene locus followed by the luciferase gene have been transfected in GH3 cells or adenovirally transduced into primary pituitary cells from Syrian hamsters. Results indicated pulsatile expression of prolactin, with a high degree of fluctuation and heterogeneity between cells (Friedrichsen *et al.*, 2006, Stirland *et al.*, 2003, Takasuka *et al.*, 1998). Of these, the h-PRL-Luc-GH3/D44 cell line (or D44 cell line as it will be referred to form now on) developed by Takasuka *et al.* in 1998 is of particular interest in relation to this project.

More recently the BACx cell lines have been developed by Adamson *et a.l* (PhD thesis). In these cell lines, the luciferase reporter in under the control of the entire human prolactin promoter, incorporated into a bacterial artificial chromosome (BAC). X refers to the clonal number, each with differing insertion sites and degrees of truncation of the BAC as it is integrated into the host DNA. The BAC2 cell line was chosen due to robustness of response to stimuli.

As with any model, the use of cell lines has its pros and cons. While cell lines have the advantage of immortality, easy transfection and growth, and spark less ethical debate than animal models, there are caveats in the system. The GH3-based D44 and Bac2 cell lines do not express the dopamine D2 receptor, which is crucial for the regulation of prolactin regulation (Ben-Jonathan *et al.*, 2008), hence an important aspect of normal physiological regulation cannot be studied. Furthermore, in cell culture systems, post-translational and up- and downstream events cannot be modelled, neither can the spatial relationship between cells and their intercommunication, and the impact of this on physiology, highlighting the importance of the *in vivo* model.

1.6.3.2. In Vivo: The development of a model to enable the real-time visualisation of prolactin gene expression in individual cells

In 2009, a former lab member Dr. Sabrina Semprini developed humanized reporter transgenic rats, expressing either a destabilised enhanced GFP (d2eGFP) or luciferase, or both, under the control of the human prolactin gene locus (Figure 1.6.). This model has enabled *in vivo* imaging from the scale of the whole body to the single cell. A BAC containing the human prolactin locus was chosen from a publicly available library. Reporter genes were knocked into the first coding exon of the prolactin gene, and the recombinant BAC was injected into the pronucleus of Fisher 344 fertilized rat oocyte. Adults were mated in order to generate transgenics expressing both transgenes. The hPRL gene locus used in the initial BAC spans 163 kbp and includes 115 kbp upstream and 38 kbp downstream of the coding region. One of the advantages of using a BAC recombineering system is the ability to include such a large fragment of DNA, allowing the reporting of appropriate regulation of the gene by distant elements, including EREs and both intra- and

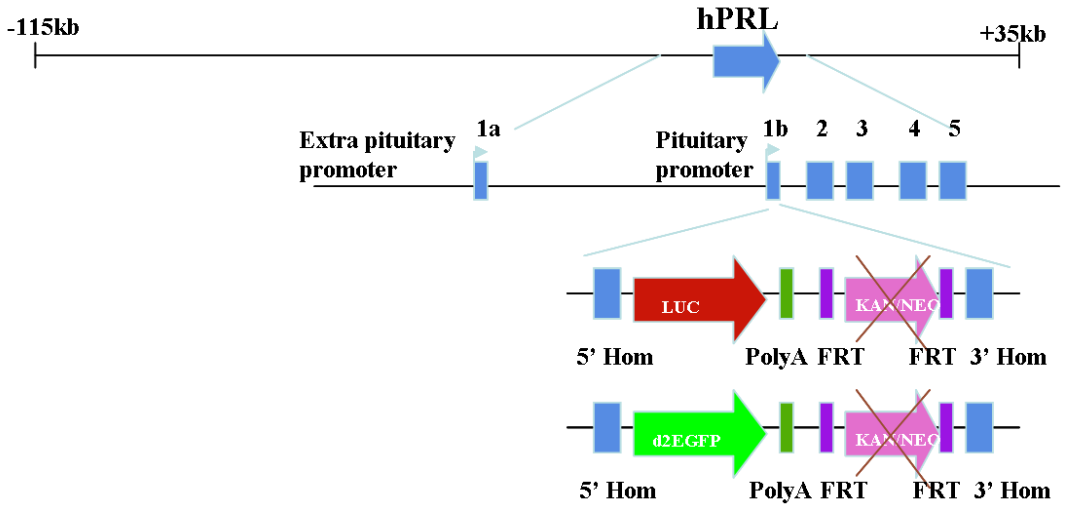

Figure 1.6. Structure of the BAC reporter gene constructs

Schematic of the BAC constructs used to develop the Fischer 344 (d2eGFP-hPRL 455) rats used. Luciferase and d2eGFP are expressed under the control of the human prolactin promoter. ***Figure from Semprini* et al. *2009.***

extra-pituitary start sites. *Photinus pyralis* luciferase and d2eGFP were chosen for their short half-lives. Due to the position of the reporter gene, translation of the prolactin protein is inhibited, maintaining the normal levels endogenous prolactin expression (Semprini *et al.*, 2009).

When transgenic rats were subjected to lipopolysaccharide (LPS) to stimulate an immune response, luciferase reporter activity for human prolactin transcription was found in the thymus and spleen. Endogenous rat prolactin was not, however, seen in these areas (Semprini *et al.*, 2009), providing further evidence of differential functions of prolactin in the immune response in humans and rodents (Ben-Jonathan *et al.*, 2008, Matera, 1996). Additional extrapituitary luminescence signal was detected in the paws and ears of both male and female rats, suggesting a human prolactin promoter-driven luciferase expression in cartilage (Semprini *et al.*, 2009).

Luciferase activity of pituitary specific prolactin expression was detectable by whole body *in vivo* imaging (Figure 1.7. a. and b.) (Semprini *et al.*, 2009). Either luminescence or single cell fluorescence signal was detected from 400μm coronal *ex vivo* tissue slices (Figures 1.7. c. and d., respectively) (Harper *et al.*, 2010). The expression of both reporter genes was found to be localized in the anterior pituitary and not the posterior and also more prominent, in lateral aspects of the gland. From dual reporter cell line studies, in which both reporters were expressed within the same cells, it became evident that expression of the two reporter genes, luciferase and d2eGFP, were not synchronised or temporally coordinated, suggesting that the pulses in prolactin gene expression are independent of cell cycle, nor are they a reflection of cellular status, environment or autocrine signalling, but rather, that pulsatility is due to an intrinsic property of the transcription process itself (Harper *et al.*, 2011, McFerran *et al.*, 2001). Single cell analysis of luciferase activity in cell cultures identified stochastic prolactin gene expression with a lack of synchronisation between the fluctuations of prolactin promoter activity between individual cells (Figure 1.7 .e.).

Upon examination of single cells in the context of whole (adult) tissue slices, promoter activity varied in pulsatility with time and location. Adjacent cells showed a heterogeneous array of transcription patterns, however, the summation of these local patterns, generated an apparently coordinated behaviour across the tissue

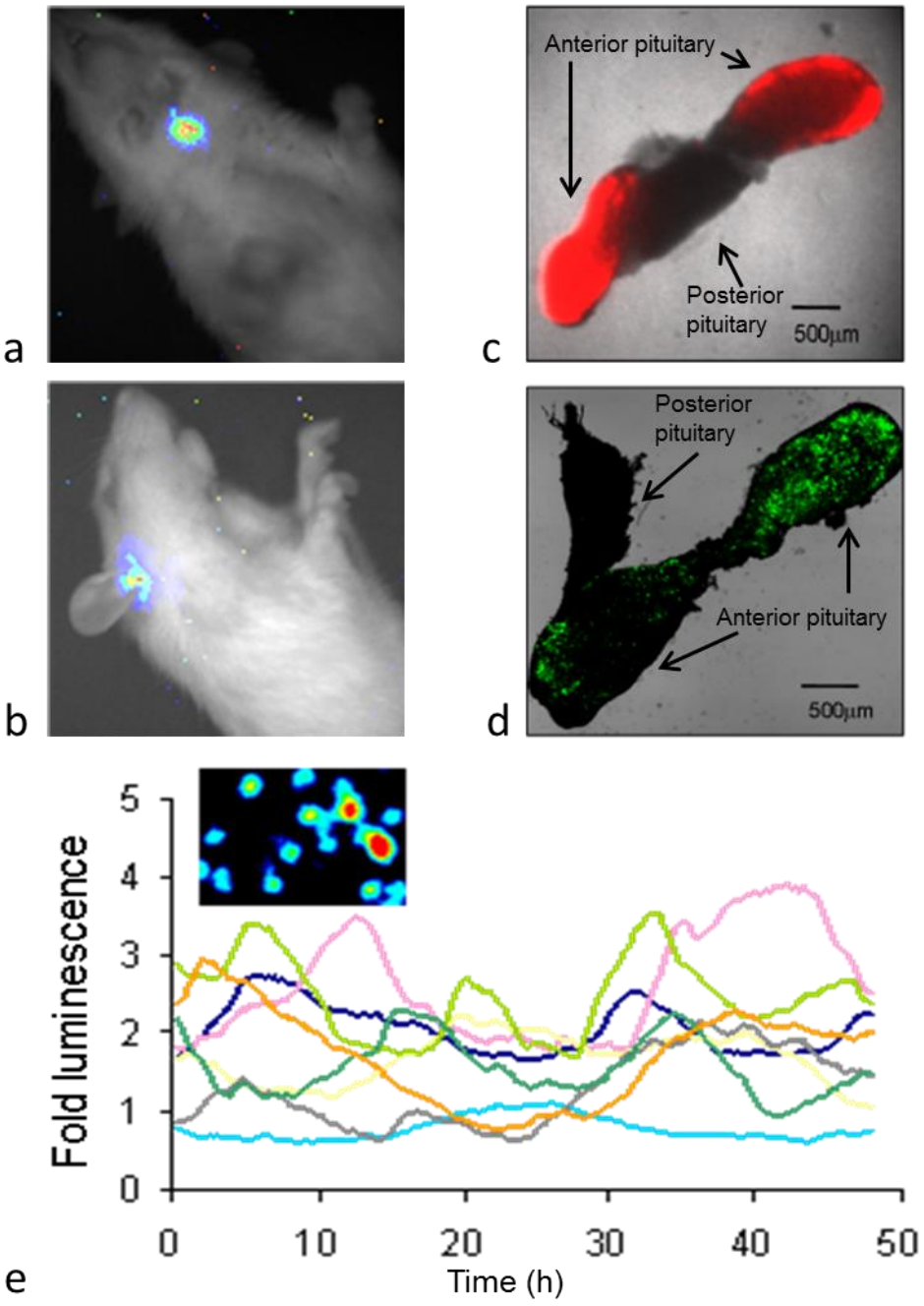

Figure 1.7. Luminescence and fluorescence activity of the human prolactin gene transcriptional reporters from the Fischer 344 (luc/d2eGFP-hPRL 455) rats

*In **a.** and **b.** pituitary luminescence can be seen by whole body imaging. **c.** and **d.** show single cell luminescence and fluorescence from pituitary tissue slice preparations, respectively. In **e.** traces of tracked single cell luminescence from dispersed pituitary tissue, with time in hours along the x-axis and fold change in luminescence along the y-axis. **Figure adapted from Semprini et al., 2009 and Harper et al., 2010.***

(Harper *et al.*, 2010). The mechanisms for the heterogeneous transcriptional pulses between cells is still unclear. Unsynchronised cycles may be due to a functional heterogeneity between cells, differences in cycle stage or oscillatory protein activity, or chromatin and transcription cycles stages, or of course, perhaps a combination of the above. A tissue with a heterogeneous mix of transcriptionally active cells, may facilitate graded responses to transient and sustained stimulation.

During the development of the pituitary, single cell prolactin gene expression is highly pulsatile in nascent lactotrophs at E16.5, with pulses with a median of c.5 hours. Later in gestation and in early neonatal life (P1.5), prolactin transcription was seen to stabilise. Interestingly, when neonatal pituitary cells are dispersed and are no longer constrained by tissue architecture or paracrine signalling, pulsatile transcriptional behaviour is regained, with cells showing a range of zero to three pulses in 48 hours with 1.2 to 8.4 fold increases in amplitude and ranging from 7 to 30 hours. These findings were consistent between males and females (Featherstone *et al.*, 2011). Transient pulses in newly derived cells may be necessary for programming of gene expression in differentiating cells.

Taken together, single cell and tissue wide results in both adult and the developing gland, indicate that the pituitary is comprised of a series of cell ensembles which, when dispersed, show an individual variety of patterns of short-term stochastic gene expression behaviour; but when grouped, as they are in tissue, cells display a degree of long-range and long-term coordination. This suggests that transcriptional patterns are constrained by tissue architecture and may be controlled by factors such as tissue environment and cellular communication.

1.6.4. Mathematical modelling of transcription

The ability to collect single cell time-lapse bioluminescent data from reporters of gene activity has lead to the need for a development of a system with which to analyse such data and to be able to relate the light produced by reporters to information about transcription.

In early work, peaks in PRL and GH promoter reporter activity were assessed visually from luminescence light intensity readings from GH3 cells and patterns were categorised into three groups: progressive rise, phasic/transient or no

response (Norris *et al.*, 2003, Takasuka *et al.*, 1998). The first mathematical determination of peaks in reporter activity utilised a combination of area under the curve (AUC) and Cluster analysis (Norris *et al.*, 2003, Veldhuis, 1996, Veldhuis & Johnson, 1986).

We have since developed the tools to obtain valuable single cell fluorescence and luminescence data, reporting promoter activity in the human prolactin transgene from the Fischer 344 (d2eGFP-hPRL 455) rat, and have thus been able to collect data on human prolactin transcription from an *in vivo* model. Using similar visual analysis, we have been able to identify pulsatile patterns in prolactin gene activity. This remains, however, an evaluation of the light intensity produced by the reporter. In collaboration with the Systems Biology Centre at the University of Warwick, algorithms have been developed in order to model the transcription dynamics of prolactin from the original fluorescence and luminescence data obtained from confocal time-lapse microscopy.

In 2011, Harper *et al*. implemented a stochastic binary switch model to describe prolactin transcription patterns from the hPRL-luc and hPRL-d2eGFP reporter genes in the dual GH3-DP1 cell line. In this algorithm, transcription was modelled to exist in two states, either 'on' or 'off' (Figure 1.8.). This model used a stochastic differential equation (SDE), to analyse fluorescence data and this was then fitted to time-series data using a Markov Chain Monte Carlo (MCMC) algorithm, using prior information on the degradation rates of the mRNA and protein of the d2eGFP reporter (Harper *et al.*, 2011).

Further statistical algorithms were used to assess the distribution of time spent in active and inactive transcription. Autocorrelation analysis was performed on the reconstructed transcription rate data. This showed that transcription cycles were occurring at each gene with a dominant period of 11.3±3.3h. The average transcriptionally 'on' phase was estimated to be 4.0±1h and the average 'off' period was estimated at 6.5±2h per transcription cycle. The mean 'off' period was never seen to last less than 3 hours, which led to the hypothesis that there was a transcriptional refractory period of at least 3 hours, during which a new cycle of transcription could not be initiated. Cycles of hPRL transcription were also observed form both reporter genes in individual clonal pituitary cells from dual BAC-

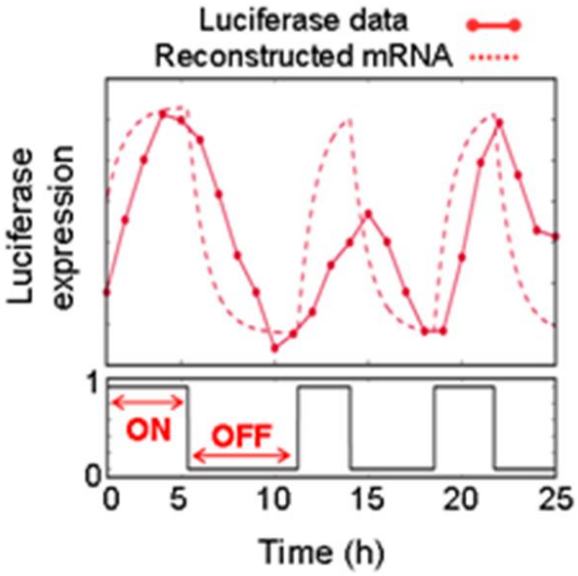

Figure 1.8. A binary model of prolactin transcription dynamics

The 'on' and 'off' times of prolactin transcription were calculated using the stochastic binary (switch) model, form hPRL-luc reporter gene data from GH3-DP1 cells. Red lines indicate the luciferase data, dotted red lines indicate reconstructed mRNA levels over time and the lower panel shows the modelled 'on' and 'off' periods of gene transcription. ***Taken from Harper* et al.*, 2011.***

reporter transgenic rats grown in primary culture, although the average period length was slightly longer, at 15.2±4.8h (Harper *et al.*, 2011).

This three hour refractory period was statistically shown to introduce cyclicity into the system. Previous studies have considered a model in which fluctuations of transcription rates follow a random telegraph process, where a gene switches between an active and an inactive state in a 'memoryless system' and mean times in each state follow an exponential distribution. In the case of prolactin transcription rates, the 'on' phase durations follow such an exponential distribution (Figure 1.9. a.), however, the 'off' phase, does not (Figure 1.9. b.). This time spent in the inactive phase effects the length of time remaining in that state. With the incorporation of a three hour refractory period (Figure 1.9. c. and d.), memory is introduced into the system and the 'on' and excess 'off' times of prolactin transcription follow an exponential distribution cycle pattern (Harper *et al.*, 2011).

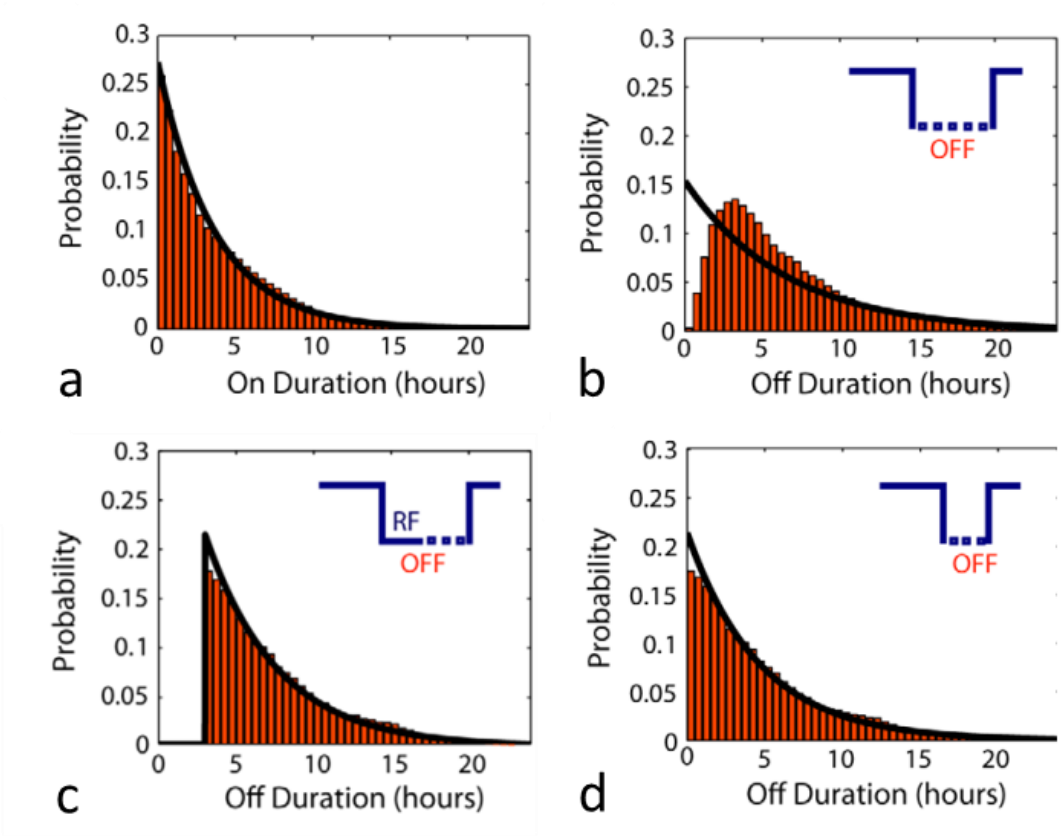

Figure 1.9. A refractory period introduces cyclicity into transcriptional cycles

*The histograms in **a.** show the probability of durations of transcriptionally 'on' times, fitting to an exponential distribution. In the case of the 'off' distributions (**b.**), however, the probability of distributions does not fit a random distribution (black line). The removal of a three hour refractory period (**c.**), gives the system memory and the distribution then follows an exponential distribution (**d.**).* ***Taken from Harper* et al., *2011.***

Our group has hypothesised that the biological significance of the three hour refractory period has to do with chromatin remodelling. In this model, the transcriptional 'off' period represents the transition between closed to open chromatin and the assembly of the transcription initiation complex (TIC). The 'on' phase then represents active transcription and ends at the point of disassembly of the TIC. The minimum 'off' period following the 'on' phase would thus take at least

the amount of time needed for the dissociation and reassembly of a new TIC. This mechanism is summarised in Figure 1.10.

To investigate the role of chromatin in prolactin transcription cycles, GH3-DP1 cells were exposed to the histone deacteylase inhibitor Trichostatin A (TSA). This resulted in a prolonged period of correlation between cells (especially when combined with forskolin and BayK-8644, activating both cAMP and $Ca2^{+}$ signalling), with less than 20% of cells reverting back to cycling. TSA increased the duration of the on-phase and the initial rate of transcription, resulting in a pronounced increase in reporter gene expression. Chromatin immunoprecipitation assays (ChIP) showed an increase in acetylated histone H3 DNA binding at the hPRL promoter following TSA treatment. Together this suggests a refractory period of transcriptional inactivity, in which chromatin remodelling may play an important role. Histone acetylation has a key role in the coordination of the temporal kinetics of transcription. Transcription of the hPRL gene might therefore require a long period of chromatin remodelling that is the source for the observed refractory period (Harper *et al.*, 2011).

Experiments in the regulation of *mCherry* as a reporter for the cytomegalovirus (CMV) promoter activity in isogenic chick cell populations, showed that TSA directly manipulated chromatin dynamics and had a marked effect on the stochasticity of gene expression. The fitting of a two-state model to describe opening and closing patterns of chromatin found that most variety was seen in the timing of the closed state between clones and that TSA affected only the opening probability, which complies with our theory (Vinuelas *et al.*, 2013).

Opposing theories have been proposed. Single molecule RNA measurement by fluorescence in situ hybridization indicated that while the levels of transcriptional activators effect average burst size, it did not alter the frequency or timing of transcriptional dynamics (Raj *et al.*, 2006). From TSA studies into the pulsatile transcription of circadian genes, Suter *et al.,* (2011) found that transcriptional kinetics were gene specific and that chromatin environment played only a secondary role in burst regulation. Studies into the stochastic transcription of the *Pho5* gene in yeast, also lead the authors to conclude that the phases of increased transcriptions remained unexplained by promoter chromatin remodelling steps (Brown *et al.*, 2013).

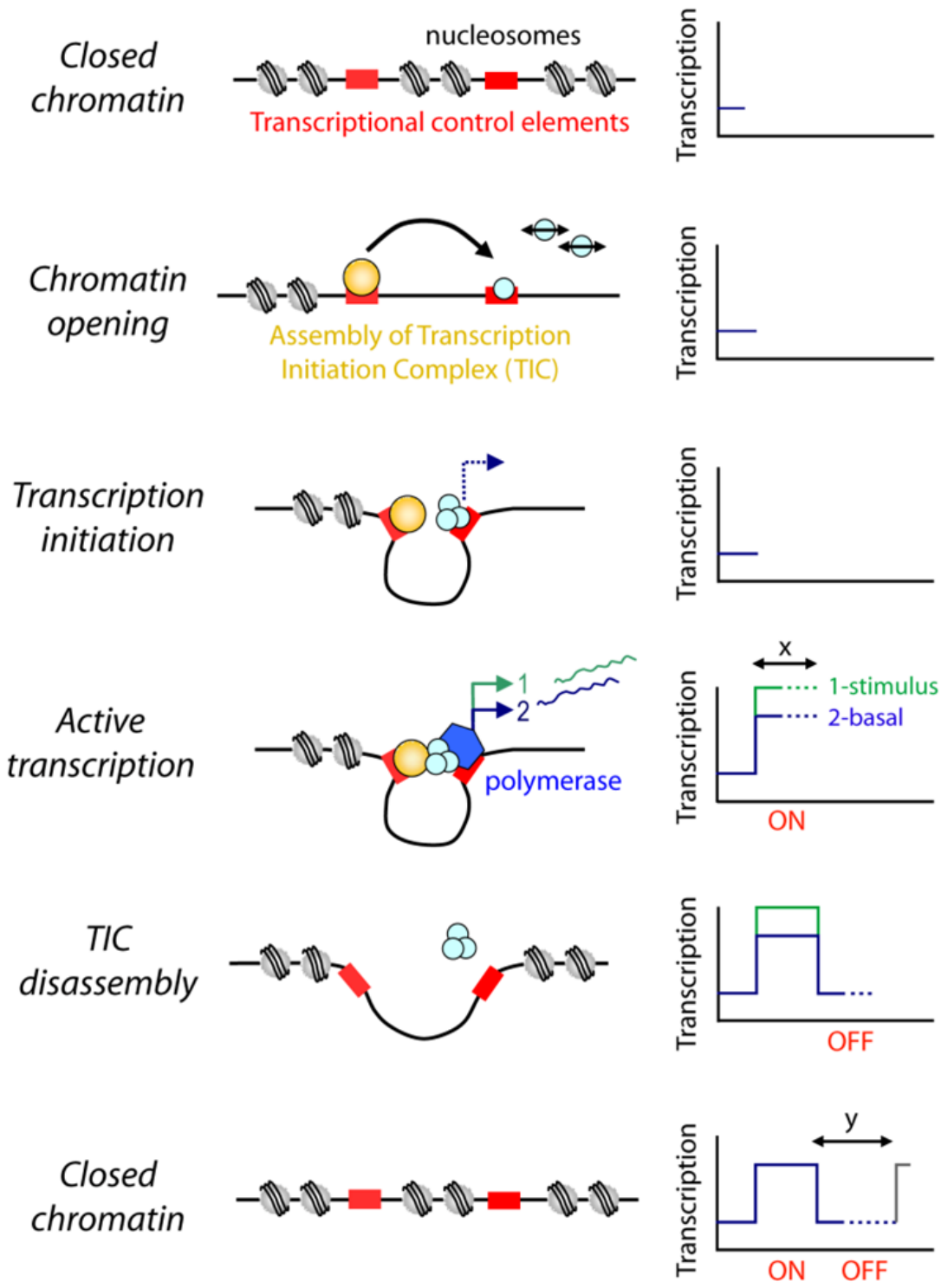

Figure 1.10. Model for the generation of transcription cycles

The above schematic, poses a theoretical model whereby the process of chromatin remodelling is the mechanism on which stochastic transcription cycles are based, with x and y denoting variable durations of time. ***Figure from Harper et al., 2011****.*

1.7. Aims

Oestrogen is a well-known modulator of prolactin transcription, secretion and the proliferation of lactotrophs. It has been shown to induce hyperplasia, resulting in prolactinomas, the pathophysiology of which is not clear. In order to understand the nature of the prolactin hypersecretion in pathological states, we must first understand the mechanisms by which prolactin gene transcription is regulated in the normal pituitary gland under physiological conditions. This can then be compared to the effects of supraphysiological doses of oestrogen and how this affects transcriptional regulation patterns.

In this study, I aimed to establish two models with which to study the effects of oestrogens on human prolactin transcription *in vivo*. First, I studied female rats expressing a destabilised GFP under the control of the human prolactin promoter, through the oestrous cycle, to analyse the effects of short-term fluctuations in endogenous oestrogen on prolactin transcription patterns. In the second model, I aimed to test the effects of longer-term supraphysiological levels of oestrogen on prolactin transcription, using male rats implanted with ALZET® micro osmotic pumps releasing a constant high dose of oestradiol over a period of 21 days.

By using live tissue time-lapse fluorescence microscopy on pituitary tissue slice preparations, I aimed to identify potential differences in the patterns of reporter gene expression in each of these models. I aimed to identifying cycles in single cell fluorescence intensity readings, by comparing the frequency, duration and amplitudes of peaks and troughs in fluorescence over 48 hour imaging periods and to identify any changes in these characteristics between high and low oestrogen states.

To further analyse transcription patterns, transcription rates were back calculated from single cell fluorescence data, using a novel transcriptional switch rate model, developed by the Systems Biology Centre at the University of Warwick. With this we hope to further highlight the nature of differences in prolactin transcriptional activity in high and low prolactin production states across both models.

Chapter 2

Materials and methods

Materials and methods

2.1. Flow cytometry

Pituitaries were removed and washed in PBS at room temperature. Posterior lobes were removed and pituitaries were sectioned into two, one half for flow cytometry and the other for wax embedding. Tissue used for primary cell culture and/or flow cytometry was sectioned using a scalpel blade, suspended in 1 ml dispersion buffer (per ml: 942.5 µl PBS, 40 µl trypsin (2.5% stock, Roche in HBSS), 13 µl BSA (250 mg/ml stock) and 4.5 µl DNase (10 mg/ml stock in water, Roche)) and transferred from the petri dish to a glass bijou with a small flea using a glass pipette (all procedures where cells are pipetted directly were carried out using a glass pipette). Bijous were placed in a water bath of 37°C with a magnetic stirrer and samples were triturated every 15 minutes for 1.5 hours to fully dissociate cells. Cells were washed in 1% BSA PSB and split in two lots, one left in PBS and the other incubated with lysis solution (ADG An Der Grub Bio Research GMBH FIX and PER cell permeabilization kit, Austria), then a primary antibody against prolactin (Lifespan 1:1500) and APC (allophycocyanin) anti-rabbit secondary (R&D Systems 1:20), before another wash in 1% BSA PSB. Both samples were then taken to the University of Manchester Faculty of Life Sciences (FLS) flow cytometry and fluorescence-activated cell sorting (FACS) unit. A minimum of 1 x 10^4 cells is needed for flow cytometry. Note that all equipment used was sterile. Statistical analysis was carried out using SPSS.

2.2. Immunohistochemistry

2.2.1. Fixing and sectioning tissue

The remaining half of the anterior pituitary tissue was incubated in 4% paraformaldehyde (PFA) or Bouins fixative (both Sigma) for 2h at room temperature, after which the tissue was washed with PBS and stored in 70% ethanol until wax embedding. A 16 hour overnight wax embedding protocol was used in which the samples were submerged and incubated in 70 to 100% ethanol, xylene and then wax in a Citadell 2000 Microm Spin. Tissues were sectioned to 5 micron thickness and mounted onto glass slides.

2.2.2. H&E

Wax was removed from tissue by subjecting slides to xylene and then decreasing concentrations of industrial methylated spirit (IMS) (100%, 95% and 70%) before being washed in tap water. Slides were stained with Shandon Gills 2 Hemotoxilin (Thermo Scientific) for four minutes, washed with water and acid alcohol before being stained with Shandon Eosin Y Alcoholic (Thermo Scientific) for 30 seconds and dehydrated and fixed.

2.3.3. Immunofluoresence staining

Tissue was dewaxed by subjecting slides to xylene and then decreasing concentrations of ethanol (100%, 90% and 70%) before antigen retrieval in 0.01 M tri-sodium citrate (pH6). After blocking in blocking buffer (per ml: 160 µl BSA (250 mg/ml), 200µl donkey serum and 640 µl PBS), for one hour at room temperature, samples were incubated with the appropriate concentration of primary antibody in the same blocking buffer (see Table 2.1.) at 4°c overnight. Secondary antibodies at the appropriate concentration in PBS were incubated for two hours at room temperature. In the case of costaining experiments, this process was repeated from the blocking stage. Cell nuclei were then stained with 4,6-Diamidino-2-phenyindole (DAPI) (Sigma) at 1: 50 000 for 10 minutes at room temperature before mounting coverslips with PermaFluor mounting media (Thermo Electron Corporation) prior to analysis using a Nikon upright confocal microscope.

2.3. Basic cell culture

Cell lines used in this project are based on the GH3 cell line, derived from a mammosomatotroph tumour of a Wistar-Furth rat (Tashjian *et al.*, 1968). Cells have a doubling time of 42-48 hours (Bancroft & Tashjian, 1971). D44 cells express luciferase under the control of a 5 kbp fragment of the human prolactin locus (Takasuka *et al.*, 1998) and in BAC 2 cells under the control of a larger fragment of the same gene locus (Adamson *et al.,* unpublished).

The following cell culturing procedures were common to GH3, D44 and BAC 2 cell lines. All cell culture procedures were carried out under sterile conditions in a Labcaire laminar flow hood and all equipment was sterilised using 70% industrial

Antibody	Raised in	Against	Manufacturer	Final concentration used
1°	rabbit	rat prolactin	Lifespan	1:500
1 °		rat prolactin	R51 (McNeilly)(*)	1:4000
1°	mouse	rat prolactin	Pierce	1:500
1°	rabbit	GH	(McNeilly) (*)	1:1000
1°	mouse	GFP	ClonTech	1:50
2° (Alexa 488)	goat	anti-rabbit	Invitrogen	1:200
2° (Alexa 456)	goat	anti-mouse/rabbit	Invitrogen	1:200

Table 2.1. Optimised antibody concentrations

* *In house antibody kindly donated by Professor Alan McNeilly at the Medical Research Council (MRC) Human Reproductive Sciences Unit, Edinburgh, Scotland.*

methylated spirit (IMS) (Genta Medical) prior to entering the hood. Viability of cells was determined visually by means of an inverted phase contrast microscope.

2.3.1. Cell stock maintenance

Cells were grown in 10 ml Phenol Red free Dulbecco's Modified Eagle's Medium (DMEM) (Gibco) supplemented with 0.1µM Ultraglutamine (Lonza) and 10% fetal bovine serum (FBS) (Invitrogen) in T75 ventilated flasks (Coring) at 37°C in a 5% CO_2 environment. Bi-yearly micoplasma testing was carried out using the PCR Micoplasma Test Kit from AppliChem.

2.3.2. Splitting cells

Once cells reached 80% confluence, approximately every 5 days, growth medium was removed and the cell sheet was washed with phosphate buffered saline (PBS). 1ml of trypsin (Lonza and later Gibco) was added to each T75 flask and incubated for 3 minutes at 37°C and 5% CO_2, until cells came loose from the dish. This reaction was stopped and cells were washed with 5 mls of culture medium (as

described above). Cells were then resuspended in 10 mls of culture medium and reseeded at a 1 in 5 dilution.

2.3.3. Cryogenic freezing and thawing

For the purpose of long term storage, aliquots of cells were frozen down and stored in liquid nitrogen (-196°C). After trypsinisation and wash with culture media, cells were resuspended in the appropriate (5 mls for a T25, 10 mls for a T75) volume of freezing media (a mixture of culture media, FCS and Di-methyl sulphoxide (DMSO; Sigma, UK) at the ratios of 6:3:1). 1ml of cell suspension was aliquoted into 2ml cryo tubes which were then slowly cooled to -80°c before allocation into liquid nitrogen storage vessels. Alternatively, $1x10^6$ cells were frozen down per aliquot.

Cell aliquots were taken from the liquid nitrogen storage as needed and placed in a 37°C water bath for 2-3 minutes to thaw. After spinning down the samples and removing the DMSO media, the cells were washed with 1 ml of culture media before resuspension and transfer to a culture dish. These processes were carried out a quickly as possible in order to minimise DMSO toxicity.

2.4. The luciferase assay

BAC2, D44 and GH3 cells were trypsinised (as before) and counted using a haemocytometer. 1×10^4 cells in 100µl were seeded per well of NUNC sterile white 96 well plates, with GH3 cells serving as a control. Cells were left to adhere overnight at 37°C and 5% CO_2 before being serum starved (for 24 hours) by removal of medium, washing each well with PBS and replacing with serum starved media (0.25 % BSA DMEM with 1% Glutamax). All stimulations were carried out using a 1000 x stock of oestradiol (E_2) (Sigma), fibroblast growth factor (FGF) (Calbiochem) or forskolin (FSK) (Sigma) with final stimulating concentrations of 10 nM, 100 pM/ml and 1 nM, respectively. Both of the latter two act as positive controls for gene expression activation. For stimulation experiments, after the allotted time of incubation with stimulant, the medium was removed, wells were washed with PBS and 50 µl of lysis buffer (for 50 mls: 12.5 ml TrisPO_4 (1M, pH7.8), 7.5 ml glycerol, 500 µl EDTA (0.5M), 500 µl MgCl (1M), 50 µl Triton X (final concentration of 0.1%), and 5mg BSA) was added to each well. Once in the luminometer (Berthold Technologies – Mithras LB 940), each well was injected with 50 µl luciferase

substrate (per ml: 300 µl 1mM luciferin (Biosynth), 660µl lysis buffer (as before), 23.4µl $dH_20$and 16.6 µl 50 mM ATP).

When sterile white 96 well plates were not available, cells were cultured in 24 well plates, where 10 x 10^5 cells in 500 µl were plated into each well. After stimulation etc. these cells were lysed using 150 µl lysis buffer (as before) and 50 µl of the lysates was transferred into non-sterile white 96 well plates for reading in the luminometer.

2.5. Live cell luminometry

1.5 x 10^4 cells were plated into each well of a 96 well white sterile plate (NUNC) in 100µl and left to adhere for 24h in the incubator. Medium was removed and replaced with serum starved media (as above) with 1mM luciferin after cells had been washed with PBS. Cells were further incubated overnight to 24 hours. For the primary stimulation, serum starved media was removed, and replaced with 100µl serum starved media with final concentrations of stimulus as shown below in figure 1 and 1mM luciferin. The plate was sealed with a Breathe-Easy® air permeable membrane (Sigma-Aldrich) and placed into the live cell luminometer (FLUOstarOmega, BMG Labtech). 5 second readings were taken every 15 minutes for 24 hours. Media were removed, wells washed with PBS and the appropriate concentration of secondary stimulus (Figure 2.1.) was added in 100µl serum starved media with 1mM luciferin. Readings were taken for a further 24 hours.

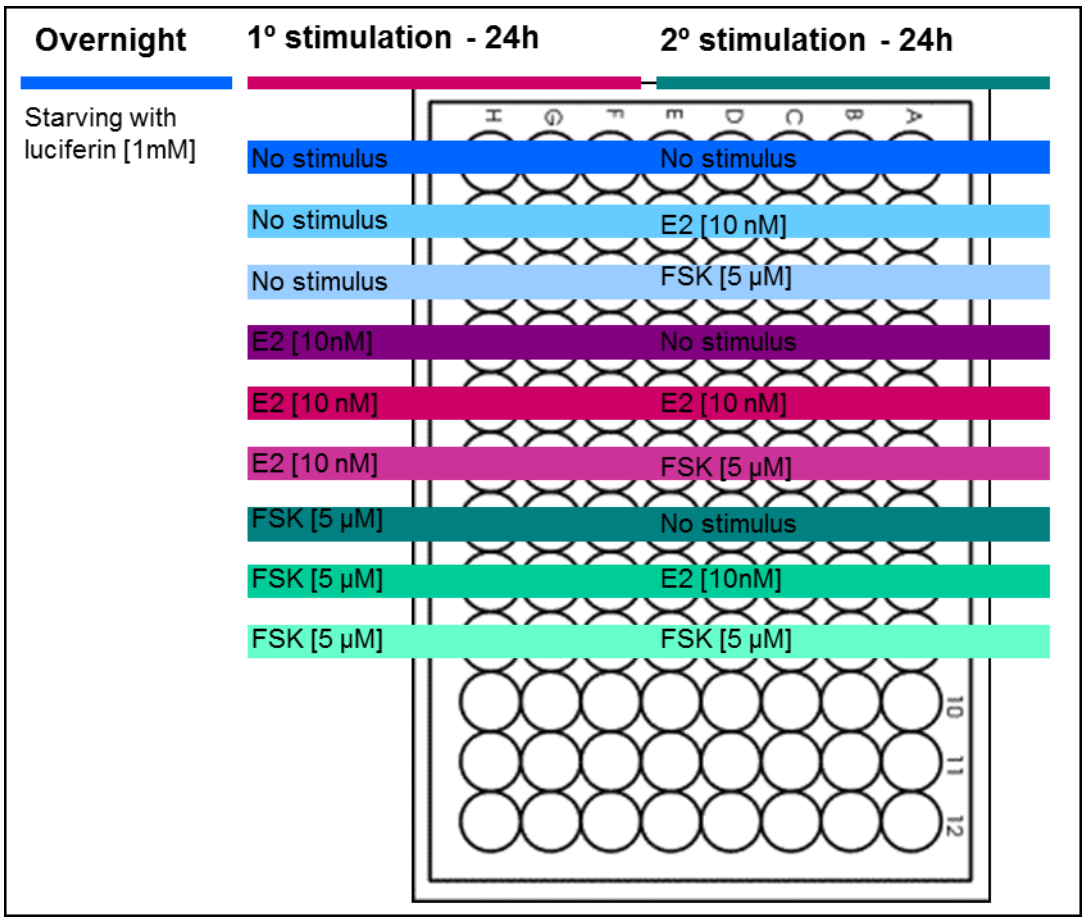

Figure 2.1. Live cell luminometry re-stimulation experimental design

Schematic diagram of a NUNC 96 well plate with an experimental time table superimposed. Coloured bars indicate stimulus and concentration to be added to each well at each round of stimulation.

2.6. Animal husbandry

The transgenic model used in this study is the Fischer 344 (d2eGFP-hPRL 455) rat, developed by Dr. Sabrina Semprini to express a destabilised enhanced GFP under the control of the human prolactin promoter (Semprini *et al.*, 2009).

Animal studies were performed under UK Home Office license (project licence no 40/3296) following review by the University of Manchester Ethics Committee. Animals were housed in temperature (20±1°c) and humidity (50±10%) controlled

condition in a 12-hour light, 12-hour dark cycle. Animals had access to water and food (Beekay rat chow, Special Diet Service, Witham, UK) *ad libitum*.

2.6.1. Genotyping

2.6.1.1. DNA isolation

One to two ear snips per animal were incubated a 1.5 ml eppendorf in 300µl DNA extraction buffer (50 mM Tris/HCl pH8, 100 mM EDTA, 100 mM NaCl, 1% SDS) and 50 µg proteinase K until tissue was fully dissociated (1-2 days). After cooling, tubes were inverted 10 times and 100 µl of a 5M NaCl solution was added, before another 10 sets of inversions. Samples were centrifuged for 10 minutes at 13000 rpm and supernatants were collected in fresh eppendorfs. After the addition of 250 µl of isopropanol and another round of inversions, the samples were incubated for at least one hour at -20°c. After centrifugation and removal of the supernatant, the pellet was washed with 70% ethanol and left to air dry and later resuspended (left on bench overnight) in 50-100 µl sterile water. DNA concentrations were determined by a combination of gel electrophoresis and nanodrop and samples were diluted in sterile water to make 20, 25 or 50 ng/µl stocks for PCR.

2.6.1.2. PCR

PCR name	Primers	PCR target size in base pairs
D2eGFP	F- 5' - GACGACGGCAACTACAAGACC -3' R- 5' - ACTCCAGCAGCACCATGTGAT -3'	531
DEGFP (old)	F- 5' - CACAAGTTCAGCGTGTC -3' R- 5' - GATCCTAGCAGAAGCAC -3'	762
Rat rennin	F- 5' - CCTGGCAGATCACAATGAAGG -3' R- 5' - GCATGATCAACTACAGGGAGC -3'	c. 600

Table 2.2. Genotyping primers

The final PCR protocol for GFP genotyping was as follows: 2µl 10 x NH_4 Reaction Buffer, 0.3 µl dNTP mix, 1 µl 50 mM $MgCl_2$ Solution, 1.4 µl forward and reverse d2eGFP (Sigma Genosys) and rat rennin (Sigma Genosys) primers and 0.3 µl BIOTAQ™ (all except primers by Bioline). 18 µl of master mix and 2 µl of DNA were used per reaction. Amplifications were carried out in a TECHNE TC-512 using a three-step thermal cycling method which consisted of a 5 minute step at 94°c followed by 40 cycles of 94°c for 30s, 58°c for 30s and 72°c for 30 s and followed by a final extension at 72°c for 5 minutes. Samples were checked visually by SDS-PAGE on a 1.5% agarose gel with 1% ethidium bromide.

2.7. Cycle stage synchronisation and staging

2.7.1. Oestrous cycle staging

The duration of the oestrous cycle can vary greatly between strains of adult female rats (Mandl, 1951). It was therefore of importance to validate the duration and efficiency of the oestrous cycle in our Fischer 344 (d2eGFP-hPRL 455) rats prior to experimentation.

For three consecutive mornings during the week prior to the experiment, vaginal lining was collected from each rat with a plastic pipette filled with 1-4 ml of sterile water, by inserting the tip into the vagina. The vaginal fluid was placed on a glass slide and cell composition was examined under a light microscope to judge the stage of the cycle the rat was in (Marcondes *et al.*, 2002). Below (Figure 2.2.), a representation of each stage is shown (samples were collected, spun down and resuspended in residual supernatant, left to settle on a poly-L-lysine slide for 10-15 minutes before a coverslip was placed over the sample and images were taken under light microscope). Note that for each rat a new pipette and glass slide were used.

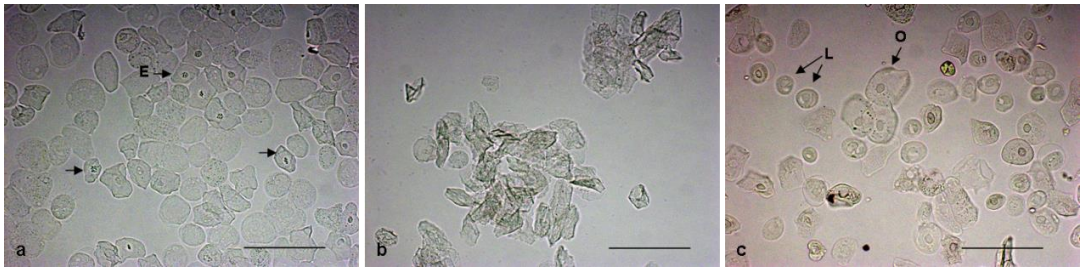

Figure 2.2. Cellular make up of vaginal lining at proestrus, oestrus and diestrus

*Light microscope micrographs show the characteristic cell combinations found in the rat uterine lining at proestrous (**a**), containing a high proportion of epithelial cells (E), as indicated by arrows, oestrous (**b**), characterised by cornified cells, clearly visible in this image and diestrous (**c**), which contains a combination of granulocytes, including leukocytes (L) and oesinophils (O). Scale bar = 10 µm.*

2.7.2. Synchronisation of the oestrous cycle

IP injection of luteinising hormone releasing hormone (LHRH) (Sigma-Aldrich) (200 µl of 20 mg/ml stock) was used to induce oestrous in transgenics. In order to synchronise animals into specific groups of oestrous cycle stages, the following schedule was used.

Injection time point : number of days prior to culling	Intended cycle stage
4.5	Proestrous
5	Oestrous
3	Diestrous

Table 2.3. Oestrous cycles induction scheme

2.7.3. Blood collection and serum analysis

After culling, blood was collected in serum collection tubes (Vacuette). Tubes are coated with microionised silica particles, which activate clotting when tubes are gently inverted. Vials were centrifuged at 15k rpm for five minutes. 200 µl serum was sent to Medical Research Council (MRC) Human Reproductive Sciences unit in Edinburgh, Scotland for serum prolactin measurement.

2.8. qPCR

2.8.1. Genomic RNA extraction

Pituitary tissue was stored in RNA *later* Solution (Ambion) and stored at -20ºc until needed. RNA was extracted using a Qiagen RNeasy mini kit, according to manufacturer's instructions. Briefly, buffer RLT with β-mercaptoethanol was added to tissue and homogenised using a 20-gauge (0.9mm) needle and a syringe. This was centrifuged for 3 minutes at maximum speed before 70% ethanol was added to the supernatant, which was then transferred to an RNeasy spin column, spun at 10k RPM for 15s and flow through discarded. The column was washed with RPE buffer and RNA was eluted using 30µl RNAse free water. This product was run on a gel to check quality.

In order to degrade any DNA contamination, samples underwent a RQ1 RNae-free DNase treatment (Progmega), according to manufacturer's instructions. In brief, RNA sample was added to 10µl RQ1 RNase-free DNase 10x reaction buffer, 2µl RQ1 RNase-free DNase 1µl RNasein and incubated at 37ºc for 30 minutes before the addition of 15µl RQ1 DNase stop solution and further incubation at 65ºc for 10 minutes.

RNA was further cleaned up on a spin column by adding RLT buffer and 100% ethanol, centrifuging at 10k RPM for 15s, adding RPE buffer and discarding flow through twice before elution of RNA in 50µl RNase free water. RNA was nanodropped to test concentration.

2.8.2. Conversion of RNA to cDNA

To convert RNA to cDNA, a Roche Transcriptor High Fidelity cDNA Synthesis Kit was used, according to manufacturer's instructions. 2µl oligoDT mix added to 1µg RNA and made up to 11.4µl with PCR grade water and incubated at 65ºc for 10 minutes in a thermocycler (Techne TC-512) for 10 minutes. Samples were cooled on ice before the addition of 4µl 5x RT buffer, 0.5µl RNAse inhibitor, 2µl 10mM dNTP mix, 1µl DTT and 1.1µl Transcriptor High Fidelity Reverse Transcriptase. Together this was incubated in the thermocycler at 29ºc for 10 minutes, 48ºc for 60 minutes, 85ºc for 5 minutes and the reaction was stopped by placing the samples on ice. Samples stored at -20º till needed.

2.8.3. qPCR

qPCR was carried out using SYBR®Green kit (Eurogentech) following instructions provided by the manufacturer. A master mix for the total number of reactions was made up, where one reaction contained 12.5µl 2x reaction buffer, 0.75µl SYBR green, 6.25µl water and 2.5µl forward and 2.5µl reverse primer. 0.5µl cDNA at a concentration of 200 ng, or water as a control, was added to each well. Three replicates were included for each condition.

The 96 well plate was placed in a thermocycler (StepOne Plus Real-Time PCR System, Applied Biosciences, held at 95ºc for 10 minutes before being subject to a PCR cycle of 40 cycles of 95ºc for 15s, 60ºc for 1 min before a melt curve analysis of one cycle of 95ºc for 15s, 60ºc for 1 min and 95ºc for 15s.

2.8.4. Primers

Below, is a table of primers used for qPCR. All were run through BLAST for analysis of secondary structure and run on sample cDNA. The GFP (2) and the two housekeeping genes, HPRT (Hypoxyanthine-guanine phosphoribosyltransferase) and calnexin, were found in literature from previous member of the lab and the prolactin primer was designed using a combination of ENSEMBLE, NCBI, primer 3, Vector NTI and BLAST softwares.

PCR name	Primers	PCR target size in base pairs
Prolactin	F- 5' - TGCAGATGAGAAAGCAGTGG -3' R- 5' - ACTCCTCCTGCTGATGATG -3'	120
GFP (2)	F- 5' - AGCAAAGACCCCAACGAGAA-3' R- 5' - TTCGTGACCGCCGCC -3'	60
HPRT	F- 5' - CAGGCCAGACTTTGTTGGAT -3' R- 5' - TCCACTTTCGCTGATGACAC -3'	115
Calnexin	F- 5' - GCATCATGCCATCTCTGCTA -3' R- 5' - GTCGTGGAATTGATCTAGGT -3'	163

Table 2.4. qPCR primers

Primers used for qPCR to look at the amount of endogenous rat prolactin mRNA as well as GFP marker for human prolactin mRNA in the rat pituitary. Sequences for the two selected housekeeping genes, HPRT and calnexin, are also shown.

2.9. Implantation of E_2 pump

2.9.1. Pump preparation

ALZET® micro-osmotic pumps (model 1004) were filled with 100µl E_2 (Sigma) dissolved in polyethylene glycol (PEG) (Aldrich Chemistry) according to the manufacturer's instructions, at a concentration of 125µg/kg/day. Control pumps were filled with PEG only. Pumps were left to equilibrate in sterile saline for 48 hours prior to implantation, in the dark at 37°c.

2.9.2. Implantation

ALZET® micro-osmotic pumps were implanted subcutaneously on the back of male Fischer 344 (455 d2eGFP-PRL) rats, as shown by the diagram in Figure 2.3.. Rats were anaesthetised with a combination of isofluorane and nitrous oxide (N_2O). Subcutaneous (SC) buprenorphine (Vetergesic, Hull, UK) [0.02 mg/kg] was used as analgesic.

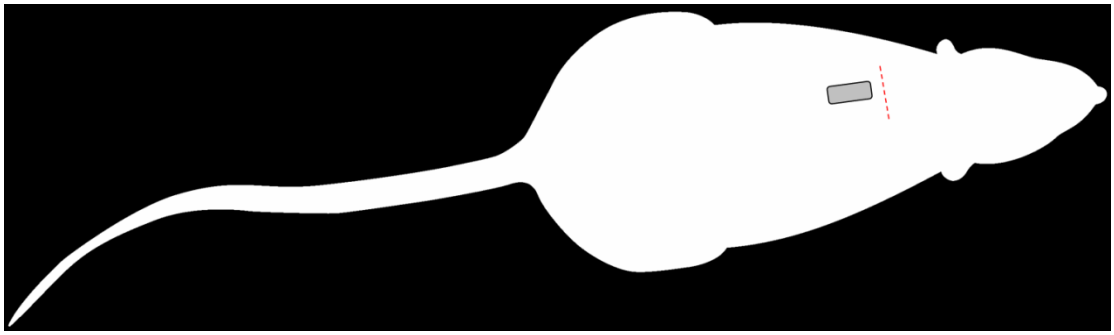

Figure 2.3. Positioning of ALZET® micro-osmotic E2 pump

2.9.3 Postoperative care

All rats were monitored postoperatively until fully recovered from anaesthetic and provided with ample feed and water as well as mash (hydrated dry feed). Weight was monitored regularly until day of culling, in particular for a drop to critical weight of -15%.

2.10. Live cell imaging

2.10.1. Fluorescence

2.10.1.1. Tissue culture and preparation

Rats were culled by exposure to N_2O followed by cervical dislocation. Trunk blood was collected for serum analysis. Pituitaries were resected from transgenic rats, washed in PBS, suspended in 4% low-melting agarose (Sigma) and sliced to 250µm thickness in the coronal orientation using a vibrating microtome (Campden Instruments).

Pituitary slices were placed on top of a Millicel (by Millipore) 0.4µm sterilised culture plate insert filter (CM low height), positioned in a 35mm glass-coverslip-based dish (Greiner) containing 1.3 ml primary cell culture media (DMEM supplemented with 4.5 g/l glucose, 10% Dextran-Charcoal treated FBS (Perbio Scientific), 50 µM Sodium Pyruvate (Sigma-Aldrich), 0.1µM Ultragluatime 1 (Lonza) and 500U

Penicillinstreptomycin (Lonza). Plates were sealed with a Breathe-Easy® air permeable membrane (Sigma-Aldrich) (Figure 2.4.).

2.10.1.2. Microscopy

Pituitaries, set up in a 35mm glass-cover-slip based dish as described above (2.10.1.1.), were images using a Carl Zeiss laser scanning microscope (LSM) 780 Microscope, LSM Pascal or LSM Excitor, all equipped with an incubator maintained at 37ºc, 5% CO_2 in humid conditions. Fluorescent images were taken with a Fluar 10x_0.5NA air objective (Carl Zeiss) with an 0.6/0.7x and 2x digital magnification for stills and time-lapse images, respectively. Time-course confocal images were obtained by z-stacking, with sequential images captured every 15 minutes using either ZEN2010 or LSM32, dependent on system used. At 24 hours of imaging,

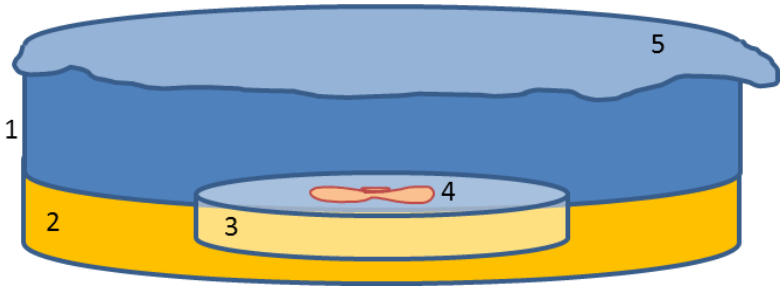

Figure 2.4. Experimental set up of pituitary slice tissue for fluorescence confocal live cell imaging

1. *35mm glass-coverslip-based dish* ***2.*** *Primary cell culture media* ***3.*** *Millicel filter* ***4.*** *250µm coronal pituitary slice* ***5.*** *Breathe-Easy® membrane.*

300µl medium was added to compensate for evaporation and at 48 hours, 300µl medium with FSK was added to the dishes giving a final concentration of 5µM, both by injection through Breathe-Easy® membrane. Prior to maximum projection stacking, optical slices were median filtered using a 5x5 kernel filter.

2.10.1.3. Cell tracking

Time course data from fluorescence microscopy was analysed using CellTracker software v.0.1 (Shen *et al.*, 2006). Single cells were selected and drawn around and manually tracked through the frames of the time course. Average intensity data was collected and normalised against an average of 10 'background cells', areas of tissue with little to no fluorescence signal.

2.10.2. Luminescence microscopy protocol

$2x10^5$ Bac 2 cells seeded into a 35mm glass-coverslip based dish (Greiner) in 1 ml standard culture media. Cells were left to adhere overnight, washed with PBS and media replaced with serum starved medium with 1mM luciferin and incubated for a further 24 hours. Media was replaced with medium containing either 10nM E_2 or equivalent volume of DMSO (as a control). The plates were covered with a Breathe-Easy® membrane and transferred to either of two incubators associated with microscopes. Images were obtained using a either a 20_0.75 NA objective and captured using a photon-counting charged coupled device (CCD) camera (Orca II; Hamamatsu Photonics) or 10_0.5 NA objective with 2x digital zoom, using a photon-counting Hamamatsu 2-stage VIM intensified camera. In both cases, sequential images were integrated over 15 minutes and analysed using Kinetic Imaging software AQM6 (Andor, Belfast, UK). Single cells were drawn around and mean intensity data was collected. Average instrument dark count (corrected from the number for pixels used) was subtracted from the luminescent signal.

2.11. Statistical analysis

2.11.1. Basic analysis and plotting of data

Basic analysis was done using GraphPad Prism6. For preliminary analysis, transcriptional 'peaks' were determined using an Area Under the Curve function. Data underwent 2^{nd} order smoothing to 10 neighbours. A peak is defined by a

crossing of the baseline, with the base line calculated for each cells to the average of the total cell fluorescence data. Peaks of less than 10% of the distance between the minimum to maximum light intensity were ignored.

2.11.2. Mathematical modelling

Algorithms for the mathematical modelling of transcriptional switches was carried out by Kirsty Hey at the University of Warwick.

Chapter 3

Results

Establishment of experimental models: the oestrous cycle and male E2 implants

Establishment of experimental models: the oestrous cycle and male E_2 implants

3.1. Introduction

3.1.1. Prolactin and oestrogen

Oestrogen is a well-known activator of the synthesis and secretion of prolactin and lactotroph proliferation (Freeman *et al.*, 2000). Oestrogen has been implicated in the pathophysiology of hyperprolactinaemia and in the development of prolactinomas (Heaney & Melmed, 1999). Serum prolactin levels follow the fluctuations of serum oestrogen (Neill, 1988). It is not, however, known if this surge in secretion is accompanied by a transcriptional surge, or if this is due simply to a release of stored prolactin protein into circulation.

17β-oestradiol (E_2), the most prominent of the oestrogens during the reproductive stage of the females, has been shown to stimulate lactotroph proliferation and prolactin gene expression (Amara *et al.*, 1987, Boockfor *et al.*, 1986, Shupnik *et al.*, 1979). E_2 exerts its genomic pituitary actions via the oestrogen receptor α (ERα), a ligand activated nuclear receptor, which resides in the cytosol and translocates to the nucleus upon binding (Scully *et al.*, 1997).

Adamson *et al.* showed in 2008 that E_2 acts through the ERα to activate the human prolactin gene transcription through a degenerate oestrogen response element (ERE) sequence found at -1189 bp relative to the transcription start site. Using GH3 cells stably transfected with a 5000-bp fragment of the human prolactin promoter linked to a luciferase reporter gene, authors found a 1.8-fold induction of prolactin gene transcription in the presence of 10nm E_2. A much larger transcriptional response is seen when the entire gene locus is included within a bacterial artificial chromosome (BAC) construct (Semprini *et al.*, 2009), suggesting the inclusion of multiple EREs.

3.1.2. Transgenic rat model

Lactotrophs have been shown to display heterogeneous patterns of prolactin transcription (McFerran *et al.*, 2001, Takasuka *et al.*, 1998). While most of this

research has been performed *in vitro* in the GH3 cell line, our lab aims to study prolactin transcriptional dynamics *in vivo*. In order to do this, Semprini *et al.* (2009) developed a transgenic Fischer 344 rat expressing a destabilised GFP (d2eGFP) (protein half-life of c. 2.5 hours) under the control of the human prolactin locus (Fischer 344 (d2eGFP-hPRL 455)). This model was generated using BAC recombineering using a 163 kbp fragment of the human prolactin genomic locus, which includes 115 kb upstream and 38 kb downstream of the prolactin gene.

Conventionally transcriptional activity has been explored using methods such as qPCR and ChIP. These techniques, however, only provide a static image of transcription. More recently, the development of fluorescent reporter genes has allowed the visualisation of temporal dynamics of transcription in stably transfected cells lines (Spiller *et al.,* 2010). Our Fischer 344 (d2eGFP-hPRL 344) model provides a novel system in which to study prolactin transcriptional dynamics in the context of intact physiology, providing a more representative insight into transcription dynamics *in vivo.*

3.2. Aim

The effects of oestrogen on the secretion of prolactin *in vivo* are well documented, as is the effect of oestrogen on prolactin transcription *in vitro.* In this project, I aimed to study the effects of oestrogen on prolactin transcription *in vivo*.

This chapter focuses on establishing a system in which to study the effects of oestrogen on prolactin transcription *in vivo*. For this investigation, Fischer 344 (d2eGFP-hPRL 455) transgenic rats expressing a destabilised form of GFP under the control of the human prolactin locus, were used, in two different physiological models.

In the first model, we studied the endogenous oestrogen fluctuations across the female oestrus cycle, analysing prolactin transcription levels at proestrus, oestrus and oestrus. With this we aimed to clarify transcriptional regulation under normal physiological conditions, across the relatively short time-scale of the 4-5 day oestrous cycle.

To model the effects of supraphysiolical levels of oestrogen on prolactin transcription while still being subjected to intact physiology, we have implanted male rats with a subcutaneous ALZET® micro osmotic pumps releasing a steady high dose of E_2 (125µg/kg/day in PEG 400) over a period of three weeks. These were compared to males with placebo (PEG 400 only) implants.

In both systems, circulating serum prolactin level was measured by ELISA. Single cell analysis of anterior pituitaries was carried out by flow cytometry to determine the quantity of expressed, and the proportion of cells expressing, the reporter gene. In addition to this, qPCR and immunofluorescence for d2eGFP and rat prolactin was carried out in all oestrogen states to compare the expression levels of the human prolactin reporter to the endogenous prolactin gene, giving an indication of whether the transgene gives a fair representation of physiological prolactin transcription.

3.3. Results

3.3.1. Validation of the oestrous cycle as a model for the effects of circulating oestrogens on prolactin transcription

To study the effects of endogenous fluctuations in oestrogens on prolactin transcription, we studied female rats across the oestrous cycle. Fischer 344 rats expressing d2eGFP under the control of the human prolactin promoter, were given an intraperitoneal injection of 40µg LHRH, forcing the cycle into oestrus (Walters *et al.*, 2008). Culling was timed at 3, 4.5 or 5 days post injection, to coincide with diestrus, oestrus and proestrus, respectively. Upon culling, serum was collected, for determination of serum prolactin. Pituitaries were harvested and either dispersed for analysis using flow cytometry or fixed for immunofluorescence or qPCR.

Serum prolactin levels were investigated by ELISA, performed by Dr. K. Niedsinska at the University of Edinburgh. Results from these analysis, collected over two separate experiments, showed median prolactin levels to be 310.8 (± 50.7, n=4), 456.4 (±77.8, n=6) and 141.0 (±78.0, n=6) ng/ml in proestrus, oestrus and diestrus, respectively (Figure 3.2.). Serum prolactin was found to be significantly higher at oestrus as compared to diestrus ($p<0.005$, unpaired t-test).

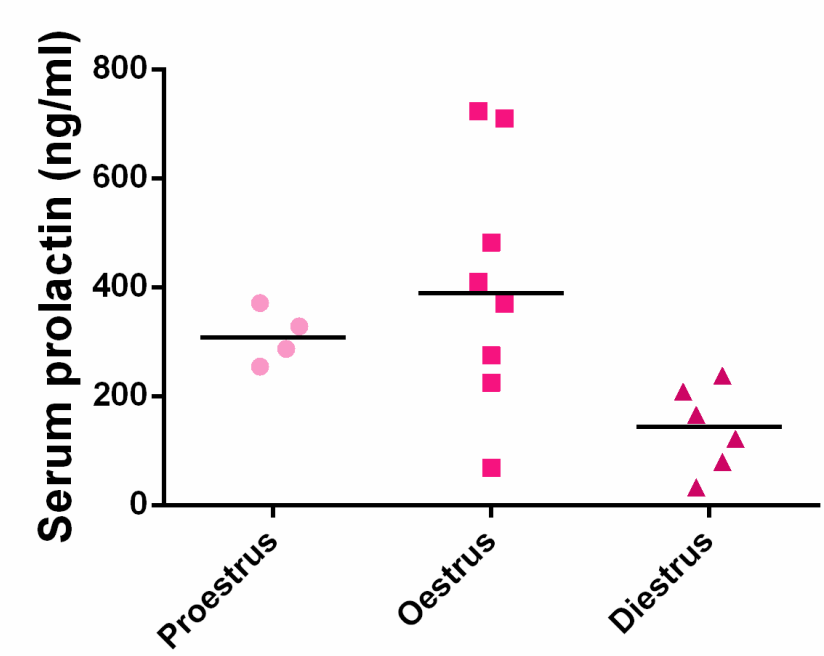

Figure 3.1. Serum prolactin across the oestrous cycle

Serum prolactin levels in ng/ml for each animal across the oestrous cycle, as measured by ELISA. Black lines indicate the median, measured to be 307.8 at proestrus, 409.9 at oestrus and 143.5 ng/ml at diestrus, with a significant difference in the means between oestrus and diestrus ($p<0.05$, t-test).

Flow cytometry results described are of data pooled from two independent experiments. Cells were gated on forward scatter and side scatter, as a measure of the size and granularity of the cells. Wild-type cells were used to establish autofluorescence levels and only transgenic cells with fluorescence above this were considered to be expressing GFP (Figure 3.2.). After gating and correction by subtraction of wild type values, the percentage of cells expressing the d2eGFP-hPRL construct in proestrus (n=2) was 21.84 % (SD ± 3.77) in oestrus (n=7) was 28.62 % (SD ± 6.46) and in diestrus (n=5) was 15.84 % (SD ± 3.91). A 1.8-fold increase in the proportion of cells expressing d2eGFP was found between diestrus and oestrus, deemed significant by t-testing ($p< 0.05$). The mean relative fluorescence was 271.89 (SD ± 57.9), 529.84 (SD ± 181) and 49.78 (SD ± 11.7), for proestrus, oestrous and diestrus, respectively. A 5.5-fold increase in fluorescence

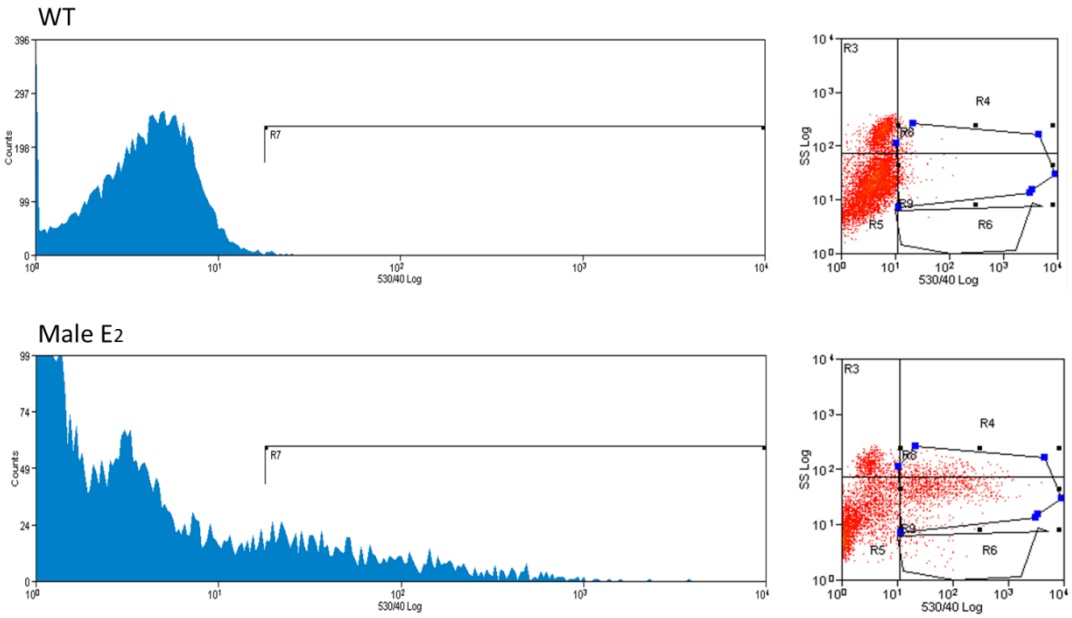

Figure 3.2. Sample of flow cytometry data

Sample of flow cytometry data from a wild type (WT) Fischer (top panel) and a male Fischer 344 (d2eGFP-hPRL 455) implanted with an ALZET® micro osmotic pump releasing E_2 for 21 days. In the left hand panels, the cell count is plotted against 530/40 Log fluorescence and on the leftthe side scatter is plotted against fluorescence. R7 and R4 indicate cells that are fluorescent in each case, respectively, showing gating against the autofluorescence of the wilt type.

per cell was found between diestrus and proestrus ($p<0.05$) as well as a 10.6-fold increase between diestrus and oestrous ($p<0.05$) (Figure 3.3.).

The increase in prolactin transcription between diestrus and oestrus was further validated by qPCR. d2eGFP expression was first detected at a δCT value of -1.26 and -3.32 in diestrus and oestrus respectively (n=9, 3x animal in given oestrus state x 3 repeats) calculated against the hypoxanthine phosphoribosyltransferase 1 (HPRT) housekeeping gene, indicating a 4.15-fold increase in d2eGFP expression between diestrus and oestrus (Figure 3.3. c.). Endogenous rat prolactin mRNA became evident at δCT -1.05 and -2.97, in diestrus and oestrus, respectively (n=9, 3x animal in given oestrus state x 3 repeats), as calculated against HPRT. This

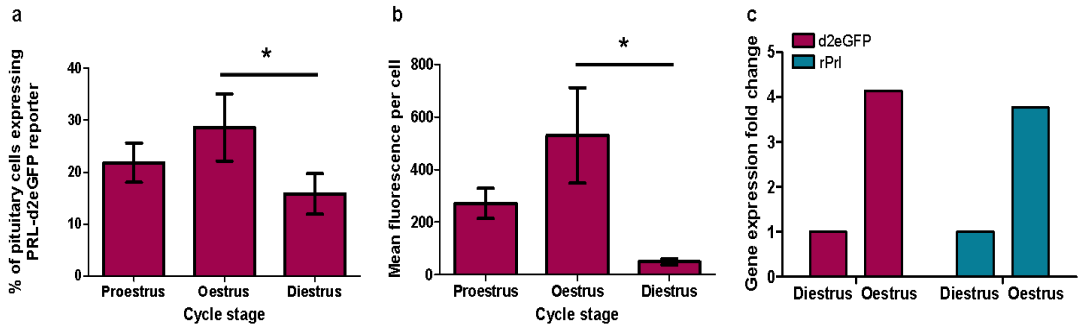

Figure 3.3. Flow cyctometry and qPCR validation of oestrous cycle model

***a**. Percentage of cells expressing d2eGFP in proestrus (n=2), oestrus (n=7) and in diestrus (n=5) (* p<0.05, ANOVA). **b.** mean fluorescence per cell of those expressing the construct (* p<0.05 ANOVA). **c.** fold changes in levels of d2eGFP (4.1-fold) and endogenous rat prolactin (Prl) (3.7-fold) mRNA between diestrus (n=3) and oestrus (n=3).*

indicated a 3.77-fold increase in endogenous rat prolactin in oestrus as compared to diestrus.

Pituitaries from females in each of the three stages of the oestrous cycle studied, were fixed for two hours in 4% paraformaldehyde (PFA), paraffin wax embedded, sectioned and stained for GFP and rat prolactin by immunofluorescence (shown in green and red, respectively in Figure 3.4.). Results indicated clear increase in the expression of d2eGFP from diestrus to proestrus, and again from proestrus to oestrus. Throughout the cycle endogenous prolactin protein staining appeared ubiquitously, with a higher level of staining towards the edge of the pituitary tissue. d2eGFP staining was widespread but less prominent towards the edges of the tissue and did not co-localise with prolactin protein. This could be an indication of a difference in location dependent functionality of lactotroph cells, with transcription occurring more actively towards the centre of the tissue and greater amounts of rat prolactin storage towards the periphery.

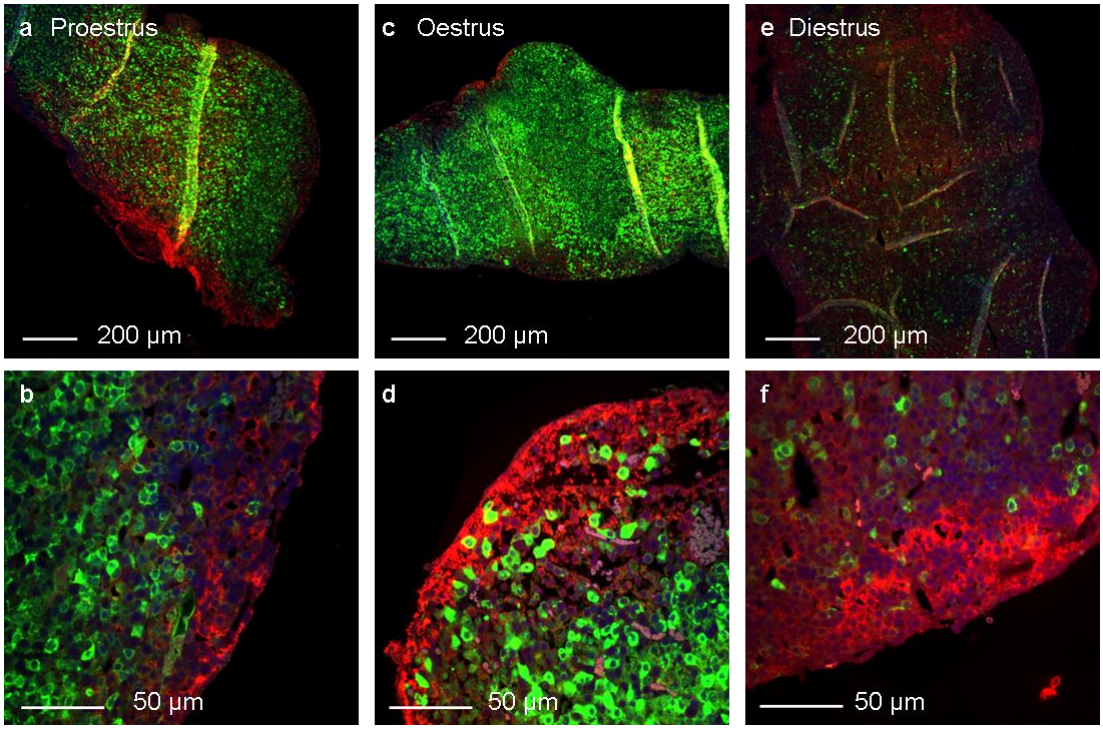

Figure 3.4. Immunofluorescent staining of Fischer 344 (d2eGFP-hPRL 455) anterior pituitaries at different stages of the oestrous cycle

*Representative micrographs of immunofluorescence staining for d2eGFP (green) and endogenous rat prolactin (red) in pituitary tissues harvested from female Fischer 344 (d2eGFP-hPRL 455) rats across the oestrus cycle. A clear increase in the proportion of cells expressing the prolactin reporter is evident between both proestrus (**a.** and **b.**) and oestrus (**c**. and **d.**) in comparison to diestrus (**e.** and **f.**). In both low and high power images, a preferential localisation of endogenous rat prolactin can be seen at the periphery of the tissue. Slides are counter stained with DAPI (blue).*

3.3.2. Validation of subcutaneous oestradiol implant in males

To study the effects of supraphysiological levels of oestrogen on prolactin transcription, we used a model in which male Fischer 344 (455 d2eGFP-PRL) rats were subcutaneously implanted with an ALZET® micro-osmotic pump. The pump released E_2 at a steady rate of 125µg/kg/day, maintaining a high level of E_2 in circulation over a period of 21 days. Rats implanted with E_2 releasing and control pumps were culled, pituitaries, testicles and serum were collected. Pituitary weights were found to increase by 2.5-fold and testis size halved in males treated with E_2 as

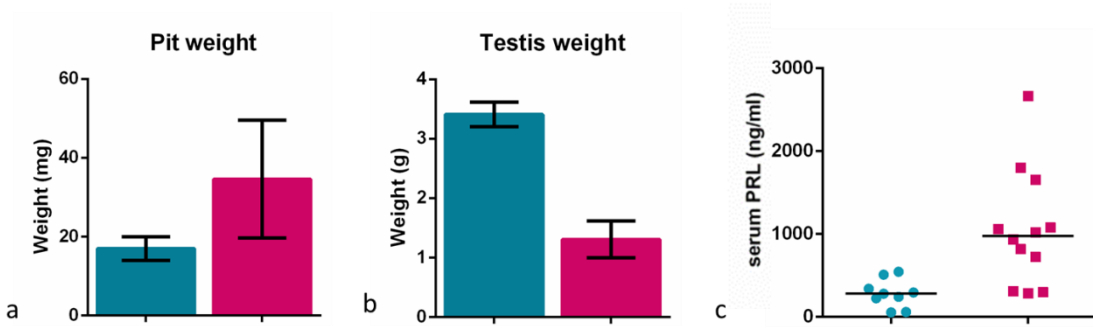

Figure 3.5. Validation of ALZET® micro-osmotic pump function

As a validation of the functionality of the ALZET® micro osmotic pump and to test that the E2 was having the desired effect, the pituitary wet weights of control and E2 treated males was recorded in ***a****., the testis weight is compared in* ***b****. and serum prolactin levels, as measured by ELISA is compared in* ***c****. Males with control implants had a median serum prolactin reading of 280.9 ng/ml as compared to the significantly higher value in males with E2 filled implants of 1041 ng/ml. All three measurements show a significant difference between control and treated males (p<0.05, t-test).*

compared to controls, indicating that E2 had the desired effect on lactotroph proliferation and anti-androgenic effects on the testes. Notably, serum prolactin increased by 3-fold. These results are summarised in Figure 3.5.

Pituitaries were dispersed and analysed using flow cytometry. The percentage of cells expressing the d2eGFP reporter for prolactin, increased from 1.59% (±1.58, n=3) to 8.27% (±0.41, n=3) in males treated with E2 ($p<0.05$). Mean fluorescence increased from 23.76 (±3.37, n=3) to 103.77 (±19.10, n=3) ($p < 0.02$). qPCR indicated σCTs of -2.29 and -3.45 for d2eGFP in control and E2 stimulated males, respectively, when compared to the housekeeping gene HPRT. Endogenous rat prolactin σCT increased from -2.29 to -3.47 in males treated with E2 (n=9, 3x animal in given oestrus state x 3 repeats). This was calculated as a 2.24 and 19.55-fold increase in mRNA expression in d2eGFP and endogenous rat prolactin, respectively. These results are summarised in Figure 3.6. Immunofluorescence shows increased staining for the reporter gene in males with E2 implants (Figure 3.7.) and serum prolactin analysis showed an increase in from 284.6 (±169, n=9) to

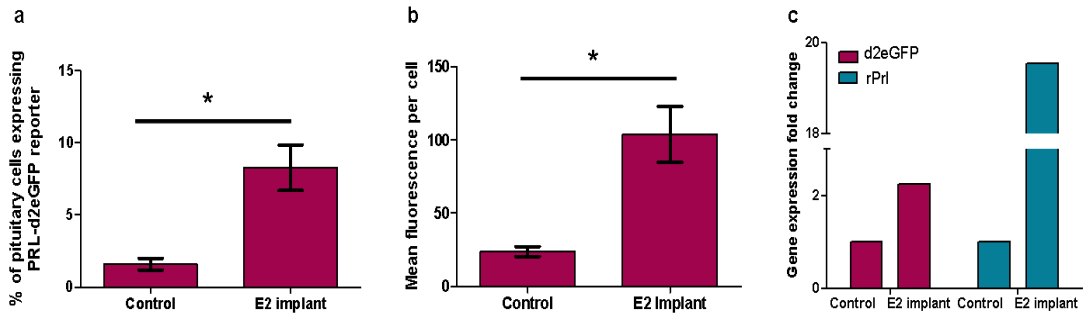

Figure 3.6. Flow cytometry and qPCR identify a significant increase in prolactin transcription in males subjected to chronic oestradiol stimulation

*In **a.** flow cytometry indicated an increase from 1.6 to 8.2% (n=3) of pituitary cells expressing the d2eGFP-hPRL transgene. **b.** indicates an increase from 23.8 to 103.8 relative fluorescence (n=3) in these cells (in both cases * p<0.05, ANOVA) **c.** shows fold changes in levels of d2eGFP (2.3-fold) and endogenous rat prolactin (Prl) (19.6-fold) mRNA between males with (n=3) and without E_2 pumps (n=3).*

1205.0 (±671, n=10), a significant difference (p<0.05, independent t-test) with a 4-fold induction in E2 treated males (Figure 3.5 c.).

3.4. Discussion

3.4.1. Validation of *in vivo* model

The aim of this PhD project is to study the effects of oestrogen on the patterns of prolactin transcription. To do this, we used a transgenic Fischer 344 rat expressing a destabilised form of GFP under the control of the human prolactin promoter. I used two physiological models, females across the oestrous cycle and males subjected to long term high doses of oestradiol supplied by a subcutaneous ALZET® micro osmotic pump. In the female model, I aimed to assess the effects of endogenous oestrogens on prolactin transcription and in the males I aimed to model a purer system, in which the effects of oestrogen are not subjected to a fluctuating basal level.

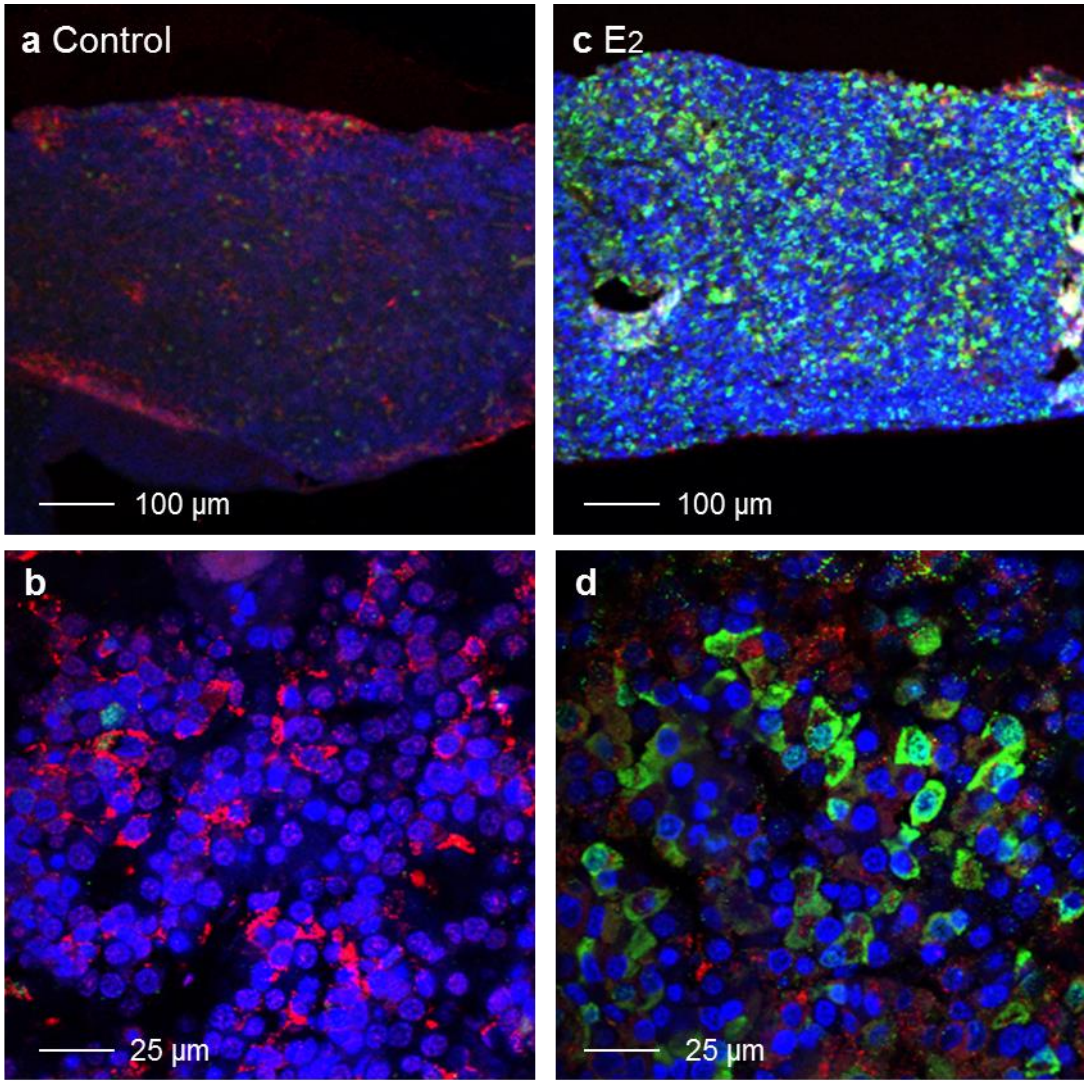

Figure 3.7. Male rats subjected to chronic oestradiol administration show an increase in prolactin gene transcription

Representative immunofluorescence micrographs, showing a marked increase in d2eGFP-PRL (green) expression in male rats when treated with suprahysiological levels of oestradiol for a period of 21 days (c. and d. as opposed to a. and b.). Red: endogenous rat prolactin, Blue: DAPI.

In this chapter, the aim was to set up and validate the above mentioned *in vivo* model. Subjects from each of the oestrogen states (female proestrus, oestrus, diestrus and male control and E_2 implanted) were subjected to serum prolactin

analysis and pituitary tissue was analysed by flow cytometry, qPCR and immunofluorescence to assess the expression of the prolactin reporter gene.

Serum prolactin was found to be significantly higher at oestrus as compared to diestrus ($p<0.005$, t-test). This result was reflected in the increase in d2eGFP expression found in immunofluorescence, qPCR and flow cytometry. Although changes in serum prolactin through the oestrous cycle are and well known (See section 1.5.7. Figure 1.5.), it was surprising to see such a robust change in transcription. Interestingly the pattern of changes in prolactin transcription through the cycle found here, does not reflect the changes in serum prolactin levels documented by Neill *et al.* (1988) and Ben-Jonathan *et al.* (2008), in which prolactin is highest at the end of proestrus. Serum prolactin remains slightly elevated during the first half of diestrus and drops to basal levels during the latter part of diestrus. The discrepancy between secretion and transcriptional timing, could be due to a replenishment mechanism, in which lactotrophs increase expression of the protein after a surge in secretion.

In males, those treated with oestradiol had a tripling in serum prolactin. Previous studies in our lab showed that three week treatment with the synthetic oestrogen Diethylstilbestrol (DES) induced a tripling of pituitary wet weight and a doubling of serum prolactin in female rats (Giles *et al.*, 2011). Oestrogen treatment in males as short as 5 days, has been shown to induce an accumulation of prolactin mRNA (Nogami *et al.*, 1985). By 14 days, mitotic activity is increased, although this is not strictly limited to lactotrophs (Nolan & Levy, 2009). In chronic oestradiol treatment of males, the proportion of lactotrophs in the anterior pituitary has been seen to rise from 24% to 42%, in particular, the proportion of the highly secretory subtype I lactotrophs increase from 45% to 81% (Takahashi & Miyatake, 1991).

In both the female and the male models, we see an increase in the d2eGFP-hPRL reporter gene expression in the higher oestrogen states ie. in oestrus as opposed to diestrus and in males with as compared to those without E_2 implants. This is seen, not only on a tissue scale in qPCR, but also on a single cell level by flow cytometry and immunofluorescence, where, not only do we see an increase in the number of cells expressing the transgene, but also an increase in expression per cell.

	Proestrus		Oestrus	Diestrus	
PRL transcription	↑		↑↑	↓	
Serum Prl (ELISA)	↑		↑↑	↓	
	Early	Late		Early	Late
Serum Prl [1]	↑	↑↑	↓	↓	↓↓

Table 3.1. Comparison of the timing of prolactin transcription and prolactin secretion

Changes of levels of prolactin transcription compared to serum levels obtained by ELISA and to data from literature (1 - Neill et al*., 1988).*

The induction of prolactin transcription by oestrogen is not in itself a novel finding, but what this does tell us is that our *in vivo* prolactin transcription reporter responds to oestrogen and reflects the action of the endogenous rat prolactin gene. This model should thus give a faithful representation of how the human prolactin gene locus responds to oestrogen *in vivo,* within the pituitary.

3.4.2. Heterogeneity and lactotroph localisation

In the female model, immunofluorescence showed an increase in d2eGFP prolactin reporter expression in the two higher oestrogen states, proestrus and oestrus as compared to diestrus. In males, reporter expression is increased with E_2 treatment. Notably, whilst endogenous rat prolactin is expressed throughout the pituitary tissue, staining appeared to be more pronounced at the periphery of the tissue (Figures 3.4. and 3.7.). Additionally, the transgene expression was decreased towards the periphery of the tissue.

A morphological and functional heterogeneity of lactotrophs has been described. In 1997 three subtypes of lactotrophs were classified, based on abundance and size of the granules. Type I lactotrophs have the least abundant and largest granules (>500nm in diameter), type II lactotrophs have 150-250nm granules, and type III cells have the smallest granules (100nm) (DePaul *et al.*, 1997). In 2005, an intermediate lactotroph was discovered, between types I and II, which act as a bihormonal mammosomatotroph (Huerta-Ocampo *et al.*, 2005). In addition to this, two forms of prolactin protein have been found to exist, a monomeric form which

was found to be loosely associated with organelles involved in its synthesis, and polymeric prolactin, found in secretory granules (DePaul *et al.*, 1997).

With a functional heterogeneity between lactotrophs and furthermore, between molecular forms of prolactin, it may be possible that we are seeing a spatial organisation of this heterogeneity, with more highly granulated cells located towards the periphery of the tissue. Or alternatively, centrally located lactotrophs may actively transcribe and translate monomeric protein for regular cyclical secretion while peripheral cells store polymeric prolactin for response to acute emergency signals.

It should be noted that the phenomenon of the endogenous rat prolactin being ubiquitously expressed throughout all cells within the pituitary tissue of females, as seen Figure 3.4. f., is unexpected, as prolactin producing cells should account for only roughly 50% of the cells within the pituitary (DePaul *et al.*, 1997). This may be due to disruption of cells during sectioning.

3.4.3. *In vitro* model of prolactin transcription

In addition to setting up an *ex vivo* model of the effects of oestrogen on prolactin transcription, an *in vitro* model was devised to test the hypothesis of oestrogen having a molecular priming effect on the chromatin structure of the prolactin gene. In parallel dishes, GH3 cells expressing luciferase under the control of a 5 kbp fragment of the human prolactin promoter were subjected to either E_2 or a DSMO control for 24 hours and then FSK for a further 24 hours, both were imaged using time lapse luminescence microscopy. We aimed to compare single cell luminescence patterns between the cells that had been pre-treated with E_2 and the controls to find any discrepancies in these patterns. Due to difficulties with establishing the model and inconsistent preliminary data, this project was not pursued to completion and is thus not covered in the body of this thesis. For preliminary experiments and setup information, please see Appendix A.

3.4.4. Effects of oestrogen on prolactin transcription patterns

To study the effects of oestrogen on prolactin transcription *in vivo*, we have used the d2eGFP-hPRL expressing Fischer rat and looked at expression throughout the oestrous cycle and in males treated with chronic oestradiol. Prolactin reporter

transcription was found to be significantly increased in higher oestrogen states ie. in females at oestrus as opposed to diestrus and in males with E_2 implants as opposed to control males with sham implants.

Prolactin transcription has been shown to occur in cycles of high and low expression. In primary cultures of adult rat tissue, these cycles displayed a predominant length of approximately 11 hours, and binary switch modelling of 'on' and 'off' periods suggest a minimum 'off' time of 3 hours (Harper *et al.*, 2011) (for further information see section 1.7.2.) . Knowing that oestrogen has an effect on the over all levels of prolactin transcription, this begs the question of whether oestrogen has an effect on the pattern of these cycles. For example, if transcription occurs in cycles with a definite peak and trough in prolactin mRNA production, does the cycle length increase if the animal is in a higher oestrogen state in order to allow the cell to generate increased synthesis and secretion? Or does the peak reach a higher amplitude, or do peaks occur more frequently? With a validated model in place, we now set out to answer questions about the timing and mechanisms of how oestrogen effects prolactin transcription.

Chapter 4

Results

Effects of oestrogen on prolactin transcription cycles

Effects of oestrogen on prolactin transcription cycles

4.1. Introduction

Mammalian genes, including the prolactin gene, have been shown to be expressed in transient pulses known as 'transcriptional bursts' (Newlands *et al.*, 1998, Raser & O'Shea, 2004, Shorte *et al.*, 2002, Suter *et al.*, 2011a). The development of reporter genes and live-cell microscopy has enabled the real-time visualisation of gene transcription.

Using our well established model, the Fischer 344 (d2eGFP-PRL 455), which expresses a destabilised GFP reporter gene under the control of the human prolactin locus (Semprini *et al.*, 2009), our lab has identified short term stochastic prolactin gene expression in dispersed lactotrophs, which together, in the context of intact tissue, display a long-term and long-range coordinated behaviour (Harper 2010). Furthermore, we have seen that patterns of transcriptional pulsatility change according to developmental stage (Featherstone *et al.*, 2011).

The aim of this chapter was to understand the effects of oestrogen on temporal patterns of prolactin gene transcription *in vivo.* To do this we have looked at Fischer 344 (d2eGFP-PRL 455) rats, in different oestrogen states in combination with live-cell time-lapse fluorescence confocal microscopy. Two models were used: in the first model, we studied the effects of endogenous oestrogen on the transcription of human prolactin, by comparing the single cell fluorescence patterns between females at diestrus and oestrus. In the second model, we studied the fluorescence patterns in males implanted with ALZET® micro osmotic pumps releasing either a high dose of E_2 over a period of 21 days, or a control pump.

4.1.1. Fluorescence microscopy

Typically, a molecule will exist in its lowest energy state. A molecule may absorb a photon of light (for example blue light), which will increase the energy state of that molecule, causing an electron to jump to an excited level. Usually this energy will quickly dissipate (within 8-10 seconds) through collisions with surrounding molecules, dropping the electron back to a lower energy level. If the surrounding molecules are not able to accept the larger energy difference needed to further

lower the molecule to its ground state, it may undergo spontaneous emission, emitting light of a longer wavelength (for example green light), as is the case in the green fluorescence protein (GFP).

In conventional fluorescence microscopy light travels through an excitation filter of a defined bandpass (usually between 445 to 515 nanometers), to the dichroic mirror. This selectively reflects light of a shorter wavelength down into the objective (Figure 4.1.). This will excite the fluorochrome within the tissue, and the emitted light of a longer wavelength passes back through the objective and the dichroic mirror. Here the mirror will reflect most of the contaminating excitation light back to the source whilst allowing emission wavelengths to pass through to be further purified by an emission filter, set to a predefined bandpass, typically 515 to 565 nanometers, corresponding to green visible light. This purified light signal travels to the eyepiece or the detection system (Semwogerere & Weeks, 2005).

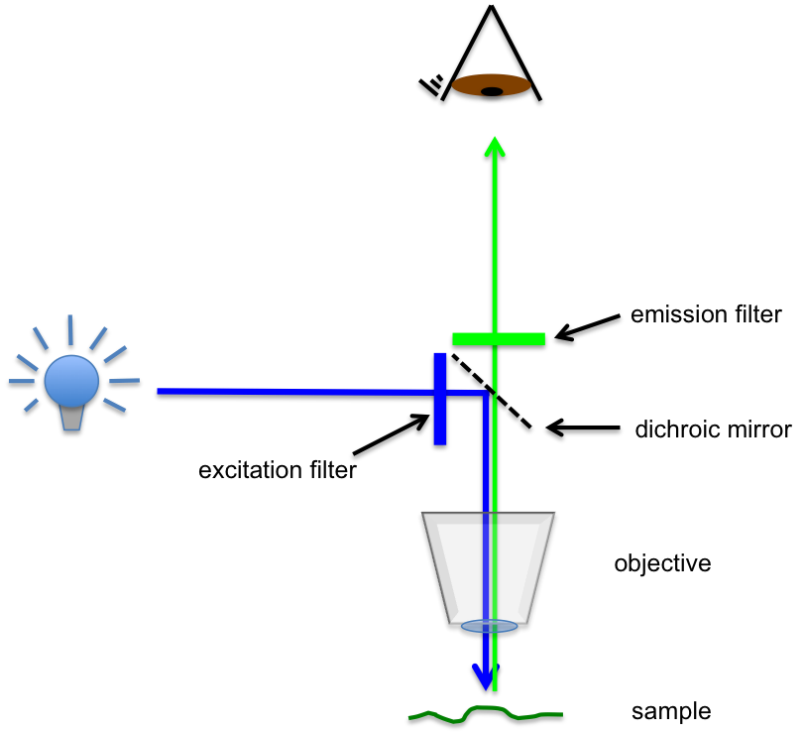

Figure 4.1. The basic concept of fluorescence microscopy

Light from the source passes through an excitation filter, to the dichroic mirror, reflects shorter wavelengths through the objective to the sample. Fluorophores within the tissue are excited and emitted light is passed back through the emission filter to the eye. ***Adapted from Semwogerere and Weeks 2005.***

4.1.2. Confocal microscopy and optical imaging

Confocal microscopy is an imaging technique pioneered in 1955 by Marvin Minsky. Light is focused to sequential points across a specimen. This light is then collected by a photomultiplier tube (PMT) after the elimination of out of focus light by a pinhole. An image of the specimen is gradually built up using a long-persistence screen.

Modern confocal microscopes are based on the same principle. Improvements in optics and electronics have significantly improved imaging quality, speed and storage. Furthermore, the combination of confocal with fluorescence microscopy has enabled the localisation of structures and proteins of interest within the specimen (Semwogerere & Weeks, 2005).

In essence, the confocal system works with two lenses that focus the light from the focal point of one lens to the focal point of the other (right hand panel of Figure 4.2.). One lens allows the light to be focused on a particular focal point of the specimen, with the help of a pinhole, while the second allows the emitted light to pass through another pinhole prior to the detection equipment, rejecting background and out of focus light, creating a sharper image. By enabling the focusing onto a focal point within a tissue specimen, an optical slice of the specimen is created. By obtaining sequential slices through the tissue, in what is called a Z-stack (left hand panel of Figure 4.2.), one can then create a 3-D image of the specimen.

4.1.3. Our systems

Two imaging systems have been used for the purpose of these experiments. The Zeiss LSM 5 Pascal and LSM 780 (Figure 4.3.) inverted laser scanning microscope systems. Both have an incubator fitted to the sample stage (Figure 4.4) to enable time-lapse live cell imaging. Imaging is controlled using the Zeiss ZEN 2010 or LSM 32 software, for the LSM 780 and Pascal, respectively. Using this system we can control imaging parameters. These include the focus, the number of optical slices in the z-stack and their position within the sample, the detector gain (the sensitivity threshold of the PMT), the amplifier gain (increases the amplitude of the signal going to the detector), pinhole size, which determines the amount of light reaching the detector and the scan speed (the longer the scan, the better the definition of the

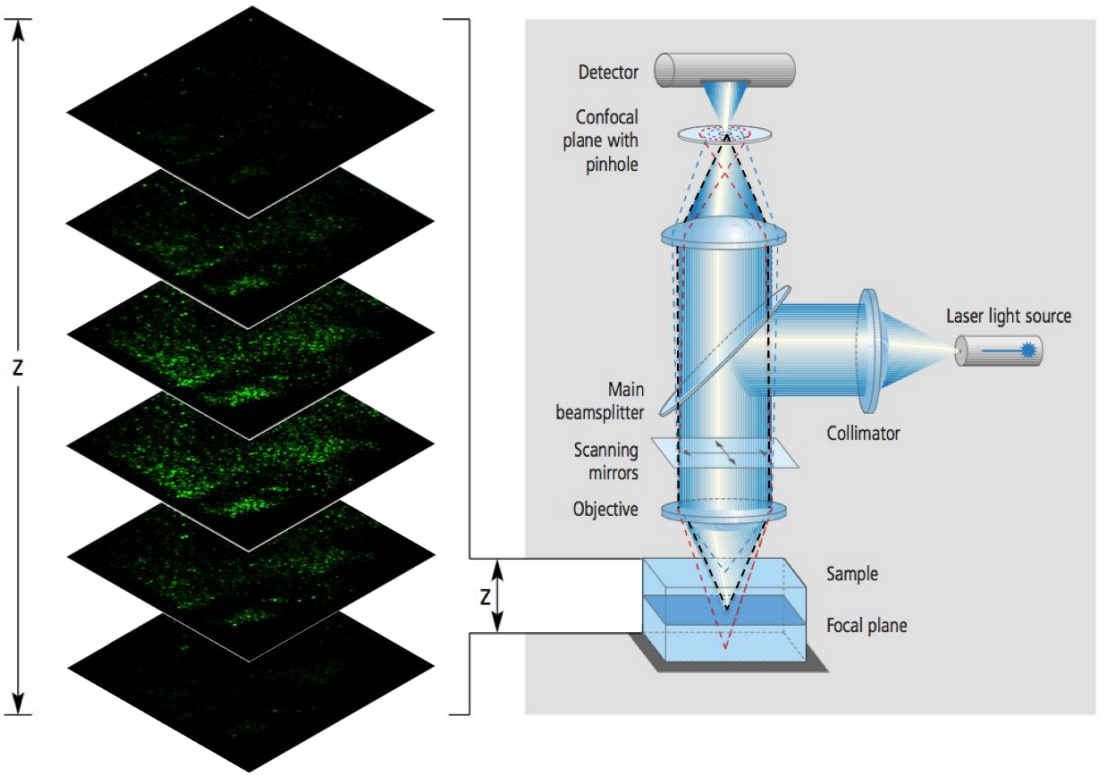

Figure 4.2. Concept of confocal microscopy based on the Zeiss Pascal Scanning Laser Microscope

Light from the source is filtering through the dichroic mirror (see right hand panel), reflected down the lens towards the specimen. The black dotted lines indicate where the lower lens has focused the light, or the focal plane. Emitted light from the specimen passes back up through the lower lens and is condensed at the second higher lens and filtered through a pinhole before the detector. The image from a particular focal plane is referred to as an optical slice. By changing the focus of the light through the z-plane of the specimen, we can collect multiple optical slices, or a z-stack, which can give an indication of the 3D structure of the tissue (see left hand panel). Red and blue dotted lines indicate light that is out of focus and is filtered out by the detector pinhole. ***Adapted from Ziess.com.***

image). All of the above determine the clarity of the image. Using the ZEN 2010 or LSM 32 software, we can also determine the time course, ie. duration of imaging and the imaging frequency, which in this case is 2 x 24 hours with an interval of 15 minutes between collection of complete z-stacks.

Figure 4.3. The LSM 780 confocal microscope at the Systems Microscopy Centre at the University of Manchester

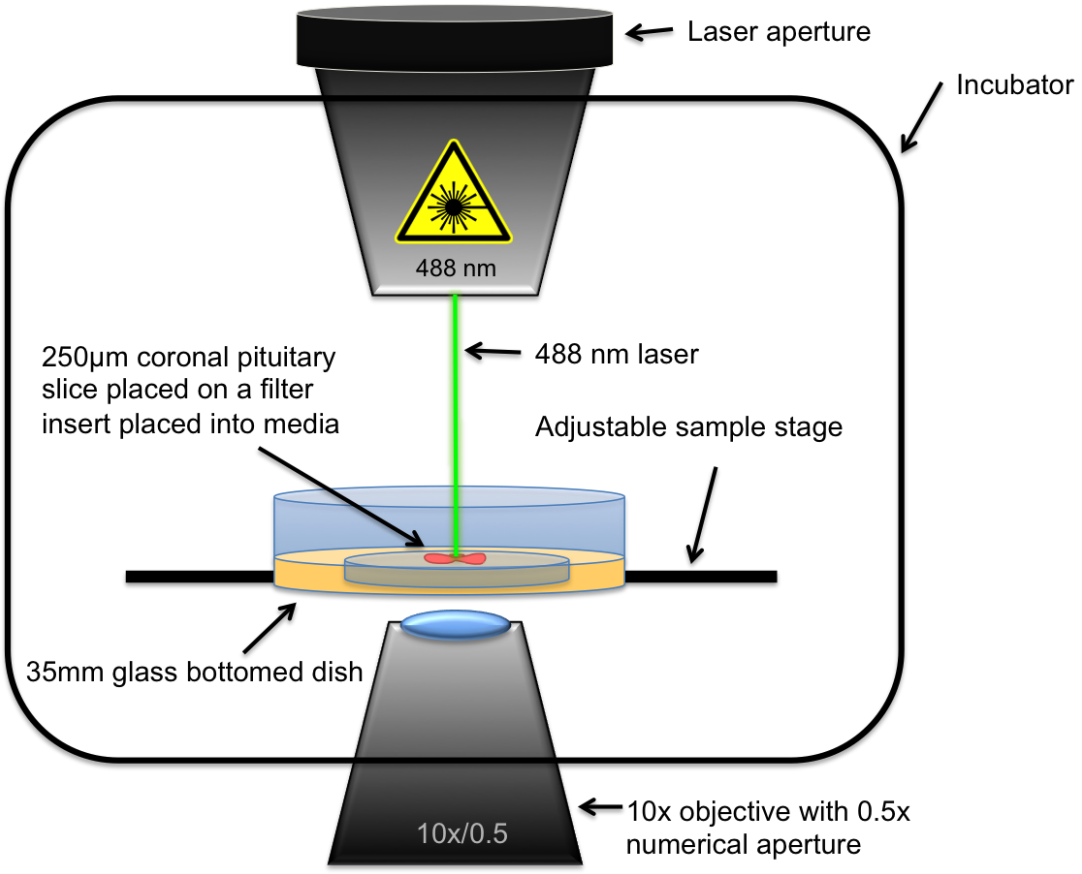

Figure 4.4. LSM 780 and LSM 5 Pascal inverted tissue imaging setup

Representative setup of tissue imaging. The tissue is placed on a MilliPore 0.4 µm filter in a 35 mm glass bottomed dish on an adjustable sample stage housed within an incubator keeping the tissue at 37°C and 5% CO_2. The light source comes from above the sample and the light emitted is collected through the objective below the sample. The objective in an inverted set up such as this one is situated directly underneath the glass bottom of the 35mm dish.

4.2. Optimisation of tissue culture for live cell imaging

To obtain optimal fluorescence time-lapse confocal microscopy, several systems were tested. Initially, a 400µm coronal pituitary slice was placed directly into a 35mm glass bottomed dish, submerged in medium and housed within the incubator associated with the microscope. In this culture setup, a large amount of tissue death was seen. It was thought that this may be due to either a lack of fresh medium, or from the inability of media to reach the side of the tissue in direct contact with the glass of the dish. In addition to this, there was a problem of movement of the tissue, which made tracking of single cells impossible.

Several methods of securing the tissue were experimented with, including the coating of the plate with poly-L-lysine and medical tissue glue. A perfusion system method was used, which in hypothesis, should prevent tissue movement by securing it between two covers slips, whilst providing a constant perfusion of fresh medium. All of the above however, lead to tissue death, as shown by propidium iodide (PI) testing (Figure 4.5.).

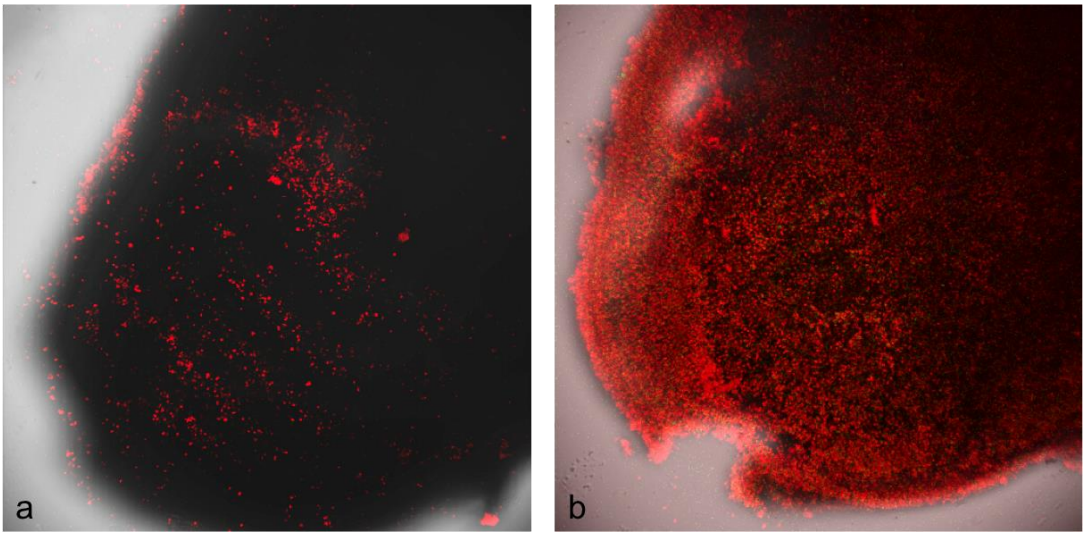

Figure 4.5. Comparison of cell viability in tissue pituitary slice kept in an incubator and in a perfusion chamber

A comparison of two PI stained 250um coronal pituitary slices from a wild-type female rat at oestrus. The tissue in ***a.*** *remained in a dish with 3ml media in an incubator. The tissue in* ***b.*** *was housed in a perfusion chamber system on the LSM 780 for 18 hours. Cells stained red with PI are dead.*

To provide the section of tissue adjacent to the objective with medium, 250µm coronal pituitary slices were elevated by placement on a Millipore plate insert filter. Medium was reduced from 3 to 1.3mls, filling the plate up to the level of the filter, providing the tissue with nutrients but reducing the probability of tissue movement. This did however pose the problem of the tissue drying out due to evaporation. The dish was covered with a BreatheEasy® polyurethane membrane, which allowed the diffusion of air into the dish, whilst reducing evaporation. After 24 hours of imaging, 300µl of medium (calculated to be the amount of evaporation over a 24 hour period) was injected through the membrane. A limited evaporation was inevitable, bringing the tissue out of focus in the z plane. To counteract this, a larger imaging stack had to be obtained, in order to be able to track single cell fluorescence activity over the full 48 hours period. Cells were found to still be viable at the end of the 48 hour imaging session by stimulation with forskolin.

After the initial optimisation was carried out, each imaging session was named by a unique data set (DS) number. These are listed in Appendix B. The data sets chosen for imaging are shown in Figures 4.6. and 10., for females and males, respectively. These were chosen for cell tracking due to stability and viability of the tissue and signal quality of the images.

4.3. hPRL-d2eGFP transgene expression across the oestrous cycle

To study the effects of endogenous fluctuations of oestrogen on human prolactin transcription, we studied the expression of the d2eGFP reporter for human prolactin transcription across the oestrous cycle of transgenic Fischer 344 rats. Z-stacks of 250 µm coronal pituitary slice preparations from animals in diestrus and oestrus were taken at 15 minute intervals, unstimulated for a period of 48 hours and then with FSK for a further 8-16h as a viability test. Two identical dishes were set up per imaging session and data was collected from two microscopes. In total three imaging series were collected from each tissue, focusing on an edge and a central region using the LSM 780 and a single location on the Pascal system. Time-lapse imaging is acquired with a Fluar 10x_0.5 NA objective and 2x optical zoom.

In an effort to promote comparability between data sets, the imaging settings (detector gain, amplifier gain and offset, pinhole size, optical slice and scan speed)

was kept as consistent as possible between tissues from the same oestrogen state. This was, however, difficult due to differing power of the laser depending on its usage, as well as inter-tissue fluctuations in fluorescence levels. There is also of course inter-microscope variation in laser power and imaging quality.

The four most consistent 48 hour imaging periods were chosen for cell tracking. This decision was based on cell viability, consistency of focus and least movement of tissue (for ease of tracking). An example of the location of imaging within the pituitary tissue is shown in Figure 4.6. and stills from the time lapse files chosen for cell tracking in females in diestrus and oestrus are shown in Figure 4.7.

Seen through the eye piece of the microscope, it is clear that there is more fluorescence in oestrus as compared to diestrus. For the purpose of time-lapse imaging, each microscope was up in such a way that little to no fluorescence is seen at time 0h, but that enables the detection of fluorescence dynamics in later hours of the time series (this is discussed in section 4.4.3.). In both high and in low oestrogen states, a surge in fluorescence activity is seen between 10 and 20 hours. This is most likely due to the release of prolactin transcription from the suppression normally experienced *in vivo* from the effect of hypothalamic dopamine. After this initial apparently coordinated increase in signal, fluorescence patterns of single cells diverge and seem to display cycles of gene activity.

The fluorescence of 100 cells from each time series were tracked and analysed using CellTracker. A central region was preferentially picked for tracking, due to high reporter staining seen by immunofluorescence (Figures 3.4 and 3.7.). To analyse patterns in reporter gene cyclicity, area under the curve function was used to determine the number of fluorescence peaks seen in each cell over a period of 48 hours. Results are displayed in Table 4.1., Figure 4.8. and Figure 4.9. Interestingly, the patterns of fluorescence activity do not differ between the high (oestrus) and low (diestrus) oestrogen states. No distinctive difference was seen in the number of peaks in fluorescence, or distribution of amplitudes or duration of peaks.

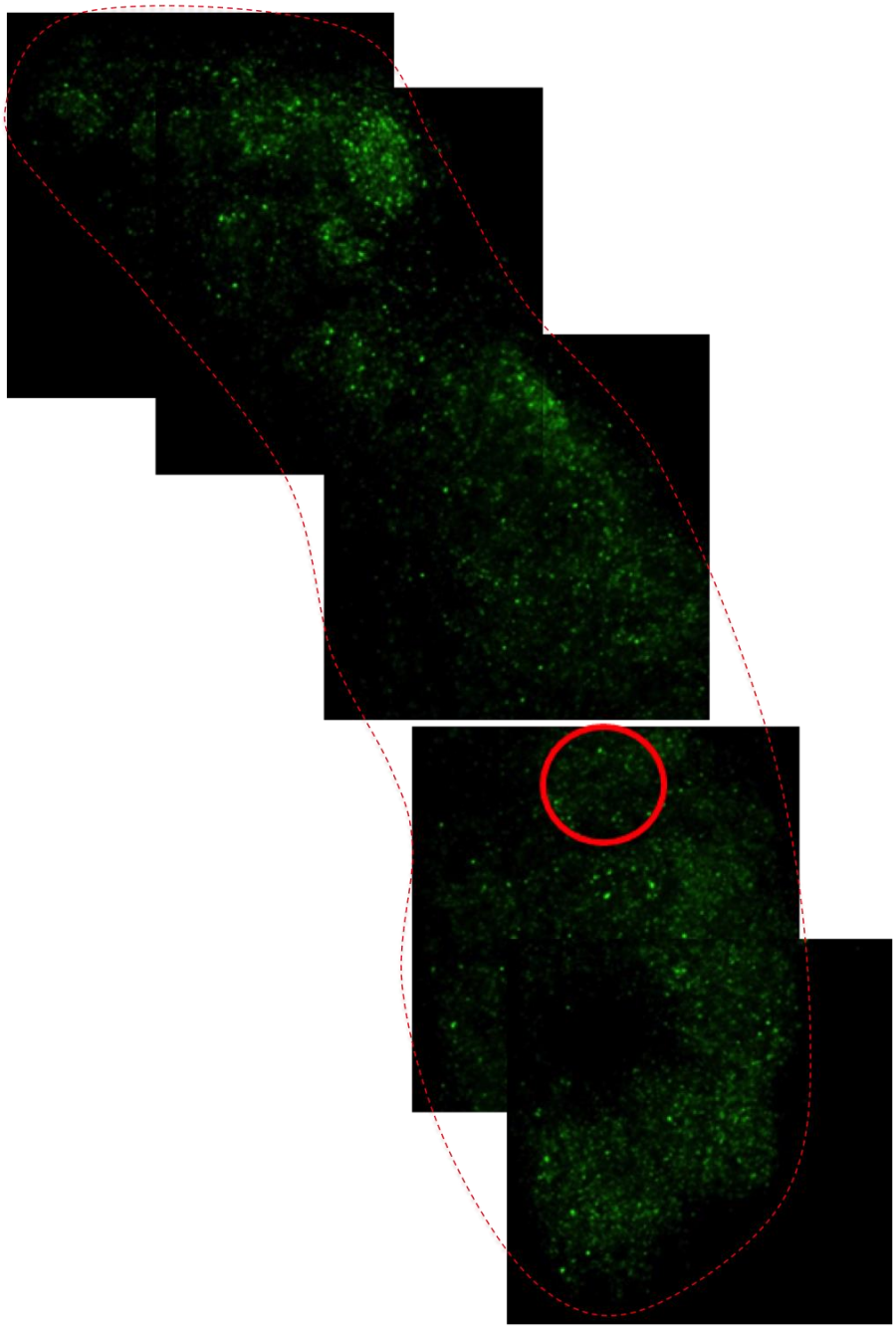

Figure 4.6. Composite image of 250 µm coronal pituitary slice at 0h of a 48 hour imaging series

Montage of maximum projection micrographs of a 250µm coronal pituitary slice on the LSM 780 at time 0h before 48h imaging. Gain set in order to show fluorescence in lactotrophs, which is later adjusted in order to capture fluorescence dynamics. Red circle indicates approximate location of imaged section of this particular pituitary slice from an oestrus female (DS18). Images taken with 10x_0.5 NA objective at 0.6x optical zoom.

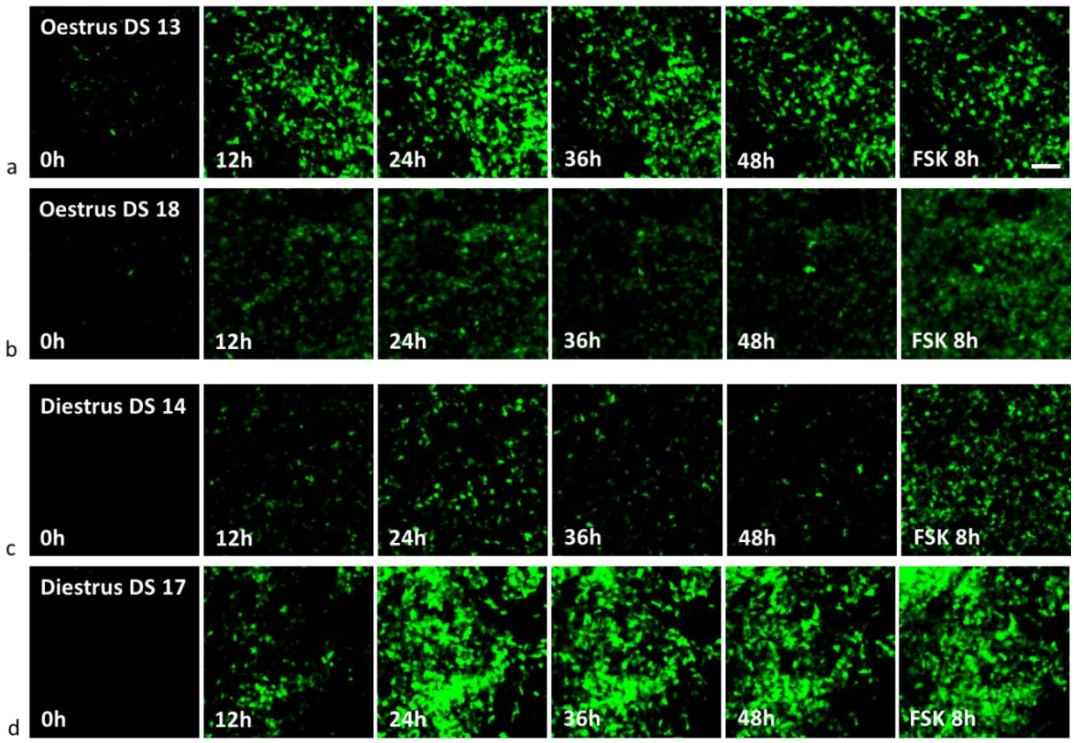

Figure 4.7. Time-lapse imaging of 250 µm coronal sections of Fischer 455 (d2eGFP-hPRL 344) female rats at oestrus and diestrus, selected for cell tracking

Stills at 12 hour intervals from 48 hour time lapse and after 8 hour FSK stimulation to show tissue viability. Panels ***a.*** *and* ***b.*** *show data sets from two tissues in oestrus and* ***c.*** *and* ***d.*** *from tissues in diestrus. Scale bar indicates 50 µm.*

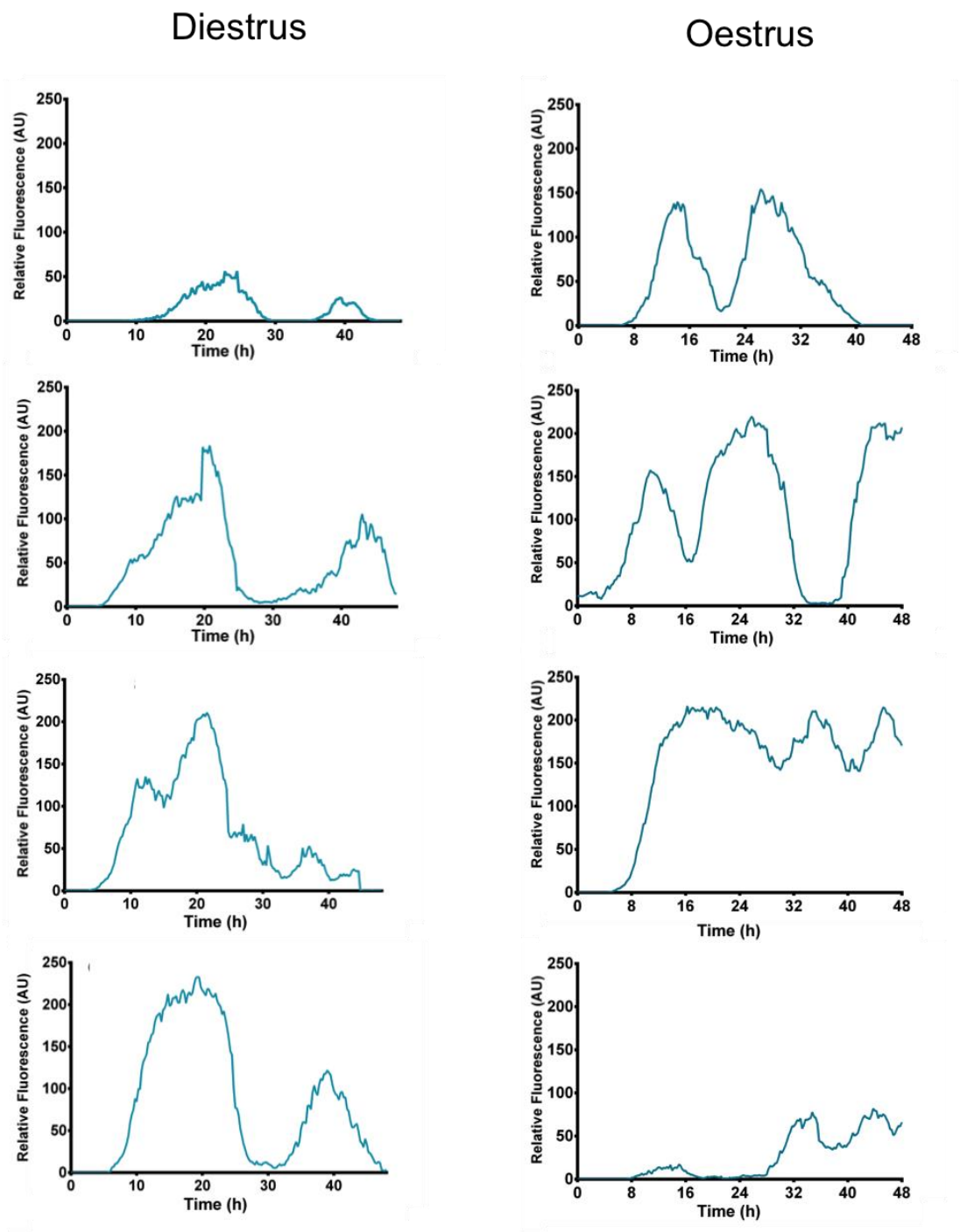

Figure 4.8. Single cell fluorescence patterns from diestrus and oestrus

Fluorescence traces of individual lactotrophs expressing d2eGFP under the control of the human prolactin promoter over a period of 48 hours. On the left, four cells from animals at oestrus and on the right, four from diestrus. The x-axis denotes time and the y-axis denotes raw relative fluorescence.

Percentage of cells displaying given number of fluorescence peaks over 48 h				
Number of peaks in fluorescence	**Diestrus (DS 14)**	**Diestrus (DS 17)**	**Oestrus (DS 13)**	**Oestrus (DS 18)**
1	75	64	51	71
2	23	36	37	26
3	2		11	2
4			1	1

Table 4.1. Distribution of fluorescence peaks across the oestrous cycle

The fluorescence of 100 individual cells was tracked over 48 hours in two examples of pituitary slice preparations in diestrus and two in oestrus (DS 14 and 16 and DS 13 and 18, respectively). Peaks in fluorescence activity were determined by area under the curve (AUC) analysis and results are plotted above.

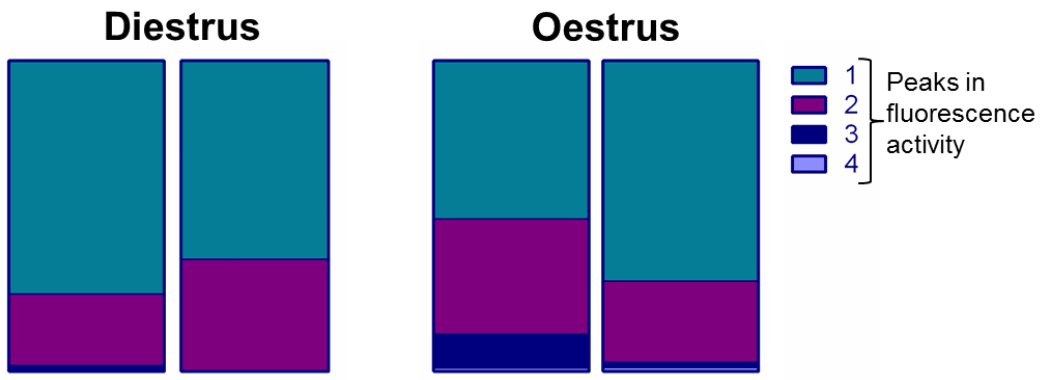

Figure 4.9. Distribution of fluorescence peaks across the oestrous cycle

Data from Table 1, plotted as a histogram. Each histogram represents the proportion of the 100 cells tracked, displaying one to four peaks in fluorescence activity, as defined by AUC analysis. On the left, two examples of pituitary slice preparations from rats culled in diestrus and on the right, two culled in oestrus. See legend for colour classification.

4.4. hPRL-d2eGFP transgene expression in males treated with chronic E_2

In order to study the effects of supraphysiological levels oestrogen on human prolactin transcription we developed a male implant model. The reasoning behind this is to produce a model of a chronic high-oestrogen state that is known to cause hyperplasia (Giles *et al.*, 2011) and to study the effects this has on prolactin gene regulation. In this model we used male Fischer 344 (455 d2eGFP-PRL) rats, subcutaneously implanted with ALZET® Micro-Osmotic pumps releasing 125µg/kg/day E_2, for a period of 21 days. Tissues were prepared and imaged as before.

E_2 treated and control tissue was imaged consecutively. Microscope imaging settings (detector gain, amplifier gain and offset, pinhole size, optical slice and scan speed) were optimised for E_2 treated male and re-used for control tissue, in order to allow direct comparison between states.

All male imaging used for cell tracking was obtained from the Pascal fluorescence confocal system. An example of the region chosen for tracking is seen in Figure 4.10, in which the red circle gives an approximation of the location of time-lapse imaging.

The phenomenon of increased fluorescence due to the release from dopamine inhibition, seen across the tissue at 10-20hours, which was seen in females, is also evident in male tissue. After this initial coordination, cells show heterogeneous patterns in fluorescence activity (Figure 4.11.).

The fluorescence signal from each of 100 cells from each tissue slice preparation was tracked (Figure 4.12.) To distinguish patterns in reporter prolactin reporter gene activity as an effect of oestrogen, we aimed to compare peaks in fluorescence activity in cells between males with and without E_2 stimulation. To do this, an area under the curve function was used. From this analysis, no prominent difference is seen in the proportion of cells with a 1, 2, 3 or 4 peaks in fluorescence between males with and without oestradiol treatment. For a summary of these results, see Table 4.2., and Figure 4.13.

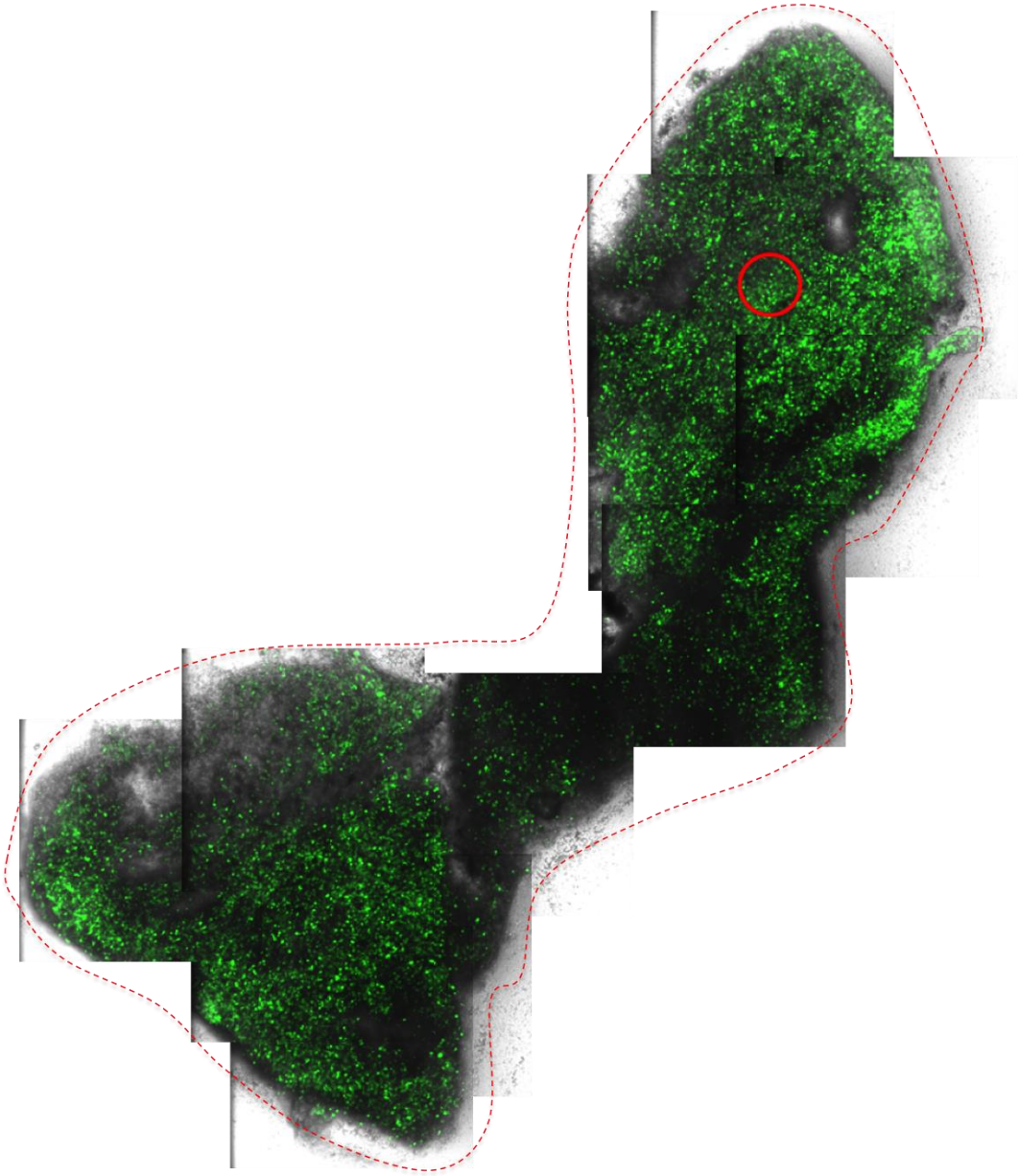

Figure 4.10. Imaging position of E_2 treated male

Montage of maximum projection micrographs of a 250µm coronal pituitary slice on the Pascal at time 0h before 48h imaging. Gain adjusted to show fluorescence in lactotrophs, which was later adjusted in order to capture fluorescence dynamics. Red circle denotes approximate location of imaged section of this tissue from a male subjected to 21 days of high E_2 stimulation. (DS16). Images taken with 10x_0.5NA objective at 0.6x optical zoom.

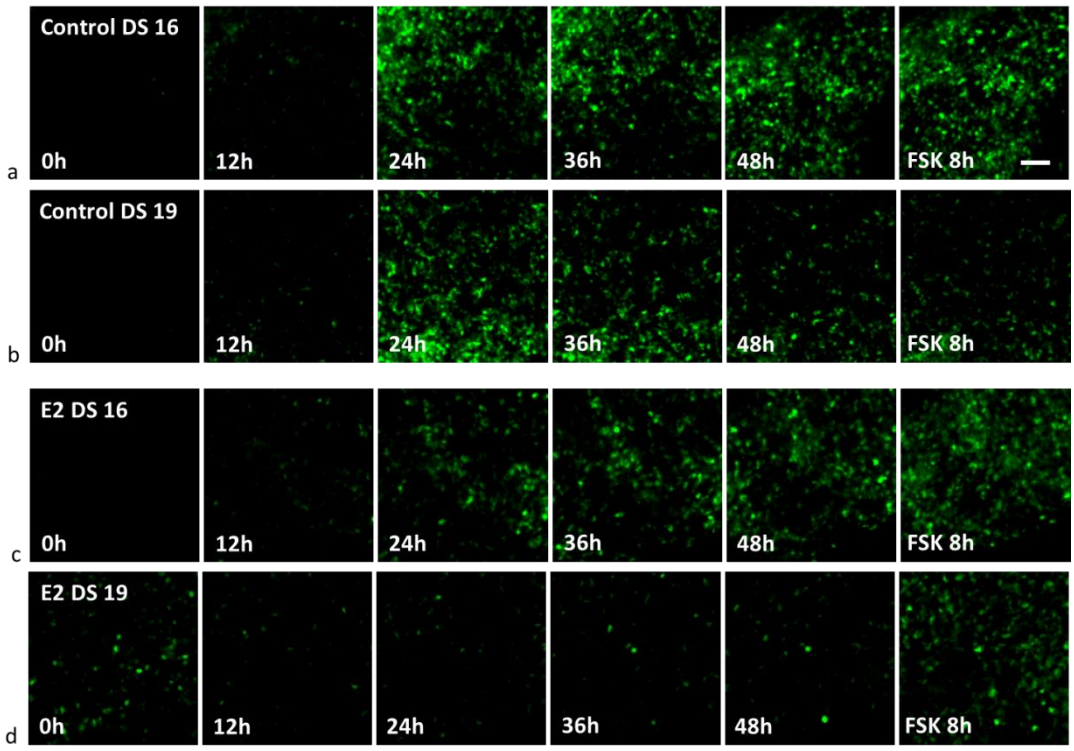

Figure 4.11. Time-lapse imaging of 250µm coronal sections of Fischer 344 (d2eGFP-hPRL 455) males treated with E_2 and controls

Stills at 12 hour intervals from 48 hour time lapse and after 8 hour FSK stimulation to show tissue viability. Panels ***a.*** *and* ***b.*** *show data sets from two tissues slice preparations from males with control pumps and* ***c.*** *and* ***d.*** *from males with E_2 implants. Scale bar indicates 50µm.*

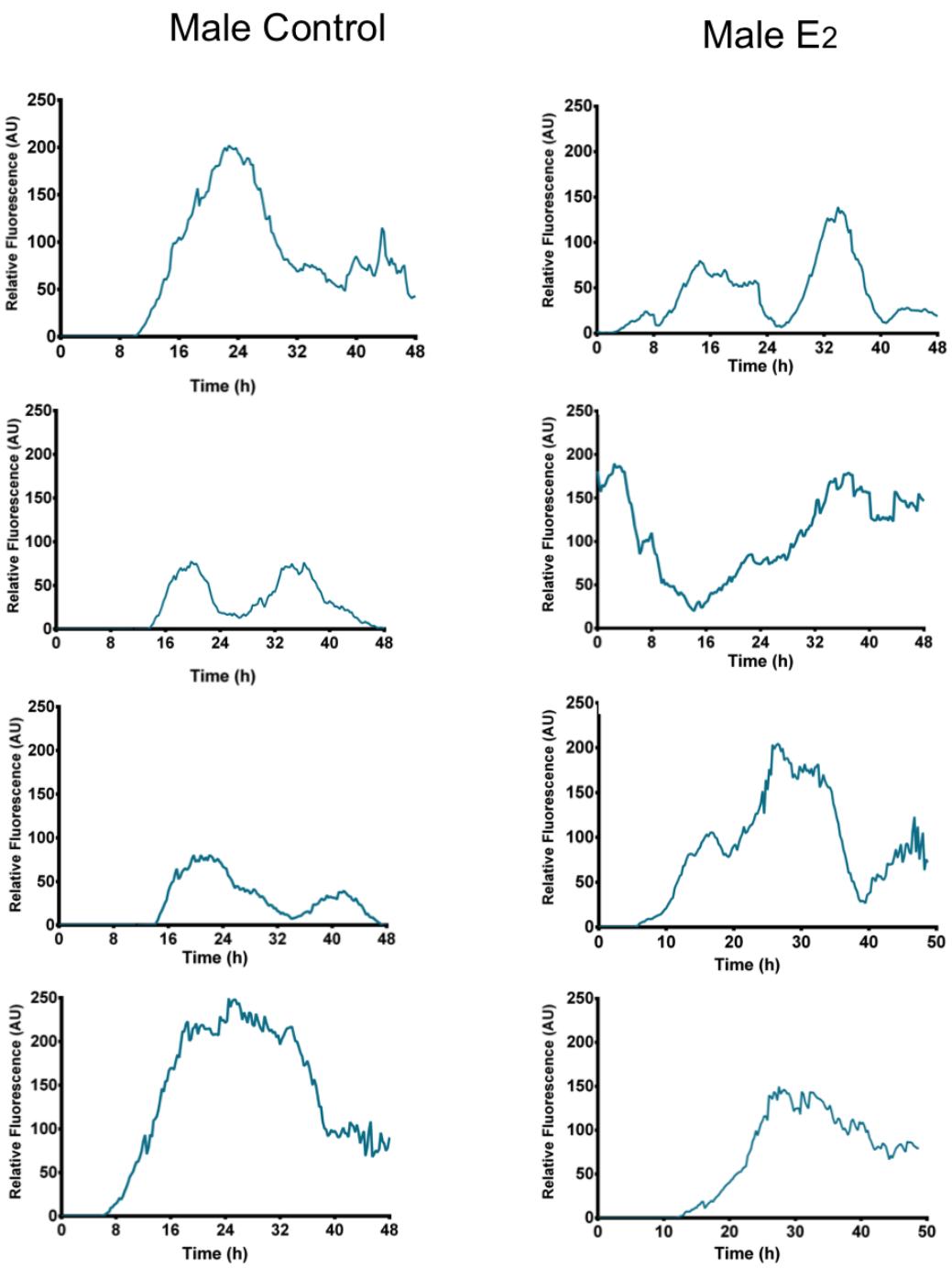

Figure 4.12. Single cell fluorescence patterns from control and E2 treated males

Examples of fluorescence traces of individual lactotrophs expressing d2eGFP under the control of the human prolactin promoter over a period of 48 hours. On the left, four individual cells from tissue slice preparations from control males and on the right, four from males treated with E2 for 21 days. The x-axis denotes time in hours and the y-axis denotes raw relative fluorescence

Percentage of cells displaying given number of fluorescence peaks over 48 h				
Number of peaks in fluorescence	**Male Control (DS 16)**	**Male Control (DS 19)**	**Male E_2 treated (DS 16)**	**Male E_2 treated (DS 19)**
1	74	78	51	45
2	26	22	38	41
3			11	13
4				1

Table 4.2. Distribution of fluorescence peaks in E_2 treated and control males

The mean fluorescence of 100 individual cells was tracked over 48 hours in two examples of pituitary slice preparations from males with control and males with micro osmotic pumps releasing a steady high dose of E_2 over a period of 21 days (DS 16 and 19). Peaks in fluorescence activity were determined by area under the curve (AUC) analysis and results are plotted above.

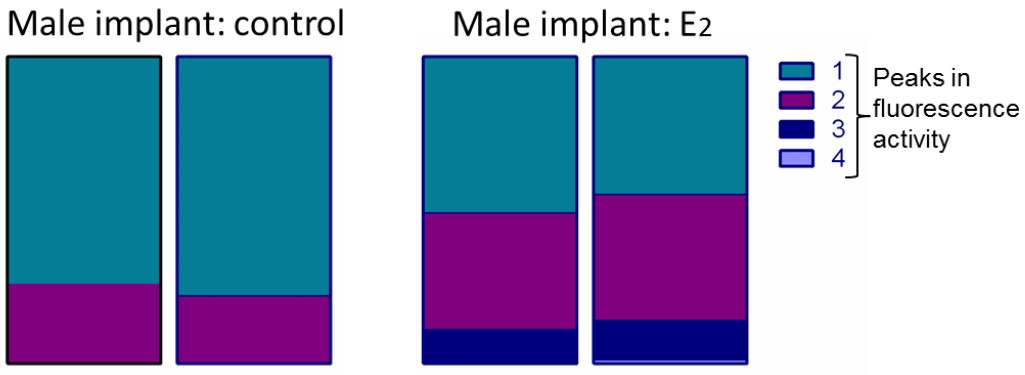

Figure 4.13. Distribution of fluorescence peaks in E_2 treated and control males

Data from Table 2, plotted as a histogram. Each histogram represents the proportion of the 100 tracked cells, displaying one to four peaks in fluorescence activity, as defined by AUC analysis, On the left, data from two tissue slice preparations from male males rats implanted with control micro osmotic pumps and on the right, from two male rats with micro osmotic pumps releasing a high dose of E_2 over a period of 21 days. See legend for colour classification

4.5. Discussion

4.5.1. High vs low oestrogen state does not alter patterns in prolactin gene expression reporter activity

To study the effects of endogenous oestrogen on patterns of prolactin gene expression, the fluorescence of 100 cells from time lapse imaging of pituitary slice preparations of Fischer 344 (d2eGFP-PRL 455) rats at diestrus and oestrus was tracked and plotted against time. The vast majority of cells showed no fluorescence from 0 to 15 hours (due to limitation of dynamic range of PMT), after which a progressive rise in the prolactin reporter transcription was seen. This rise is most probably due to the release of prolactin transcription from the suppression normally experienced *in vivo* from the effect of hypothalamic dopamine. After this coordinated rise in transcription, single cell fluorescence patterns tend to diverge. By using an area under the curve (AUC) method, the number of peaks in fluorescence activity in each lactotroph was determined.

We had hypothesised, that with an increase in oestrogen, we would see a difference in the fluorescence patterns. For example, an increase in the amplitude, frequency, or duration of the transcriptional bursts might be expected. Interestingly, no major differences were seen between the high and the low oestrogen states in the female. The proportion of cells with high and low frequencies of fluorescence pulses was not dramatically different between oestrus and diestrus.

In one of the two oestrus tissues tracked, the level of serum prolactin was low, showing a plasma concentration close to the median expected at diestrus (see Appendix B), as defined by the validation studies carried out in chapter 3. This similarity in serum prolactin could indicate a reason for the similarity in transcription pattern, however, validation studies did indicated that the serum prolactin can vary greatly in short period of time rats spend in oestrus and the presence of cornified cells in the vaginal smear used to determine cycle stage, did confirm that animals used were in oestrus.

With the male E_2 implant study, we aimed to model the effects of chronic oestrogen stimulation on prolactin transcription *in vivo*. The fluorescence of 100 individual cells from two pituitaries from males with control implants and from two males implanted

with osmotic pumps releasing a controlled high dose of oestradiol over a period of 21 days, was tracked. In a similar way to the females, fluorescence remained below the threshold level until c. 15 hours, after which a progressive rise in fluorescence was seen, again likely to be due to the release from dopamine inhibition *in vivo*. After this first prolonged peak, the patterns of fluorescence signal between individual cells became more heterogeneous.

E_2 and control treated males were imaged at the same settings, so fluorescence results should be directly comparable. The imaging series appeared to indicate an approximately similar fluorescence signal overall in the images analysed here. The reason for this is not entirely clear, as validation studies had consistently shown that prolactin transcription occurred at a significantly higher level in males treated with the E_2 implants by flow cytometry and qPCR and serum prolactin was shown to increase by 18 fold in the animals whose tissue was used for these analyses (Chapter 3. Figure 3.5.). Despite any likely post-translational changes in mRNA stability, with the half-life of human prolactin being only 30 minutes (Guyda *et al.*, 1971), it is not possible that the discrepancy between serum prolactin and transcribed prolactin is due to protein accumulation. This problem highlights the fact that imaging techniques are not strictly quantitative, as well as the need for absolute quantification of the levels of transcription such as those carried out in our validation studies.

Simple analysis of the proportion of cells showing between one and four peaks in fluorescence activity showed that there was a slight decrease in the proportion of cells with only one peak in fluorescence activity and an increase in the proportion of cells displaying 3 or more peaks. But these differences are relatively small, and seem unlikely to be biologically significant, and would need larger numbers of replicate analyses to detect a significant and consistent difference in pattern.

Taken together, the data indicate that in high oestrogen states (and high prolactin production states), either oestrus vs. diestrus, or males treated with high dose oestrogen, there is clear evidence of continuing cyclicity in prolactin gene expression in individual cells within the context of tissue slices. There is no marked change in the proportions of cells displaying different numbers of transcriptional cycles over the 48h period of observation *ex vivo*. However, these analyses were relatively crude, relying simply on the raw fluorescence signal. In the light of our

previous studies of similar transcriptional patterns in cell lines, it was therefore important to apply more rigorous analysis to these systems: in particular the data could be analysed using mathematical derivation of the transcription rate, taking account of the half-lives of d2eGFP mRNA and protein. This will be described in detail in the following chapter.

4.5.2. Dopamine

The effects of the release of prolactin transcription from the inhibitory control of dopamine *in vivo* is clearly visible in the first 20 hours of the imaging of all tissues, both in males and in females and in high and low oestrogen states. Previous studies from our group (Harper *et al.*, 2010), had indicated that the replacement of dopamine into the slice culture system would prevent this transcriptional surge, suggesting that this phenomenon was indeed likely to be due to release from dopaminergic suppression *in vivo*. This response to removal of dopamine influences the imaging window and also creates a moving baseline of the fluorescence activity seen, which is evident from the stabilisation of fluorescence from 20 hours and the heterogeneity that becomes apparent after the initial coordinated transcriptional surge.

This prominent effect of dopamine does beg the question of whether we are seeing true dynamics of prolactin transcription *in vivo* in a system where the tissue is removed from this control. It can be argued that what we are creating is an *in vitro* model of dopamine withdrawal, similar to the mechanism thought to underlie the prolactin surges seen during stress and lactation.

We are confident that regardless of the dopamine state, we see true prolactin transcription cycles. In work published by Harper *et al.* in 2010, our group had found evidence for prolactin gene expression pulsatility in adult pituitary tissue slice preparations *ex vivo*. These pulses were present both in the presence and absence of dopamine, but at different levels. Furthermore, our colleague Dr. Anne McNamara is currently performing studies in which dopamine suppression in the culture system is maintained by using with dopamine agonists Cabergoline and Bromocriptine. In these experiments we have continued to see prolactin reporter gene expression pulses, with the difference that pulses are of lower amplitude (McNamara *et al*, unpublished data). Taken together, this suggests that pulsatility is

a fundamental feature of prolactin transcription, whether in states of low production or high production. Dopamine and oestrogen clearly alter the overall level of transcription, as shown by my and others' previous data, but do not appear to mediate this through changes in the frequency or duration of transcriptional pulses.

4.5.3. Imaging

The Zeiss LSM 5 Pascal and 780 are both state of the art imaging systems, allowing high resolution single cell time-lapse microscopy. As with every technique, this too has its caveats. The principal problem encountered is the dynamic range of the detector, which does not have a wide enough dynamic range to capture the full range of fluorescence emitted by the samples. As a result, we can only capture a partial view of the dynamics that cells actually display. This poses two separate issues.

Below (Figure 4.14. a.) is a schematic of an example of the fluorescence dynamics of a single cell, shown in blue, with time in hours along the x-axis and relative fluorescence on the y-axis. The red dotted lines indicate the span of the detectors sensitivity and the chosen window of fluorescence capturing. At time 0 of imaging, we are able to detect signal from single cells, however, the increase in signal is so dramatic, that, if we would set the detection threshold to a level where cells at time 0 are visible, after the release of prolactin from dopamine inhibition, we would no longer be able to see the transcription dynamics, as these would surpass the saturation level of the detector. In an effort to circumvent this problem, we chose to set the detection threshold to a higher level, moving the detection window upwards, as indicated by the dotted red lines. In most cases, the emission of cells between 0 and c. 15 hours is lower than the detection threshold, giving the impression that transcription is absent, as shown by event 1 in Figure 4.14.a. In some cases, cells can still exceed the fluorescence detection capacity of PMT systems (event 2). In most cases, we were able to capture the peaks and troughs of fluorescence emitted by cells after the initial release from dopamine inhibition peak, as shown in event 3. In some cases (4), the trough may fall below the threshold of the detector, which does not necessarily mean that transcription has been turned off, but simply that it falls outside of the detector range.

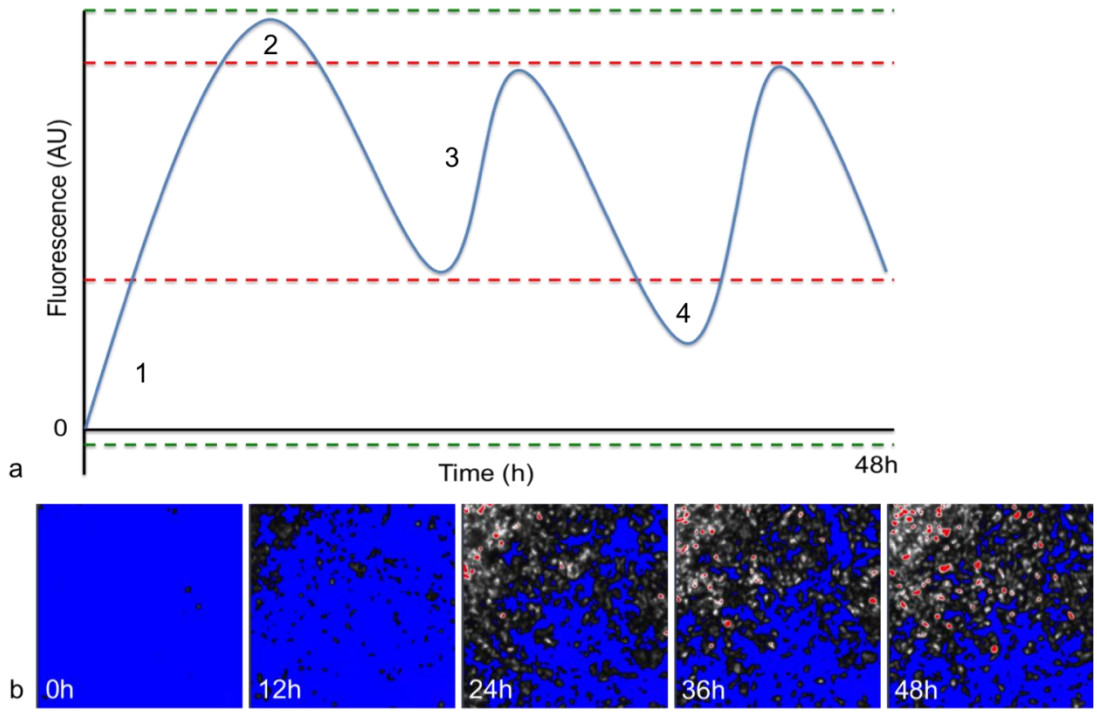

Figure 4.14. Detector sensitivity

*In panel **a.** a schematic diagram of the theoretical fluorescence range of a single cell (shown in blue) over a period of 48 hours. Green dotted lines represent the ideal range of the signal detector. Red dotted lines indicate the real detector range. Numbers indicate events described in the text. In 1. fluorescence below the detector threshold will be read as no transcription, in 2. fluorescence saturates the detector system, in 3. a peak and trough fit within the detector window, allowing the visualisation of the full dynamics of the pulse and in 4. fluorescence falls below the detector level, indicating the turning off of transcription. In panel **b.** stills from a female diestrus tissue that has been tracked and analysed. Blue indicates no signal, grey scale is signal within range and red denotes areas where the detector has reached saturation.*

This poses the problem that the full dynamics of emitted fluorescence cannot be captured, thus not giving a true image of prolactin transcription dynamics, but showing only a window. However, by capturing the more dynamic higher range of fluorescence and with the assumption that the first 0 to c. 15 hours shows a steady increase in transcription (as shown by previous experiments, not shown here), it seems that using this window is the most effective and informative use of the system.

In an effort to circumvent this problem, members of group are trying to develop a high dynamic range (HDR) based system with which to capture a fuller range of fluorescence from our pituitary tissue. This system aims to capture the lower range of fluorescence (seen from 0 to 15 hours) and the higher range of fluorescence (seen from 15 hours onwards) and to combine the two images to create one single time point.

The second issue lies in comparability between data sets. If the imaging window has to be optimised for each tissue, this begs the question of whether the single cell fluorescence patterns are comparable between tissues imaged. Taken together with the results from the validation studies described in chapter 3, in which the increase in the overall level of prolactin transcription is evident in oestrus as opposed to diestrus and in males treated with E_2 as opposed to controls, the more subtle dynamics seen here, can still be compared.

Alternative methods of live cell imaging include optogentics, in which the light source and light detection systems are embedded within the tissue of the living animal (Deisseroth *et al.*, 2006). The use and benefits of using light sheet microscopy are discussed in chapter 6.4.

4.5.4. Cell tracking

To measure the fluorescence activity in individual cells within the pituitary tissue, cells were tracked using the CellTracker program designed by the group of Douglas Kell in collaboration with Mike White at the University of Manchester and further developed by the group of Till Bretscheider at the University of Warwick. We were not able to use the automated cell tracking facility due to the nature of tracking single cells in the context of tissue. Adjacent cells were frequently regarded as a single cell by the algorithm depending the activity of cells around the cell of interest. In addition to this, cells that temporarily fell below the detection level of the imaging system, were lost and not recovered when fluorescence reappeared. Tissue movement both in the x,y and in the z, plane, which often resulted in the need for refocusing and restarting of imaging in different points throughout the time series acquisition, added further complications to tracking. As a result, single cells had to be tracked by hand, frame by frame, taking on average three weeks to track 100 cells for each tissue slice preparation.

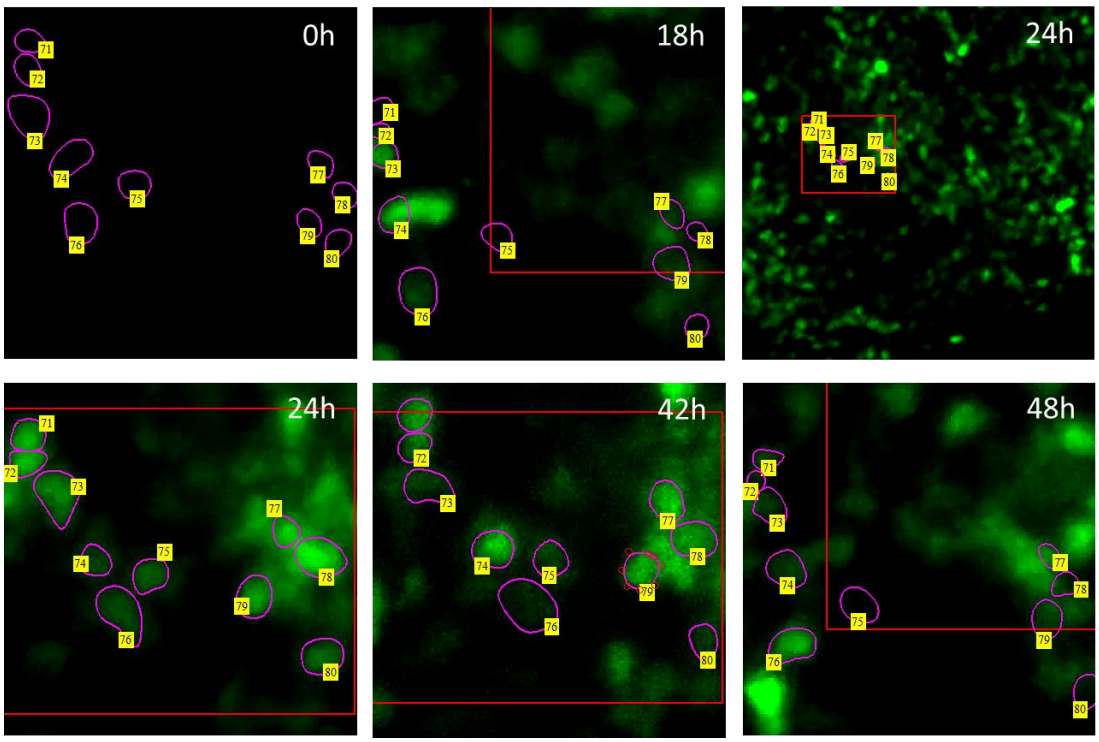

Figure 4.15. Single cell fluorescence tracking using CellTracker

Still from the time-lapse imaging of tissue from a male Fischer 344 (d2eGFP-hPRL 455) treated with a chronic high dose of E_2 over a period of 21 days. 10 cells were chosen (pink circles), in this case, at time point 24 hours and tracked backwards between 0 and 24 due to cells falling below the dynamic range of the PMT detector system associated with the LSM Pascal microscope. The red box (shown in the context of the field of view in the top right panel and zoomed in in the rest of the panels for ease of tracking) indicates the region of interest, which remains constant through the time series, however, with movement of tissue, cells move relative to the designated region of interest. The overlapping of fluorescence from neighbouring cells can clearly be seen in cell 78, which further highlights the need for manual cell tracking.

4.5.5. Determination of fluorescence cycles

In this study, I have used a simple area under the curve (AUC) function of smoothed data to identify the peaks in fluorescence activity to analyse patterns of prolactin transcription in our four different model states. Methods for identification of peaks and troughs has been thoroughly discussed and researched with fellow lab member

Dr. Karen Featherstone. An alternative method used in the lab is a system in which a peak is determined as a doubling from baseline (the overall average of the data for all cells tracked) and a second peak will be a doubling from the lowest point of the through of the previous peak. We are currently working to find a more suitable method for peak determination using a MatLab based wavelet analysis method.

Whilst the data on the patterns of fluorescence as a reporter for prolactin transcription through different oestrogen states obtained using these methods is valuable, what we aim to study is not reporter activity, but rather the rate of transcription at the prolactin gene locus. To apply more rigorous analysis to these data, we have been in close collaboration with the Systems Biology team at the University of Warwick, who have developed an algorithm that can mathematically derive the transcription rate of individual lactotrophs from the fluorescence data. This is described in the next chapter.

Chapter 5

Results

Mathematical modelling of prolactin transcription dynamics

Mathematical modelling of prolactin transcription dynamics

5.1. Introduction

5.1.1. Prolactin transcription cycles

Pulsatility in the expression of prolactin promoter activity was first seen during the 90's (Castano *et al.*, 1994, Castano *et al.*, 1996, Shorte *et al.*, 2002, Takasuka *et al.*, 1998, Villalobos *et al.*, 1999). By using single cell bioluminescent imaging microscopy, the group identified 'on'/'off' gene expression bursts, occurring in a distinctly non-circadian oscillatory pattern, in primary lactotrophs. Both Takasuka *et al.,* (1998) and Norris *et al.,* (2003) showed temporal variation and heterogeneous patterns in gene expression in pituitary GH3 cells transfected with a luciferase reporter gene linked to a 5000 bp fragment of the human prolactin gene.

In 2010, Harper *et al.* used fluorescence live cell imaging to the study temporal and spatial arrangement of prolactin transcription in Fischer 344 (d2eGFP-hPRL 455) rats. Enzymatically dispersed cell cultures showed unsynchronised fluctuations in promoter activity. In whole tissue studies, while single cells across different regions of the gland showed varying amplitudes and timings of transcriptional response, all regions displayed similar overall patterns of reporter gene expression over a 50-hour imaging period. This implies either that individual cell patterns are summated to generate similar overall patterns, or that the stochastic behaviour of single cell prolactin gene expression becomes, a coordinated cell behaviour when constrained by tissue architecture. The latter poses a possible role for cell-cell communication. Featherstone *et al.,* (2011) studied fetal and neonatal pituitary gene expression to assess dynamic patterns of transcription throughout development. The authors showed that gene expression in single cells is highly pulsatile at the time that endocrine cells first appear, but become stabilised as the tissue develops in neonatal life, substantiating the hypothesis that transcription patterns may depend on tissue architecture or paracrine signalling.

To investigate the origins and functional relevance of the stochastic nature of prolactin transcription, Harper *et al.,* (2011) quantitatively analysed this variability using mathematical tools developed in collaboration with Prof. David Rand and colleagues at the Centre for Systems Biology, University of Warwick. This system

reconstructed the transcription rates of two different reporter genes, d2eGFP and firefly luciferase, controlled by identical fragments of the human prolactin promoter in the same living cell, using dual-transfected clonal cell lines. Using this system, they were able to analyse the time-dependence and cyclicity of transcription pulses over periods of 25 hours and distinguish phases of active and inactive transcription, establishing a binary model in which prolactin transcription exists in two phases, 'on' or 'off'. The average cycle period was found to be 11 hours, with a minimum refractory period of three hours. This minimum refractory period is hypothesised to correspond to a phase of chromatin remodelling, significantly increasing the cyclicity of the system. The mechanisms facilitating the cyclical behaviour of gene transcription are still in dispute. In a similar modelling study, the cyclicity of circadian genes was investigated. Results here also indicated that for the 'on' times to follow a random distribution a minimum refractory period was needed, but came to a dissimilar conclusion in that chromatin structure plays only a secondary role in the development of cyclicity (Suter *et al.*, 2011a). Both the mathematics and the mechanisms are further discussed in the introduction in 1.7.2. and in the discussion chapter 6.0.

5.1.2. The hierarchical model

Previously, prolactin transcription has been mathematically described as binary (Harper *et al.*, 2011) in a binary 'Transcriptional Switch Model'. Here we describe a modified transcriptional model, developed in close collaboration with Kirsty Hey and co-workers at the University of Warwick.

This modified algorithm is based on a Bayesian hierarchal model. It works to back calculate transcription rates from fluorescence activity from individual cells obtained through cells tracking, as described in chapter 4. Using a Bayesian Hierarchical model means that prior information can be incorporated into the calculation. Here, the degradation rates of both d2eGFP mRNA and protein are incorporated into the equation. These rates were obtained experimentally from studies with actinomycin, which blocks transcription by preventing RNA elongation (Sobell, 1985), and cycloheximide, which blocks the translocation step in the protein translation (Schneider-Poetsch *et al.*, 2010), performed by Dr. Karen Featherstone.

The hierarchy of modelling consist of two layers of data analysis, and has been used previously to look at single cell transcription dynamics (Woodcock *et al.*, 2013). The first layer incorporates variation within a single cell. The second layer then incorporates the variation between cells, for example extrinsic noise and heterogeneity. This provides more information across the cells and allows comparison between them.

The outcome of the algorithm gives a statistical estimation of the rate of transcription and of the number of switches in this rate. In this model, in contrast to a binary system, where transcription can only exist in one of two states, a cell can now switch from any given stable rate, which can take any value from a continuous scale from zero to 3000 molecules per hour, to a new stable rate, that is either higher or lower than the previous one. To calculate this output, the algorithm is run 100,000 to 150,00 times on a group of ten cells at a time. On the basis of the data for each cell containing the fluorescence data of 48 hours of measurements with imaging intervals of 15 minutes, the time it takes to make these iterations can range from 6 to 50 hours, depending on the processing power of the computer used. The single output that we see and have analysed here, is the outcome with the highest statistical probability.

In the context of data shown here, where the fluorescence signal from 100 single cells is tracked in four different oestrogen states, females in diestrus and oestrus and in males subjected to E_2 stimulation or not, the hierarchy works as follows: Layer one, or the 'hyper parameter' incorporates the mRNA and protein degradation rates into the algorithm. Layer two factors in the 'hyper-prior information', which is the mean and the variance of the distribution of these degradation rates. As a result, the prolactin transcription rates over a 48h period are calculated per lactotroph, within the context of each tissue in each oestrus state. The hierarchical model, thus provides information on 100 lactotrophs in a particular context, ie. oestrogen state of the tissue, as opposed to providing 100 results, independent of each other.

5.1.3. Effects of oestrogen on patterns in prolactin transcription rates

Data presented so far in this thesis has been based on analysis of the fluorescence activity of the d2eGFP reporter of human prolactin gene expression. We have observed pulsatile fluorescence patterns across all oestrogen states examined,

females at diestrus and oestrus and in males with and without high oestrogen stimulation.

In this chapter we move from the simple description of GFP expression patterns to a more complex modelling of calculated prolactin transgene transcription rates. By doing so we hope to identify key characteristics of gene expression patterns and any alteration in these that may occur in different oestrogen states, for example changes in the frequency of switches or the duration of low- or high-level expression. The idea behind systems biology is to find a model that fits to the data, which will lead to new questions and predictions, which can be tested by the experiment. This modelling could thus, not only help us to identify transcription patterns, but also give insight into unanticipated mechanisms, that could lead us to our next questions. Here I present preliminary algorithm output data from both models and interpretations thereof.

5.2. Prolactin transcription rates across the oestrous cycle

To analyse the patterns of prolactin transcription rates in females across the oestrous cycle, single cell fluorescence data from 100 cells per tissues from oestrus and diestrus were analysed using the Bayesian Hierarchical Model described in 5.1.2., by Kirsty Hey of the University of Warwick. In the tracking and analysis, cells were treated as independent entities, without taking into account their relative position in the tissue.

The algorithm provides an indication the transcription rates displayed by a single cell over a period of 48 hours, and an estimated time point at which a cell switches from one transcription rate to another (shown as red bars in the upper panels of graphs in Figure 5.1.). Transcription rate was therefore not assumed to be a binary phenomenon, as it was in the analysis by Harper *et al.* (2011), but rather it could be assigned any value from a continuous scale (see Figure 5.1 lower panels).

Output data was received as graphs in individual PDF files for each cell, as well as in the form of a spread sheet denoting the transcription rate of the cell and estimated time points of transcription. From this data, it was possible to analyse the frequency of ‘switches’ per cell in each tissue. This analysis is summarised in Table 5.1. The proportions of cells showing 2 to 8 switches in transcription rate were then

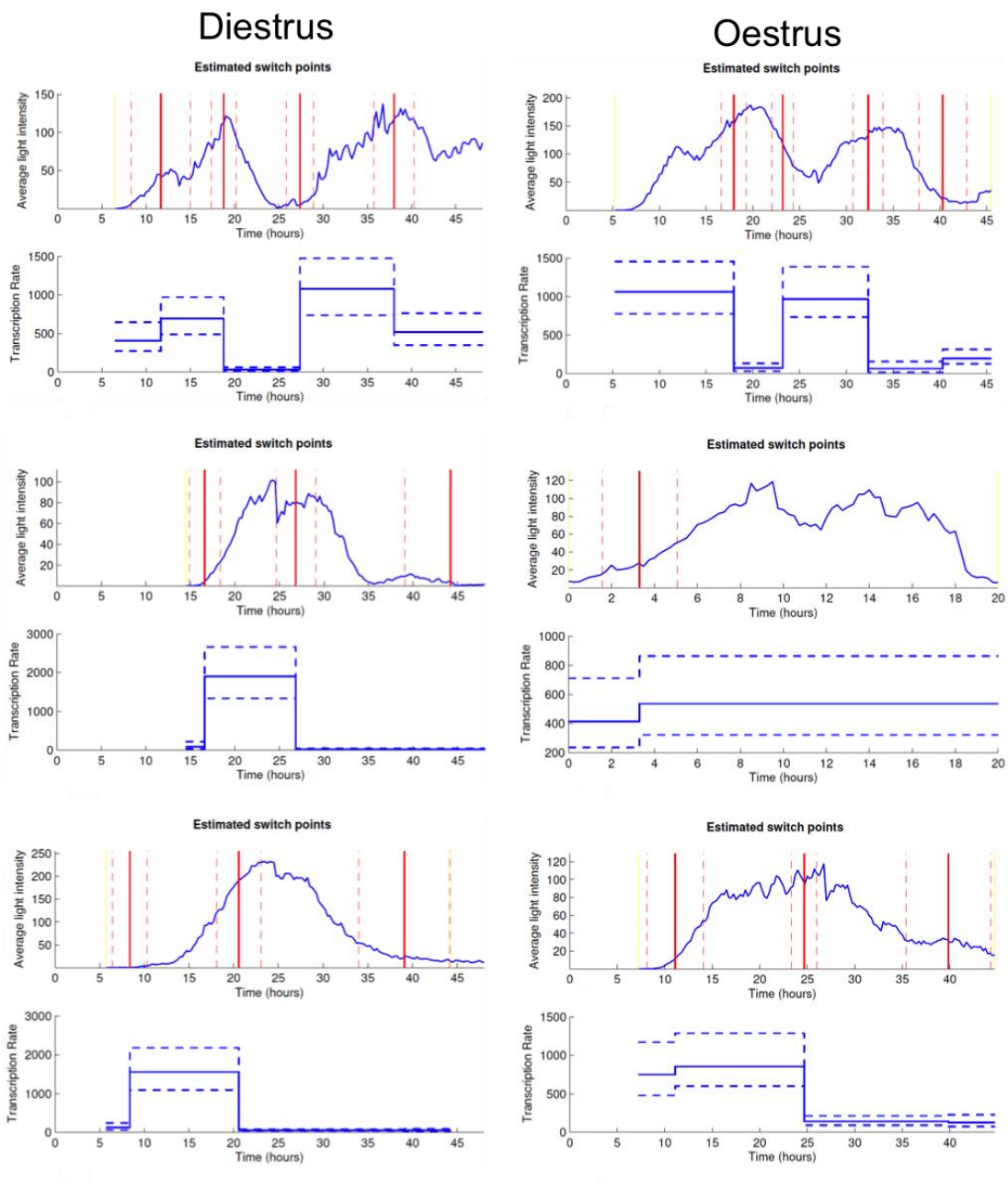

Figure 5.1. Switch rate model algorithm outputs for females in oestrus and diestrus

Representative data outputs from the hierarchical transcription switch rate model algorithm, with diestrus on the left and oestrus on the right. The top panel of each graph shows the light intensity of a cell, with below it the corresponding transcription rate as represented by blue lines. Red lines indicate estimated time of rate switch. Dotted lines indicate 95% confidence intervals. Yellow lines indicate the time series data that was included in the analysis by the algorithm. Graphs courtesy of Kirsty Hey, University of Warwick.

Proportion of cells per tissue displaying a given number of switches in transcription rate in 48 hours			
Number of switches	**Diestrus (DS 14) (n=100)**	**Diestrus (DS 17) (n=94)**	**Oestrus (DS 13) (n=97)**
2	7	7	8
3	29	47	30
4	39	34	40
5	18	5	15
6	3	1	3
7	2		1
8	2		

Table 5.1. Frequency of estimated switches in transcription rate per cell across the oestrous cycle

The number of cells in a tissue from diestrus or oestrus showing between two and eight switches in transcription rate, are plotted above. The number of switches was counted from the algorithm output received from Kirsty Hey at the University of Warwick. The DS number refers to the numbering of the data set, as described in Appendix B.

compared between tissues in oestrus and diestrus (Figure 5.2. a.). It had been assumed that rate and switch frequency might be altered in the high-production or low-production states, but in fact no clear difference was seen.

To allow a more intuitive insight into the data, heat maps were created to amalgamate single cell time series data. Heats maps (Figure 5.2. b. c. and d., created by Dr. Hiroshi Momiji, University of Warwick, using the CoAST software). give an indication of the time course data for each individual cells (as denoted on the x axis). The colour range gives an indication of the level of transcription. This thus gives a concise overview of the transcriptional activity of 100 individual cells, over the course of 48 hours, within the context of the tissue and its oestrogen state. This additional analysis did not identify any differences in transcription patterns between oestrus and diestrus, but does give an indication of the coordinated increase in transcriptional activity seen in the majority of lactotrophs between 10

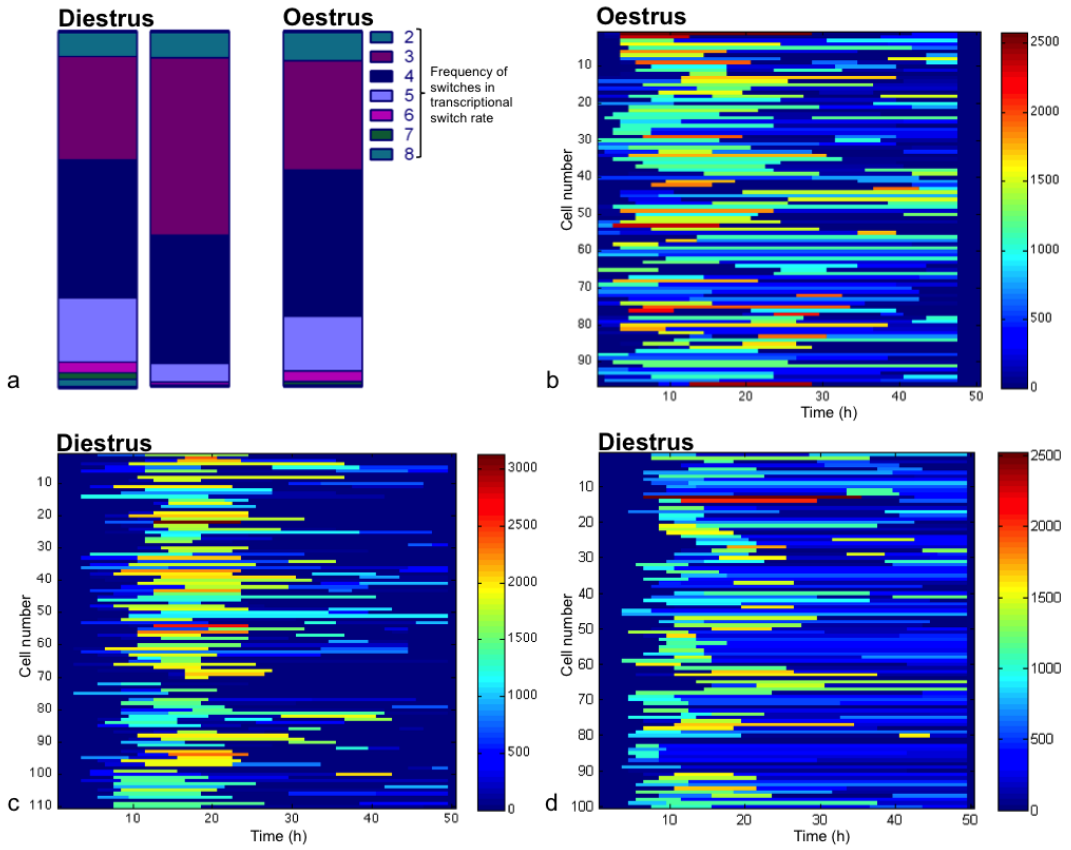

Figure 5.2. Summary of prolactin transcription rate switch model algorithm output for females at diestrus and oestrus

*In **a.** each parts of the whole histogram represents the proportion of cells per tissue showing two to eight switches in transcription rate. The data from tissues represent pituitary slice preparations taken from female rats in diestrus or oestrus, in which the fluorescence signal from 100 individual living cells have been tracked every 15 minutes for 48 hours. The number of switches corresponds to the key on the right. Panels **b**, **c**. and **d**. show the transcription rate time course data for all 100 tracked cells per tissue in the form of a heat map, for one tissue in oestrus and two in diestrus, respectively. The y-axis indicated the number of the cell, the x- axis is time in hours and the colour range gives an indication of the transcription rate, in molecules per hour, with warmer red colours indicating a higher rate. This gives an indication of the transcription rate of each cell and when this cell changes from one rate to another, within the context of the entire tissue. Heat maps were provided by Dr. Hiroshi Momiji, University of Warwick.*

and 20 hours, due to release from dopamine inhibition and the divergence from this coordination in the hours thereafter, between individual cells in the same tissue.

5.3. Prolactin transcription rates in male high and low oestrogen sates

The estimated transcription rates of 100 cells from male rats with chronic oestradiol treatment and controls was calculated from fluorescence data (Figure 5.3). The same Bayesian Hierarchial Model used to analyse female data was applied to single cell 48 hour time series data from male tissue.

From these data the frequency of switches in transcription rate per cell per tissue was counted, with the progression from undetectable signal to the first transcription rate, being counted as the first switch. The proportions of cells with two to nine switches in rate are shown below numerically (Table 5.2.) and graphically (Figure 5.4 a.)

Male data were collated in the form of a heat map, in which the transcription rates of 100 individual cells in a tissue in a given oestrogen state is plotted against the 48 hours of observation (Figure 5.4. b. and c.). From this preliminary analysis it appears that the frequency of periods of higher transcription rates after the initial coordination between 10 and 20 hours, is higher in males with E_2 implants, however, to reach any firm conclusions, further studies would have to be carried out.

5.4. Discussion

5.4.1. Patterns in prolactin transcription cycles and the effects of oestrogen

Mammalian gene expression kinetics have been shown to display cycles or transcriptional bursts. Our group has previously shown prolactin transcription to occur in cycles of 11 hours, with a minimum refractory period of three hours in individual living lactotrophs. This cycle pattern was highlighted with the help of a binary model of transcription, in which transcription can cycle between only two states, ‘on’ or ‘off’.

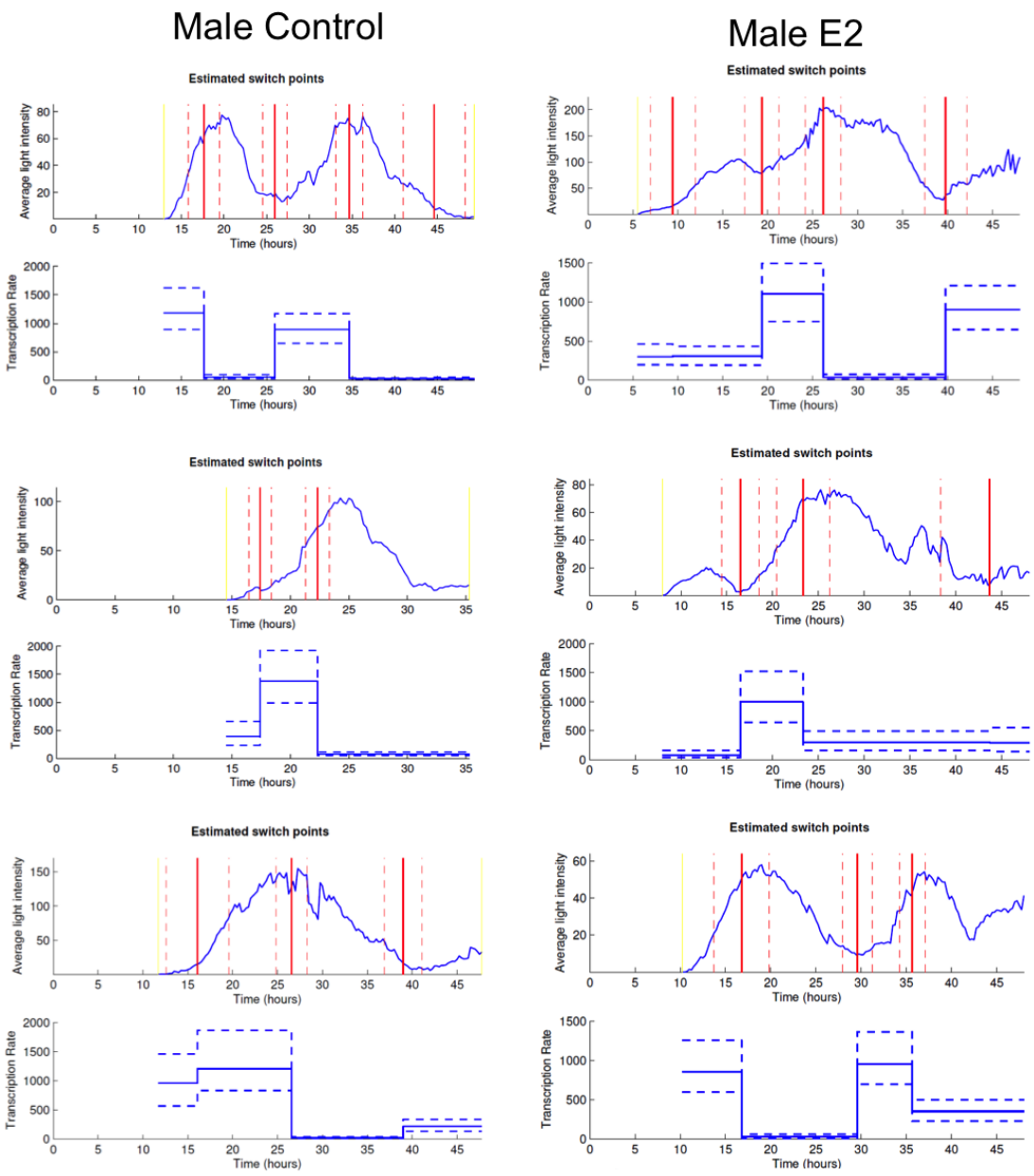

Figure 5.3. Switch rate model outputs from males with and without E_2 treatment

Representative switch model outputs. On the right three cells from males implanted with ALZET® micro osmotic pumps releasing a high dose of E_2 over a period of three weeks, prior to culling and on the left three traces from controls. Each set of graphs gives the light intensity of the cell, with below it the transcription rate model data. Red lines indicate the estimated time point of the switch of a cell from one rate to the next and corresponds to the transcription rate data below, in which blue lines indicate estimated transcription rate. Dotted lines indicate 95% confidence intervals. Yellow lines indicate time series data included in analysis by the algorithm. Graphs courtesy of Kirsty Hey, University of Warwick.

Proportion of cells per tissue displaying a given number of switches in transcription rate in 48 hours

Number of switches	Male E_2 Treated (DS 16) (n=100)	Male Control (DS 19) (n=98)
2	4	0
3	33	46
4	44	43
5	16	9
6	0	
7	0	
8	2	
9	1	

Table 5.2. Frequency of estimated switches in transcription rate per cell, in males with E_2 implants and controls

The number of cells in a tissue from males that have been implanted with an ALZET® micro osmotic pump releasing a high dose of E_2 over a period of 21 days prior to culling, as compared to control males, showing between two and nine switches in transcription rate, are plotted above. Data generated from tissues represent pituitary slice preparations, in which the fluorescence signal from at least 100 individual living cells have been tracked every 15 minutes for 48 hours. The number of switches was counted from the algorithm output received from Kirsty Hey at the University of Warwick. The DS number refers to the numbering of the data sets, as described in Appendix B.

In this chapter we aimed to elaborate the transcriptional modelling to study the effects of oestrogen on prolactin transcription cycles *in vivo*. Two physiological models of oestrogen states were used. In the first, the fluorescence of 100 individual cells from pituitary tissues of female Fischer 344 (d2eGFP-hPRL) rats at diestrus and oestrus were analysed. In the second model, cells of male rats subjected to chronic oestradiol treatment and controls were analysed. Differences in transcription cycle patters, for example the length, amplitude and frequency of 'on' phases would be compared in order to define the effects of oestrogen on prolactin transcription.

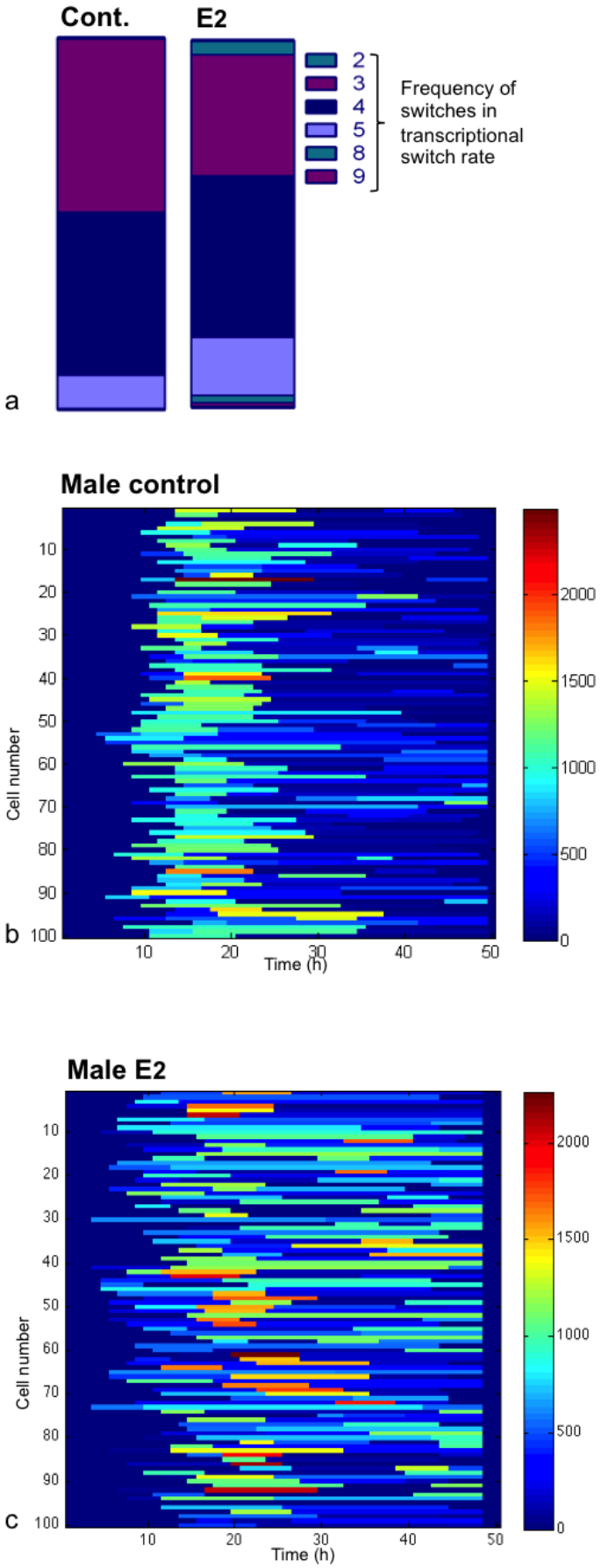

Figure 5.4. Summary of prolactin transcription rate model outputs for E2 treated and control males

*Each parts of the whole histogram (**a**) represents the proportion of cells per tissue, from a male rat treated with a high dose of E2 for 21 days and a control male, showing two to nine switches in transcription rate. The number of switches corresponds to the key on the right. Panels **b**. and **c**. show the transcription rate time course data for all 100 tracked cells per tissue in the form of a heat map, for one tissue in a control and an E2 treated male, respectively. The y-axis indicates cell number, the x- axis is time in hours and the colour range gives an indication of the transcription rate, in molecules per hour, with warmer red colours indicating a higher rate. Heat maps are courtesy of Dr. Hiroshi Momiji, University of Warwick.*

To carry out these comparisons, a novel algorithm is in development, in order to model stochastic transcription reporter activity data. This model is fundamentally different to the binary switch model described by Harper *et al*., (2011). While the binary switch model determined transcription to be either on or off, the transcription rate switch model described in this thesis, gives estimations of single cell transcription rates on a continuous scale, using a hierarchical system.

Analysis of algorithm outputs indicated that the distribution of switches in transcription rate between high and low oestrogen states was similar. This reflects the observations made of the analysis of fluorescence signal (without the mathematical derivation of transcription rate estimates) of the reporter gene in chapter 4. While no significant change was found in the frequency of transcription pulses, further analysis is required to investigate the period and the amplitude of these pulses before any final conclusions can be drawn.

In conclusion, we have studied the effects of oestrogen on prolactin transcription patterns *in vivo* by combining fluorescence live cell time lapse imaging with the application of a novel transcription rate switch model in order to analyse complex stochastic data. We have seen that the production of prolactin in individual living lactotrophs oscillates within the context of tissue, not in a binary fashion, but rather that transcription can occur at any given rate from a continuous scale. Taken together with data from chapters 3 and 4, it is clear that a higher oestrogen state increases the overall level of prolactin transcription of the tissue, but that pulsatility in individual cells is maintained in both high and low oestrogen states. This suggests that cyclical prolactin transcription is a fundamental feature of the lactotroph.

5.4.2. Development of the transcription rate switch model

The binary model of prolactin transcription (Harper *et al.*, 2011), worked on the basis of a random telegraph model, in which the distribution of the ‘on’ times of transcription followed a random distribution, but only with the condition of a minimum of a three hour ‘off’ period, which was termed the refractory period, during which it was assumed that no new transcriptional burst could be initiated. This refractory period was proposed as crucial for introducing cyclicity to the system. The new transcription rate switch interpretation works on the basis of a hierarchical model. This system back-calculates transcription rates from the original

fluorescence data of reporter gene activity and outputs are continuous and thus do not give a definitive on or off phase.

As discussed in section 4.4.3, there is an ongoing issue with the sensitivity of the fluorescence detection system, in that only the higher range dynamics of reporter gene activity are captured, giving the impression that transcription is absent in the first c. 15 hours of imaging. This is indeed not the case, this is purely a thresholding effect enforced by the range of the imaging systems. This does pose a problem for rate modelling and imposes an apparent transcriptional 'off' period in all cells. Furthermore, in data not included in this thesis, we have encountered problems where the trough of a fluorescence peak drops to below this imaging threshold which not only gives the impression of an off phase, but causes further problems in that the algorithm then splits this data, recognising each peak as an individual cell.

5.4.3. Further analysis

The data presented in this chapter are derived from the second version of the transcription rate switch model algorithm. As mentioned previously, this is still under development by collaborators at the Systems Biology Centre of the University of Warwick. At the point of writing this thesis, data is currently being run through a newer version of this algorithm. Once the total of eight data sets, two females at diestrus, two at oestrus, two males with E_2 treatment and two controls, has been modelled, we can further analyse and compare the prolactin transcription cycle patterns between the oestrogen states. In addition to comparing the frequency of transcription rate switches, we aim to compare time spent in active transcription and the frequency of transcription rates. Using this data, we can then compare the average time cells spend in high, medium and low levels of prolactin transcription in each oestrogen state.

An example of such possible analysis has been performed on the transcription rate data of a male treated with oestradiol. By plotting the transcription rate against the duration that this rate was held for (Figure 5.5. b.) we get an indication of the distribution of time cells in a particular tissue spent in higher or lower transcription rates. Another layer of information is added into this figure with the colour of the points plotted. A blue downward pointing arrow indicated that the rate after the switch has decreased from the previous rate, whereas and red upward red arrow

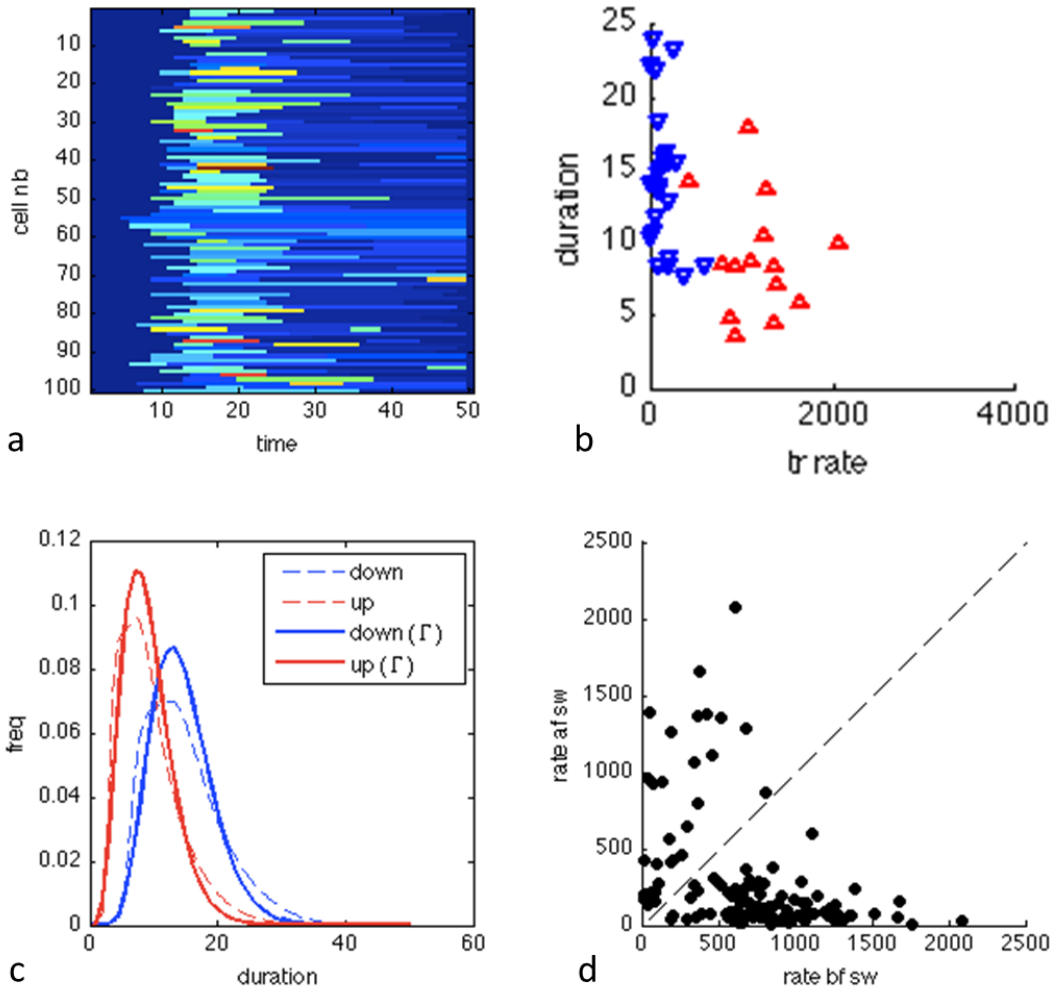

Figure 5.5. Statistical analysis of transcription rate data

A summary figure of possible analysis possible to be performed on new algorithm output data from a male control tissue slice, based on the information gathered from 100 cells. Note, data differs main body of this chapter. In ***a.*** *a heat map giving an indication of the time series data of 100 cells in the tissue, with time in hours on the x axis, the cell number on the y axis and the colour range indicating the rate of transcription of a given cell. In* ***b.*** *the post switch transcription rate is plotted against the duration of this rate, with the blue downward pointing arrows indicating a downward switch and red upward pointing arrows indicating that the switch was to a higher rate. The duration (in hours) of rates that have risen from a previous rate (red) and rates that have decreased (blue) are plotted against frequency in a probability density function shown in* ***c.*** *with uninterrupted lines representing parametric estimation and dashed lines indicating non-parametric estimations. The rate of a cell's transcription before a switch is plotted against the rate after the switch in panel* ***d.*** *The dashed line indicates no change in transcription rate. Figure courtesy of Dr. Hiroshi Momiji of the University of Warwick.*

indicates that the rate of transcription has increased. By comparing similar analyses between oestrogen states, we aim to study discrepancies between the duration of the time spent in upward and downward switches. The comparison of upward to downward switches would provide information about transcription cycles, similar to that obtained by analysing ‘on’ and ‘off’ phases of transcription in the binary model.

In addition to this, we can plot the frequency with which cells in a given oestrogen state, have increased in, or decreased in transcription rate (Figure 5.5. c.). This would give an indication of whether oestrogen induces more frequent increases in transcription rate. By plotting the rate before the switch against the rate after the switch (Figure 5.5. d.), we can again get an indication of the range of the amplitudes of the switches and the variation between transcription rates in each oestrogen state.

Chapter 6

Discussion

Discussion

Oestrogens have been shown to modulate prolactin transcription, prolactin secretion and lactotroph proliferation. Furthermore, oestrogens have been suggested to play a role in the hyperproliferation of lactotrophs in the formation of prolactinomas and in their occasional progression to more aggressive behaviour. In this project, I set out to characterise the stochastic nature of human prolactin gene expression and how this is affected by oestrogen. I have studied two models, females across the oestrous cycle and males subjected to chronic oestradiol stimulation. Single cell fluorescence from hPRL-d2eGFP transgenic rat pituitary tissue was analysed using time lapse confocal microscopy and the data were subjected to mathematical modelling in order to analyse and compare the effects of differential oestrogen states *in vivo* on prolactin transcription.

6.1. Stochastic gene expression

The stochastic nature of mammalian gene expression has become well established, particularly in pituitary tissue, both in adult rat pituitary cells (Harper *et al.*, 2010, Harper *et al.*, 2011, Norris *et al.*, 2003, Takasuka *et al.*, 1998) and the during development of the pituitary (Featherstone *et al.*, 2011). The Systems Biology approach of combining biological data with mathematical modelling aims to discover emerging properties from the biological systems, clarifying patterns seen and bringing to light new questions about the mechanisms of the biology. Many groups have set out to explore the origin of transcriptional stochasticity with the help of mathematical modelling, using a variety of systems, mostly in isolated bacteria, yeast and mammalian cell systems rather than in intact tissue (Brown *et al.*, 2013, Lipniacki *et al.*, 2006, Metivier *et al.*, 2006, Paszek *et al.*, 2005, Pedraza & Paulsson, 2008, Sanchez *et al.*, 2013, Segal & Widom, 2009, Suter *et al.*, 2011a, Vinuelas *et al.*, 2013).

6.2. Oestrogen *in vivo* promotes the transcription of prolactin

In this study, I aimed to investigate the transcription dynamics of a human prolactin transgene and how these dynamics may be affected by oestrogen. Two model systems were tested and validated, one to study the effects of short-term endogenous oestrogen fluctuations on the transcriptional regulation of prolactin, and

the other to study the effects of chronic exposure to oestrogen. In the first model, the reporter activity of female Fischer 344 (d2eGFP-hPRL 455) rats, expressing a destabilised GFP reporter under the control of a large human prolactin genomic fragment, was investigated at high (oestrus) and low (diestrus) oestrogen states through the oestrous cycle. In the second model, male Fischer 344 (d2eGFP 455) rats were subcutaneously implanted with ALZET® micro osmotic pumps either releasing a high dose of oestradiol over a period of three weeks, or control pumps. In both models, we found a higher oestrogen state to induce a higher level of prolactin gene transcription and protein synthesis, as judged by immunofluorescence, qPCR, flow cytometry data and serum analysis.

In order to study the mechanism of this increase in prolactin transcription, the fluorescence of 100 single cells from the time-lapse confocal microscopy of tissue slice preparations was tracked and analysed for patterns in prolactin reporter gene expression. No significant change was found in prolactin patterns between high (oestrus and E_2 treated males) as compared to low (diestrus and control males) oestrogen states, in regard to frequency, amplitude or duration of reporter activity peaks and cycles. This same data was subjected to Bayesian hierarchical modelling, in which fluorescence data is run through an algorithm which uses the transcription and translation rate of the reporter as prior knowledge, in order to calculate transcription rate from light intensity data. From this, the time each individual cell spends in a given transcription rate is observable, as is the estimated point at which the given cell changes from one rate to another. Using these analyses, it is possible to look at the single cell data in the context of the tissue and start to make comparisons of the transcriptional behaviour between oestrogen states.

Having moved away from a binary switch model of transcriptional behaviour, as was previously implemented in our group (Harper *et al.*, 2011), we have, in collaboration with the Systems Biology Centre of the University of Warwick, developed a model in which transcription can be modelled to occur at any given rate along a continuous scale from 0 to 3000 molecules per hour. If each cycle consists, of a trough, followed by a peak and then another trough, we see a similar distribution of cells expressing one to eight cycles between low and high transcription states. We found that the amplitude of these bursts of transcription remain roughly constant, over a period of 48 hours, in each of the different oestrogen states. Preliminary

investigations into the durations of high and low periods of transcription in male control studies, indicate that the duration of high transcription periods tends to be shorter than periods of low transcription. Although cycle lengths have not so far been formally calculated, we can estimate that the transcription cycles seen here are on average about 10-15 hours. This length is approximately in keeping with previous estimates, which showed cycles in transcription in the dual reporter (hPRL-luc and hPRL-d2eGFP) GH3-DP1 cell line to have a 6.5±2h 'off' and 4.0±1h transcriptionally 'on' period with a total cycle period of on average 11.3±3.3h. In primary dispersed pituitary cell cultures, the average cycle was slightly longer at 15.2±4.8h (Harper *et al.*, 2011).

Taken together, the results of this study indicate that the cyclical nature of prolactin transcription is a robust phenomenon, that occurs regardless of oestrogen or dopamine state. We have found that a high oestrogen state clearly leads to a high prolactin production state, but in both high and low oestrogen states temporal patterns in prolactin reporter gene activity and transcription rate cycle patterns remain similar.

6.3. Origins of cyclical activity

Cyclicity is a phenomenon seen in many aspects of biology. In endocrine cells, for example, the secretion of proteins, transcription of genes, and binding of transcription factors have been seen to oscillate. The cyclical pattern of prolactin transcription could, in principle, arise from an accumulation of various intracellular cyclical events, but in previous work we have proposed that there is a fundamental chromatin remodelling cycle involved as an intrinsic property of the transcription start site (Figure 1.10.). However, the molecular mechanisms of the 10-15 hour transcription cycles seen here, remains incompletely explained.

Experiments have indicated that the expression of prolactin may indirectly be under circadian control (Bose & Boockfor, 2010, Guillaumond *et al.*, 2011, Leclerc & Boockfor, 2005). The cycles observed here, however, do not follow a 24 hour circadian pattern. Prolactin transcription cycles can also not be accounted for by cell cycle length, as GH3 cells have been shown to have a cycle length of 40 hours, which is significantly longer than the transcription cycles seen in cell line studies (Harper *et al.*, 2011, McFerran *et al.*, 2001).

While a continuous or multi rate model such as the one described here may be more plausible than a binary model of transcription, it may still be possible that the multiple levels of transcription we are seeing could simply be a summing effect of multiple insertion sites, each with their own onset and offset characteristics. An ideal model system to analyse this would have a cell with a single copy transgene, to rule out this possibility, whereas the transgenic Fischer 344 (d2eGFP-hPRL 455) rat has a low copy number of between two and four (Semprini *et al.*, 2009). It would be useful to apply our new multi-level modelling approach to the D44 cell system (copy number of between one and two), to determine how many different levels of transcriptional activity can be ascribed to the data. If a binary model of transcription applied to each individual prolactin reporter transcription initiation site, the new modelling algorithm might predict either two rates (on or off in the case of one copy) or three rates (in the case of a copy number of two, if transcription in on in both copies, on in one and off in the other, or the third option, if both are off). If similar multi-level transcription could be modelled from such a 1-2-copy system, then we could conclude more confidently that this behaviour is genuinely attributable to individual transcription start sites.

What we propose from the present data is that oscillations persist in both high- and low- prolactin production states, but that the basal level of transcription nonetheless varies between high and low oestrogen states (Figure 6.1.). The mechanism by which a 'base line' might move upwards in a higher prolactin production state is not yet clear. Having moved away from the binary switch model, in which prolactin transcription exists in two states, 'on' or 'off', the theory of a switch between open and closed chromatin may be too simplistic, given that the model used in this study assumes that prolactin transcription can occur at any rate as a continuous variable.

The basal level of transcription increasing in high oestrogen states, could have to do with changes in the receptor distributions in the anterior pituitary, for example, oestrogen receptors are more abundant at proestrus and at oestrus (Gonzalez *et al.*, 2008) and the concentration of dopamine receptors is decreased (Zabavnik *et al.*, 1993) (Table 6.1.). This should result in more initiation and less inhibition of prolactin gene expression, respectively. Perhaps, the binding of the transcription apparatus (TA) (consisting primarily of general transcription factors, the mediator and transcriptional activators) which acts as a physical clamp (Wang *et al.*, 2013), is bound for a set length of a cycle, but allows varying numbers of transcriptional

Oestrous phase	Proestrus		Oestrus	Diestrus	
h-PRL expression	↑		↑↑	↓	
PRL [2]	Early	Late		Early	Late
		↑↑	↑	↓	
Da [1]			↑↑		
D2[1]				Early	Late
	↓		↓↓	↑	↑↑
E2 [2]	↑↑		↑	↓	
				Early	Late
ER[3]	↑↑		↑	↓	↓↓

Table 6.1. Changes in relative levels of prolactin, oestrogen and dopamine and their receptors, through the oestrous cycle

Expression levels of human prolactin (h-PRL) data are obtained from the study at hand. These are compared to varying levels of circulating prolactin (PRL), dopamine (Da), dopamine receptor (D2), oestradiol (E2) and oestrogen receptor (ER) in the rat. ***1 - Zabivink*** **et al.,** ***1993, 2 - Ben-Jonathan*** **et al.,** ***2008, 3 - Gonzalez*** **et al.,** ***2008***

initiations per cycle, based on the intranuclear levels of oestrogen available. Alternatively, the characteristics of promoter-proximal pausing of Pol II (Adelman & Lis, 2012) may be altered. In high prolactin producing states, the degree of pausing may be reduced, allowing more frequent elongation of transcripts.

Metivier *et al.*, (2003) have shown that, at least at the pS2 promoter, cycles of ER mediated transcription is pre-empted by an initial non-productive cycle, which may poise the chromatin (through longer term methylation) to be conducive to a higher or lower amount of transcription per cycle. The active cycle periods of ER binding to the pS2 gene in that study were only 40 minutes, which were followed by Pol II binding with a lag of 10 minutes, but this timing could be gene dependent (Muramoto *et al.*, 2012, Suter *et al.*, 2011b), accounting for the discrepancy in cycle times between pS2 and prolactin.

To test these hypotheses, it is necessary to study the binding of such transcription factors and histone modifications around the prolactin gene. Both chromatin

immunoprecipitation (ChIP) (Collas, 2010) and immunohistochemistry (Zluvova *et al.*, 2001) can be used to study histone modifications. ChIP however, can only be performed on bulk samples, which would not give the single cell definition needed to establish the transcription factor binding profiles in our single cell transcription patterns. Immunohistochemistry, despite being able to achieve single cell definition, like ChIP, cannot give an indication of which point of the transcription cycle is being studied. A high-throughput 'living' microarray has been pioneered by a group in Canada, which has enabled the measuring of transcriptional changes in real time in single mammalian cells (Rajan *et al.*, 2011). Although this study implemented a reverse transfection microarray, it could be amenable to a system using primary cells.

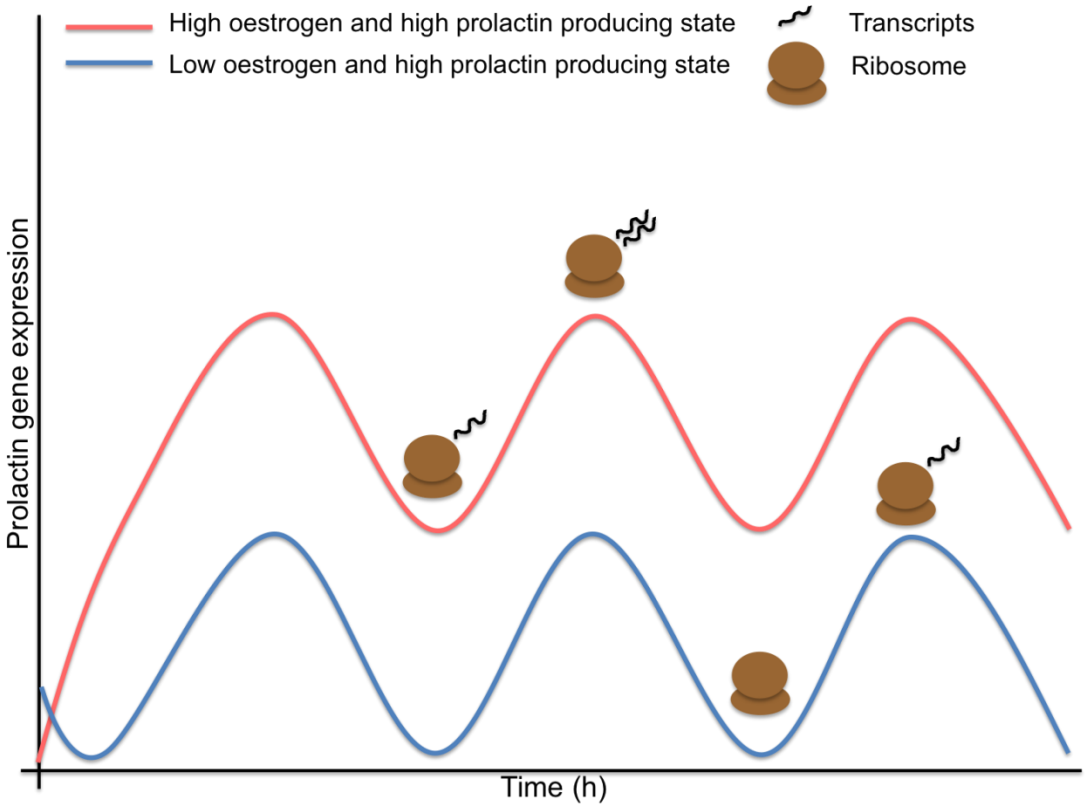

Figure 6.1. Model for the mechanism of single cell prolactin transcription cycles in high and low prolactin producing states

6.4. Future work

Mathematical modelling

As with most modelling approaches, the mathematical modelling of transcription rates is a method that is continuing to evolve and be under refinement. At the point of writing this thesis, fluorescence data was being run through an updated version of the algorithm used to calculate the data presented here. Analysis will be carried out on these algorithm outputs, for example correlation analysis to identify average lengths of high and low transcription rates and to formally investigate the amplitude of changes in rates between peaks and troughs in transcription. Durations of high and low rates will be compared between high and low oestrogen states, in order to distinguish changes in prolactin transcription dynamics as a result of altering the oestrogen state *in vivo*.

Endocrine cell networks

Work in our group by Dr. Karen Featherstone has highlighted the importance of cellular location and connectivity on the patterns of prolactin expression. The idea of a 3D endocrine cell network has been explored by other groups, particularly in somatotrophs.

Reconstructive two photon excitation microscopy was used to image the entire pituitary of GH-eGPF mice. This study provided evidence of a homotypic network of GH cells, connected by adherens junctions, as opposed to a collection of dispersed cells. The tissue was shown to have the three primary features thought to constitute a biological network: a robust architecture that holds constant throughout the lifespan, a modularity correlating to both GH content and growth patterns and lastly, connectivity between cells that synchronise to coordinate cellular activity. This cellular organisation and communication within the gland has been suggested to be important for cellular function, in the coordination of hormonal secretion from somatotrophs (Bonnefont *et al.*, 2005). Evidence for functional connectivity has also been seen between lactotrophs, with inter-cellular signalling through gap junctions (Hodson *et al.*, 2012), which may be involved in a similar function in secretory coordination of prolactin.

The recently trialled Zeiss Multiview Light Sheet Fluorescence Microscope Z.1 (LSFM) will allow the study of prolactin reporter gene expression from Fischer 344 (d2eGFP-hPRL 455) tissue slices over time, in 3D. While the confocal microscopy used to collect single cell fluorescence data in this project uses z-stacking, giving in theory, a 3D view through the tissue slices, this data is compacted for the purpose of cell tracking. The LSFM, on the other hand, can obtain both Z-stack information as well as rotational optical sections (Figure 6.2.). These images can be combined to render a 3D image. The LSFM enables the illumination of single thin sections at a time, by exciting fluorescence from only the in-focus plane, as compared to the illumination of the whole tissue, as is the case in conventional fluorescence confocal microscopy. This system allows high temporal resolution of sub cellular components within the context of 3D structures, with limited phototoxicity (microscopy.zeiss.com). This technology will aid the study of the nature of the spatial relationship between lactotrophs within the pituitary currently being undertaken by Dr. Featherstone, who is looking into the possibility of relating transcription patterns to a function of cell-to-cell distance and location within the gland.

New models

In keeping with the current Fischer 344 (d2eGFP-hPRL 455) rats used for this study, additional states of interest include pregnancy and lactation. I would like to compare any changes seen in prolactin transcription dynamics in the more subtle fluctuations of oestrogen through the oestrous cycle with the yet further increased circulating oestrogen seen during pregnancy and in the high prolactin producing state of lactation. Ovariectomy in the female and the study of prolactin producing tumours would provide a comparison of the deficient and excess states of prolactin production.

The incorporation of a nuclear marker into the model system would enable the use of automated cell tracking. This could be achieved by for example tagging a fluorescence protein to histone 2B (Saffin *et al.*, 2005). Whilst our current model was generated in the rat, due to ease of dissection of the large pituitary and the oestrogen sensitivity of this particular strain, new transgenic models, including for example such a nuclear marker, could conveniently be developed in the mouse, reducing the cost of housing significantly. Furthermore, with the wide spread use of

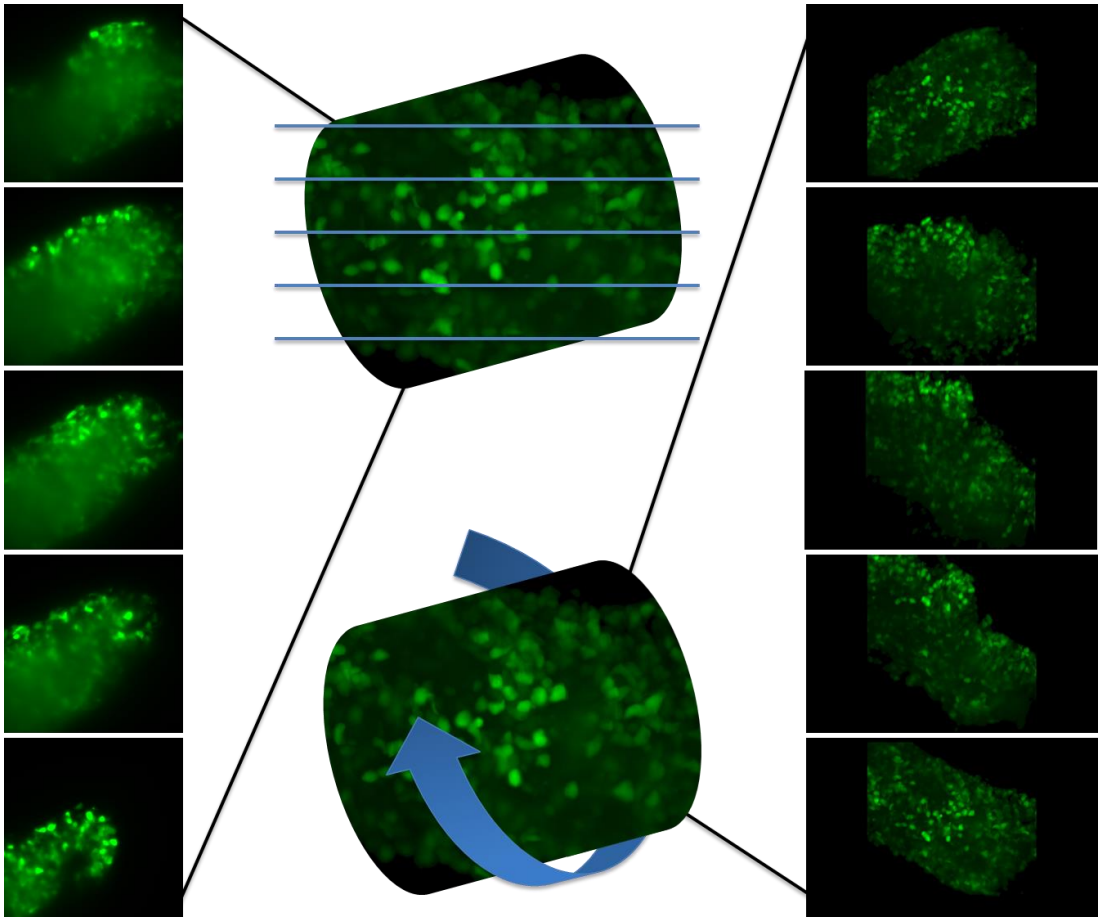

Figure 6.2. Light sheet microscopy

Conceptual schematic of The Zeiss Multiview Light Sheet Fluorescence Microscope's ability to collect both z-stack and rotational optical slices through a 250µm section of pituitary tissue from a Fischer 344 rat expressing d2eGFP under the control of the human prolactin promoter. The sequence on the left show a selection of images through the z-plane and images on the right shows a selection of optical slices through a 180º rotation of the same tissue. ***Figure based on data obtained by Dr. Karen Featherstone.***

the mouse as a model, would hold the further advantage of crossing with other conditional transgenics. By endeavouring to create a transgenic model with a single insertion copy number we can eliminate the possibility of the cycles of single cell reporter gene activity being due to a cumulative signal from the 2 to 4 insertion sites of our current model.

6.5. Conclusion

In this study I have used live tissue time-lapse fluorescence confocal microscopy in combination with mathematical modelling to show that prolactin is transcribed in cycles of approximately 10 to 15 hours. We have found that single cells within the context of pituitary tissue display heterogeneous transcription patterns, which may facilitate a graded response to the various transient and sustained stimulations that the body is subjected to, by affecting not only the transcription rate of the individual cell, but also the number of cells recruited to the expressing cell population. We have shown that overall mRNA output of prolactin expression is dependent on the *in vivo* oestrogen status of the rat, with increased oestrogen inducing a higher prolactin producing state, but that regardless of oestrogen status, the fundamental mechanism of cycling transcription remains unaltered in both high-production and low-production states.

References

References

Acconcia, F. & Kumar, R. (2006) Signaling regulation of genomic and nongenomic functions of estrogen receptors. *Cancer Letters,* 238(1).

Adamson, A. D., Friedrichsen, S., Semprini, S., Harper, C. V., Mullins, J. J., White, M. R. H. & Davis, J. R. E. (2008) Human prolactin gene promoter regulation by estrogen: Convergence with tumor necrosis factor-alpha signaling. *Endocrinology,* 149(2)**,** 687-694.

Adelman, K. & Lis, J. T. (2012) Promoter-proximal pausing of rna polymerase ii: Emerging roles in metazoans. *Nature Reviews Genetics,* 13(10)**,** 720-731.

Amara, J. F., Vanitallie, C. & Dannies, P. S. (1987) Regulation of prolactin production and cell-growth by estradiol - difference in sensitivity to estradiol occurs at level of messenger-ribonucleic-acid accumulation. *Endocrinology,* 120(1)**,** 264-271.

Andersen, B. & Rosenfeld, M. G. (2001) Pou domain factors in the neuroendocrine system: Lessons from developmental biology provide insights into human disease. *Endocrine Reviews,* 22(1)**,** 2-35.

Andrews, Z. B. (2005) Neuroendocrine regulation of prolactin secretion during late pregnancy: Easing the transition into lactation. *Journal of Neuroendocrinology,* 17(7)**,** 466-473.

Asa, S. L. & Ezzat, S. (1998) The cytogenesis and pathogenesis of pituitary adenomas. *Endocrine Reviews,* 19(6)**,** 798-827.

Bancroft, F. C. & Tashjian, A. H. (1971) Growth in suspension culture of rat pituitary cells which produce growth hormone and prolactin. *Experimental Cell Research,* 64(1)**,** 125-&.

Belandia, B., Orford, R. L., Hurst, H. C. & Parker, M. G. (2002) Targeting of swi/snf chromatin remodelling complexes to estrogen-responsive genes. *Embo Journal,* 21(15)**,** 4094-4103.

Ben-Jonathan, N. & Hnasko, R. (2001) Dopamine as a prolactin (prl) inhibitor. *Endocrine Reviews,* 22(6)**,** 724-763.

Ben-Jonathan, N., Lapensee, C. R. & Lapensee, E. W. (2008) What can we learn from rodents about prolactin in humans? *Endocrine Reviews,* 29(1)**,** 1-41.

Berno, V., Amazit, L., Hinojos, C., Zhong, J., Mancini, M. G., Sharp, Z. D. & Mancini, M. A. (2008) Activation of estrogen receptor-alpha by e2 or egf induces temporally distinct patterns of large-scale chromatin modification and mrna transcription. *Plos One,* 3(5).

Berwaer, M., Martial, J. A. & Davis, J. R. E. (1994) Characterization of an up-stream promoter directing extrapituitary expression of the human prolactin gene. *Molecular Endocrinology,* 8(5)**,** 635-642.

Berwaer, M., Monget, P., Peers, B., Mathyhartert, M., Bellefroid, E., Davis, J. R. E., Belayew, A. & Martial, J. A. (1991) Multihormonal regulation of the human prolactin gene-expression from 5000 bp of its upstream sequence. *Molecular and Cellular Endocrinology,* 80(1-3)**,** 53-64.

Bodner, M., Castrillo, J. L., Theill, L. E., Deerinck, T., Ellisman, M. & Karin, M. (1988) The pituitary-specific transcription factor-ghf-1 is a homeobox-containing protein. *Cell,* 55(3)**,** 505-518.

Bole-Feysot, C., Goffin, V., Edery, M., Binart, N. & Kelly, P. A. (1998) Prolactin (prl) and its receptor: Actions, signal transduction pathways and phenotypes observed in prl receptor knockout mice. *Endocrine Reviews,* 19(3)**,** 225-268.

Bonnefont, X., Lacampagne, A., Sanchez-Hormigo, A., Fino, E., Creff, A., Mathieu, M. N., Smallwood, S., Carmignac, D., Fontanaud, P., Travo, P., Alonso, G., Courtois-Coutry, N., Pincus, S. M., Robinson, I. & Mollard, P. (2005) Revealing the large-scale network organization of growth hormone-secreting cells. *Proceedings of the National Academy of Sciences of the United States of America,* 102(46)**,** 16880-16885.

Boockfor, F. R., Hoeffler, J. P. & Frawley, L. S. (1986) Estradiol induces a shift in cultured-cells that release prolactin or growth-hormone. *American Journal of Physiology,* 250(1)**,** E103-E105.

Bose, S. & Boockfor, F. R. (2010) Episodes of prolactin gene expression in gh(3) cells are dependent on selective promoter binding of multiple circadian elements. *Endocrinology,* 151(5)**,** 2287-2296.

Brown, C. R., Mao, C., Falkovskaia, E., Jurica, M. S. & Boeger, H. (2013) Linking stochastic fluctuations in chromatin structure and gene expression. *PLoS Biol,* 11(8)**,** e1001621.

Budry, L., Lafont, C., El Yandouzi, T., Chauvet, N., Conejero, G., Drouin, J. & Mollard, P. (2011) Related pituitary cell lineages develop into interdigitated 3d cell networks. *Proceedings of the National Academy of Sciences of the United States of America,* 108(30)**,** 12515-12520.

Cadigan, K. M. & Nusse, R. (1997) Wnt signaling: A common theme in animal development. *Genes & Development,* 11(24)**,** 3286-3305.

Campbell, N. & Reece, J. (2005) *Biology,* (7th edn) (Pearson).

Carreau, S., Wolczynski, S. & Galeraud-Denis, I. (2010) Aromatase, oestrogens and human male reproduction. *Philosophical Transactions of the Royal Society B-Biological Sciences,* 365(1546)**,** 1571-1579.

Castano, J. P., Kineman, R. D. & Frawley, L. S. (1994) Dynamic fluctuations in the secretory activity of individual lactotropes as demonstrated by a modified sequential plaque-assay. *Endocrinology,* 135(5)**,** 1747-1752.

Castano, J. P., Kineman, R. D. & Frawley, L. S. (1996) Dynamic monitoring and quantification of gene expression in single, living cells: A molecular basis for secretory cell heterogeneity. *Molecular Endocrinology,* 10(5)**,** 599-605.

Chen, D. G., Huang, S. M. & Stallcup, M. R. (2000) Synergistic, p160 coactivator-dependent enhancement of estrogen receptor function by carm1 and p300. *Journal of Biological Chemistry,* 275(52)**,** 40810-40816.

Christian, H. C., Chapman, L. P. & Morris, J. F. (2007) Thyrotrophin-releasing hormone, vasoactive intestinal peptide, prolactin-releasing peptide and dopamine regulation of prolactin secretion by different lactotroph morphological subtypes in the rat. *Journal of Neuroendocrinology,* 19(8)**,** 605-613.

Christian, H. C. & Morris, J. F. (2002) Rapid actions of 17 beta-oestradiol on a subset of lactotrophs in the rat pituitary. *Journal of Physiology-London,* 539(2)**,** 557-566.

Collas, P. (2010) The current state of chromatin immunoprecipitation. *Molecular Biotechnology,* 45(1).

Corish, P. & Tyler-Smith, C. (1999) Attenuation of green fluorescent protein half-life in mammalian cells. *Protein Engineering,* 12(12)**,** 1035-1040.

Craig, F. F., Simmonds, A. C., Watmore, D., Mccapra, F. & White, M. R. H. (1991) Membrane-permeable luciferin esters for assay of firefly luciferase in live intact-cells. *Biochemical Journal,* 276(637-641.

Davis, J. R. E., Farrell, W. E. & Clayton, R. N. (2001) Pituitary tumours. *Reproduction,* 121(3)**,** 363-371.

Day, R. N., Koike, S., Sakai, M., Muramatsu, M. & Maurer, R. A. (1990) Both pit-1 and the estrogen-receptor are required for estrogen responsiveness of the rat prolactin gene. *Molecular Endocrinology,* 4(12)**,** 1964-1971.

Deisseroth, K., Feng, G., Majewska, A. K., Miesenbock, G., Ting, A. & Schnitzer, M. J. (2006) Next-generation optical technologies for illuminating genetically targeted brain circuits. *Journal of Neuroscience,* 26(41)**,** 10380-10386.

Demssie, Y. N. & Davis, J. R. E. (2008) Hyperprolactinaemia. *Clinical Medicine,* 8(2)**,** 216-219.

Depaul, A. L., Pons, P., Aoki, A. & Torres, A. I. (1997) Heterogeneity of pituitary lactotrophs: Immunocytochemical identification of functional subtypes. *Acta Histochemica,* 99(3).

Dewet, J. R., Wood, K. V., Deluca, M., Helinski, D. R. & Subramani, S. (1987) Firefly luciferase gene - structure and expression in mammalian-cells. *Molecular and Cellular Biology,* 7(2)**,** 725-737.

Diamond, S. E. & Gutierrez-Hartmann, A. (2000) The pit-1 beta domain dictates active repression and alteration of histone acetylation of the proximal prolactin promoter. *Journal of Biological Chemistry,* 275(40)**,** 30977-30986.

Dimattia, G. E., Gellersen, B., Bohnet, H. G. & Friesen, H. G. (1988) A human-b-lymphoblastoid cell-line produces prolactin. *Endocrinology,* 122(6)**,** 2508-2517.

Dimattia, G. E., Gellersen, B., Duckworth, M. L. & Friesen, H. G. (1990) Human prolactin gene-expression - the use of an alternative noncoding exon in decidua and the im-9-p3 lymphoblast cell-line. *Journal of Biological Chemistry,* 265(27)**,** 16412-16421.

Duplessis, T. T., Williams, C. C., Hill, S. M. & Rowan, B. G. (2011) Phosphorylation of estrogen receptor alpha at serine 118 directs recruitment of promoter complexes and gene-specific transcription. *Endocrinology,* 152(6)**,** 2517-2526.

Eberharter, A. & Becker, P. B. (2002) Histone acetylation: A switch between repressive and permissive chromatin - second in review series on chromatin dynamics. *Embo Reports,* 3(3)**,** 224-229.

El-Kasti, M. M., Christian, H. C., Huerta-Ocampo, I., Stolbrink, M., Gill, S., Houston, P. A., Davies, J. S., Chilcott, J., Hill, N., Matthews, D. R., Carter, D. A. & Wells, T. (2008) The pregnancy-induced increase in baseline circulating growth hormone in rats is not induced by ghrelin. *Journal of Neuroendocrinology,* 20(3)**,** 309-322.

Elowitz, M. B., Levine, A. J., Siggia, E. D. & Swain, P. S. (2002) Stochastic gene expression in a single cell. *Science,* 297(5584).

Enmark, E. & Gustafsson, J. A. (1999) Oestrogen receptors - an overview. *Journal of Internal Medicine,* 246(2).

Farrell, W. E. & Clayton, R. N. (1998) Molecular genetics of pituitary tumours. *Trends in Endocrinology and Metabolism,* 9(1)**,** 20-26.

Featherstone, K., Harper, C. V., Mcnamara, A., Semprini, S., Spiller, D. G., Mcneilly, J., Mcneilly, A. S., Mullins, J. J., White, M. R. H. & Davis, J. R. E. (2011) Pulsatile patterns of pituitary hormone gene expression change during development. *Journal of Cell Science,* 124(20).

Featherstone, K., White, M. R. H. & Davis, J. R. E. (2012) The prolactin gene: A paradigm of tissue-specific gene regulation with complex temporal transcription dynamics. *Journal of Neuroendocrinology,* 24(7)**,** 977-990.

Freeman, M. E., Kanyicska, S., Lerant, A. & Nagy, G. (2000) Prolactin: Structure, function, and regulation of secretion. *Physiological Reviews,* 80(4)**,** 1523-1631.

Friedrichsen, S., Harper, C. V., Semprini, S., Wilding, M., Adamson, A. D., Spiller, D. G., Nelson, G., Mullins, J. J., White, M. R. H. & Davis, J. R. E. (2006) Tumor necrosis factor-alpha activates the human prolactin gene promoter via nuclear factor-kappa b signaling. *Endocrinology,* 147(2)**,** 773-781.

Fullwood, M. J., Liu, M. H., Pan, Y. F., Liu, J., Xu, H., Bin Mohamed, Y., Orlov, Y. L., Velkov, S., Ho, A., Mei, P. H., Chew, E. G. Y., Huang, P. Y. H., Welboren, W. J., Han, Y. Y., Ooi, H. S., Ariyaratne, P. N., Vega, V. B., Luo, Y. Q., Tan, P. Y., Choy, P. Y., Wansa, K., Zhao, B., Lim, K. S., Leow, S. C., Yow, J. S., Joseph, R., Li, H. X., Desai, K. V., Thomsen, J. S., Lee, Y. K., Karuturi, R. K. M., Herve, T., Bourque, G., Stunnenberg, H. G., Ruan, X. L., Cacheux-Rataboul, V., Sung, W. K., Liu, E. T., Wei, C. L., Cheung, E. & Ruan, Y. J. (2009) An oestrogen-receptor-alpha-bound human chromatin interactome. *Nature,* 462(7269)**,** 58-64.

Gaytan, F., Bellido, C., Morales, C. & Sanchez-Criado, J. E. (2001) Luteolytic effect of prolactin is dependent on the degree of differentiation of luteal cells in the rat. *Biology of Reproduction,* 65(2)**,** 433-441.

Gellersen, B., Dimattia, G. E., Friesen, H. G. & Bohnet, H. G. (1989) Prolactin (prl) messenger-rna from human decidua differs from pituitary prl messenger-rna but resembles the im-9-p3 lymphoblast prl transcript. *Molecular and Cellular Endocrinology,* 64(1)**,** 127-130.

Gellersen, B., Kempf, R., Telgmann, R. & Dimattia, G. E. (1994) Nonpituitary human prolactin gene-transcription is independent of pit-1 and differentially controlled in lymphocytes and in endometrial stroma. *Molecular Endocrinology,* 8(3)**,** 356-373.

Gellersen, B., Kempf, R., Telgmann, R. & Dimattia, G. E. (1995) Pituitary-type transcription of the human prolactin gene in the absence of pit-1. *Molecular Endocrinology,* 9(7)**,** 887-901.

Gerlo, S., Davis, J. R. E., Mager, D. L. & Kooijman, R. (2006) Prolactin in man: A tale of two promoters. *Bioessays,* 28(1051-1055.

Giles, A., Madec, F., Friedrichsen, S., Featherstone, K., Chambers, T., Harper, C. V., Resch, J., Brabant, G. & Davis, J. R. E. (2011) Wnt signaling in estrogen-induced lactotroph proliferation. *Journal of Cell Science,* 124(4).

Gonzalez, M., Reyes, R., Damas, C., Alonso, R. & Bello, A. R. (2008) Oestrogen receptor alpha and beta in female rat pituitary cells: An immunochemical study. *General and Comparative Endocrinology,* 155(3)**,** 857-868.

Gonzalezparra, S., Chowen, J. A., Segura, L. M. G. & Argente, J. (1996) Ontogeny of pituitary transcription factor-1 (pit-1), growth hormone (gh) and prolactin (prl) mrna levels in male and female rats and the differential expression of pit-1 in lactotrophs and somatotrophs. *Journal of Neuroendocrinology,* 8(3)**,** 211-225.

Gothard, L. Q., Hibbard, J. C. & Seyfred, M. A. (1996) Estrogen-mediated induction of rat prolactin gene transcription requires the formation of a chromatin loop between the distal enhancer and proximal promoter regions. *Molecular Endocrinology,* 10(2)**,** 185-195.

Gourdji, D. & Laverriere, J. N. (1994) The rat prolactin gene - a target for tissue-specific and hormone-dependent transcription factors. *Molecular and Cellular Endocrinology,* 100(1-2)**,** 133-142.

Green, S., Walter, P., Kumar, V., Krust, A., Bornert, J. M., Argos, P. & Chambon, P. (1986) Human estrogen-receptor cdna - sequence, expression and homology to v-erb-a. *Nature,* 320(6058).

Grosdemouge, I., Bachelot, A., Lucas, A., Baran, N., Kelly, P. A. & Binart, N. (2003) Effects of deletion of the prolactin receptor on ovarian gene expression. *Reproductive biology and endocrinology : RB&E,* 1(12.

Gruber, C. J., Tschugguel, W., Schneeberger, C. & Huber, J. C. (2002) Mechanisms of disease - production and actions of estrogens. *New England Journal of Medicine,* 346(5)**,** 340-352.

Grunstein, M., Carmen, A., Rundlett, S., Strahl-Bolsinger, S. & Hecht, A. (1997) Histone acetylation and deacetylation. *FASEB Journal,* 11(9)**,** A1300.

Guillaumond, F., Boyer, B., Becquet, D., Guillen, S., Kuhn, L., Garin, J., Belghazi, M., Bosler, O., Franc, J. L. & Francois-Bellan, A. M. (2011) Chromatin remodeling as a mechanism for circadian prolactin transcription: Rhythmic nono and sfpq recruitment to hltf. *Faseb Journal,* 25(8)**,** 2740-2756.

Guyda, H., Hwang, P. & Friesen, H. (1971) Radioimmunoassay for human prolactin. *Journal of Clinical Investigation,* 50(6)**,** A41-&.

Hall, W. A., Luciano, M. G., Doppman, J. L., Patronas, N. J. & Oldfield, E. H. (1994) Pituitary magnetic-resonance-imaging in normal human volunteers - occult adenomas in the general-population. *Annals of Internal Medicine,* 120(10)**,** 817-820.

Harper, C. V., Featherstone, K., Semprini, S., Friedrichsen, S., Mcneilly, J., Paszek, P., Spiller, D. G., Mcneilly, A. S., Mullins, J. J., Davis, J. R. E. & White, M. R. H. (2010) Dynamic organisation of prolactin gene expression in living pituitary tissue. *Journal of Cell Science,* 123(3)**,** 424-430.

Harper, C. V., Finkenstaedt, B., Woodcock, D. J., Friedrichsen, S., Semprini, S., Ashall, L., Spiller, D. G., Mullins, J. J., Rand, D. A., Davis, J. R. E. & White, M. R. H. (2011) Dynamic analysis of stochastic transcription cycles. *Plos Biology,* 9(4).

Heaney, A. P. & Melmed, S. (1999) Pituitary tumour transforming gene: A novel factor in pituitary tumour formation. *Best Practice & Research Clinical Endocrinology & Metabolism,* 13(3)**,** 367-380.

Heim, R., Cubitt, A. B. & Tsien, R. Y. (1995) Improved green fluorescence. *Nature,* 373(6516)**,** 663-664.

Hodson, D. J., Molino, F., Fontanaud, P., Bonnefont, X. & Mollard, P. (2010) Investigating and modelling pituitary endocrine network function. *J Neuroendocrinol,* 22(12)**,** 1217-25.

Hodson, D. J., Schaeffer, M., Romano, N., Fontanaud, P., Lafont, C., Birkenstock, J., Molino, F., Christian, H., Lockey, J., Carmignac, D., Fernandez-Fuente, M., Le Tissier, P. & Mollard, P. (2012) Existence of long-lasting experience-dependent plasticity in endocrine cell networks. *Nature Communications,* 3(

Huerta-Ocampo, I., Christian, H. C., Thompson, N. M., El Kasti, M. M. & Wells, T. (2005) The intermediate lactotroph: A morphologically distinct, ghrelin-responsive pituitary cell in the dwarf (dw/dw) rat. *Endocrinology,* 146(11)**,** 5012-5023.

Hume, D. A. (2000) Probability in transcriptional regulation and its implications for leukocyte differentiation and inducible gene expression. *Blood,* 96(7)**,** 2323-2328.

Ingraham, H. A., Chen, R., Mangalam, H. J., Elsholtz, H. P., Flynn, S. E., Lin, C. R., Simmons, D. M., Swanson, L. & Rosenfeld, M. G. (1988) A tissue-specific transcription factor containing a homeodomain specifies a pituitary phenotype. *Cell,* 55(3)**,** 519-529.

Jenuwein, T. & Allis, C. D. (2001) Translating the histone code. *Science,* 293(5532)**,** 1074-1080.

Kansra, S., Yamagata, S., Sneade, L., Foster, L. & Ben-Jonathan, N. (2005) Differential effects of estrogen receptor antagonists on pituitary lactotroph proliferation and prolactin release. *Molecular and Cellular Endocrinology,* 239(1-2)**,** 27-36.

Kievit, P. & Maurer, R. A. (2005) The pituitary-specific transcription factor, pit-1, can direct changes in the chromatin structure of the prolactin promoter. *Molecular Endocrinology,* 19(1)**,** 138-147.

Klinge, C. M. (2001) Estrogen receptor interaction with estrogen response elements. *Nucleic Acids Research,* 29(14)**,** 2905-2919.

Kouzarides, T. (2007) Chromatin modifications and their function. *Cell,* 128(4)**,** 693-705.

Kuiper, G., Enmark, E., Peltohuikko, M., Nilsson, S. & Gustafsson, J. A. (1996) Cloning of a novel estrogen receptor expressed in rat prostate and ovary. *Proceedings of the National Academy of Sciences of the United States of America,* 93(12)**,** 5925-5930.

Lannigan, D. A. (2003) Estrogen receptor phosphorylation. *Steroids,* 68(1)**,** 1-9.

Leclerc, G. M. & Boockfor, F. R. (2005) Pulses of prolactin promoter activity depend on a noncanonical e-box that can bind the circadian proteins clock and bmal1. *Endocrinology,* 146(6)**,** 2782-2790.

Li, W. B., Notani, D., Ma, Q., Tanasa, B., Nunez, E., Chen, A. Y., Merkurjev, D., Zhang, J., Ohgi, K., Song, X. Y., Oh, S., Kim, H. S., Glass, C. K. & Rosenfeld, M. G. (2013) Functional roles of enhancer rnas for oestrogen-dependent transcriptional activation. *Nature,* 498(7455)**,** 516-+.

Li, X. Q., Zhao, X. N., Fang, Y., Jiang, X., Duong, T., Fan, C., Huang, C. C. & Kain, S. R. (1998) Generation of destabilized green fluorescent protein transcription reporter. *Journal of Biological Chemistry,* 273(52)**,** 34970-34975.

Lipniacki, T., Paszek, P., Marciniak-Czochra, A., Brasier, A. R. & Kimmel, M. (2006) Transcriptional stochasticity in gene expression. *Journal of Theoretical Biology,* 238(2)**,** 348-367.

Liu, X. F. & Bagchi, M. K. (2004) Recruitment of distinct chromatin-modifying complexes by tamoxifen-complexed estrogen receptor at natural target gene promoters in vivo. *Journal of Biological Chemistry,* 279(15)**,** 15050-15058.

Llovera, M., Touraine, P., Kelly, P. A. & Goffin, V. (2000) Involvement of prolactin in breast cancer: Redefining the molecular targets. *Experimental Gerontology,* 35(1)**,** 41-51.

Magoulas, C., Mcguinness, L., Balthasar, N., Carmignac, D. F., Sesay, A. K., Mathers, K. E., Christian, H., Candeil, L., Bonnefont, X., Mollard, P. & Robinson, I. (2000) A secreted fluorescent reporter targeted to pituitary growth hormone cells in transgenic mice. *Endocrinology,* 141(12)**,** 4681-4689.

Malayer, J. R. & Gorski, J. (1995) The role of estrogen-receptor in modulation of chromatin conformation in the 5'-flanking region of the rat prolactin gene. *Molecular and Cellular Endocrinology,* 113(2)**,** 145-154.

Mandl, A. M. (1951) The phases of the oestrous cycle in the adult white rat. *Journal of Experimental Biology,* 28(4)**,** 576-584.

Mann, P. E. & Bridges, R. S. (2001) Lactogenic hormone regulation of maternal behavior. *Progress in brain research,* 133(251-62.

Marcondes, F. K., Bianchi, F. J. & Tanno, A. P. (2002) Determination of the estrous cycle phases of rats: Some helpful considerations. *Brazilian Journal of Biology,* 62(4A)**,** 609-614.

Matera, L. (1996) Endocrine, paracrine and autocrine actions of prolactin on immune cells. *Life Sciences,* 59(8)**,** 599-614.

Maurer, R. A. (1982) Estradiol regulates the transcription of the prolactin gene. *Journal of Biological Chemistry,* 257(5)**,** 2133-2136.

Mcferran, D. W., Stirland, J. A., Norris, A. J., Khan, R. A., Takasuka, N., Seymour, Z. C., Gill, M. S., Robertson, W. R., Loudon, A. S. I., Davis, J. R. E. & White, M. R. H. (2001) Persistent synchronized oscillations in prolactin gene promoter activity in living pituitary cells. *Endocrinology,* 142(7)**,** 3255-3260.

Metivier, R., Penot, G., Hubner, M. R., Reid, G., Brand, H., Kos, M. & Gannon, F. (2003) Estrogen receptor-alpha directs ordered, cyclical, and combinatorial recruitment of cofactors on a natural target promoter. *Cell,* 115(6)**,** 751-763.

Metivier, R., Reid, G. & Gannon, F. (2006) Transcription in four dimensions: Nuclear receptor-directed initiation of gene expression. *Embo Reports,* 7(2)**,** 161-167.

Mitrunen, K. & Hirvonen, A. (2003) Molecular epidemiology of sporadic breast cancer - the role of polymorphic genes involved in oestrogen biosynthesis and metabolism. *Mutation Research-Reviews in Mutation Research,* 544(1)**,** 9-41.

Mosselman, S., Polman, J. & Dijkema, R. (1996) Er beta: Identification and characterization of a novel human estrogen receptor. *Febs Letters,* 392(1).

Muramoto, T., Cannon, D., Gierlinski, M., Corrigan, A., Barton, G. J. & Chubb, J. R. (2012) Live imaging of nascent rna dynamics reveals distinct types of transcriptional pulse regulation. *Proceedings of the National Academy of Sciences of the United States of America,* 109(19).

Murdoch, F. E., Byrne, L. M., Ariazi, E. A., Furlow, J. D., Meier, D. A. & Gorski, J. (1995) Estrogen-receptor binding to dna - affinity for nonpalindromic elements from the rat prolactin gene. *Biochemistry,* 34(28)**,** 9144-9150.

Neill, J. (1988) *Knobil and neill's physiology of reproduction,* (3rd edn) (Academic Press).

Nelson, L. R. & Bulun, S. E. (2001) Estrogen production and action. *Journal of the American Academy of Dermatology,* 45(3)**,** S116-S124.

Neville, M. C., Mcfadden, T. B. & Forsyth, I. (2002) Hormonal regulation of mammary differentiation and milk secretion. *Journal of Mammary Gland Biology and Neoplasia,* 7(1)**,** 49-66.

Newlands, S., Levitt, L. K., Robinson, C. S., Karpf, A. B. C., Hodgson, V. R. M., Wade, R. P. & Hardeman, E. C. (1998) Transcription occurs in pulses in muscle fibers. *Genes & Development,* 12(17)**,** 2748-2758.

Nogami, H., Yoshimura, F., Herbert, D. C., Aufdemorte, T. B., Gates, G. A., Holt, G. R. & Sheridan, P. J. (1985) Changes in the nuclear uptake and retention of h-3 estrogen in gonadotrophs and lactotrophs as a function of age. *Anatomical Record,* 212(3)**,** 288-291.

Nolan, L. A. & Levy, A. (2009) The trophic effects of oestrogen on male rat anterior pituitary lactotrophs. *Journal of Neuroendocrinology,* 21(5)**,** 457-464.

Norris, A. J., Stirland, J. A., Mcferran, D. W., Seymour, Z. C., Spiller, D. G., Loudon, A. S. I., White, M. R. H. & Davis, J. R. E. (2003) Dynamic patterns of growth hormone gene transcription in individual living pituitary cells. *Molecular Endocrinology,* 17(2)**,** 193-202.

Nowakowski, B. E. & Maurer, R. A. (1994) Multiple pit-1-binding sites facilitate estrogen responsiveness of the prolactin gene. *Molecular Endocrinology,* 8(12)**,** 1742-1749.

Nye, A. C., Rajendran, R. R., Stenoien, D. L., Mancini, M. A., Katzenellenbogen, B. S. & Belmont, A. S. (2002) Alteration of large-scale chromatin structure by estrogen receptor. *Molecular and Cellular Biology,* 22(10)**,** 3437-3449.

O'lone, R., Frith, M. C., Karlsson, E. K. & Hansen, U. (2004) Genomic targets of nuclear estrogen receptors. *Molecular Endocrinology,* 18(8).

Paszek, P., Lipniacki, T., Brasier, A. R., Tian, B., Nowak, D. E. & Kimmel, M. (2005) Stochastic effects of multiple regulators on expression profiles in eukaryotes. *Journal of Theoretical Biology,* 233(3)**,** 423-433.

Pedraza, J. M. & Paulsson, J. (2008) Effects of molecular memory and bursting on fluctuations in gene expression. *Science,* 319(5861)**,** 339-343.

Peers, B., Voz, M. L., Monget, P., Mathyhartert, M., Berwaer, M., Belayew, A. & Martial, J. A. (1990) Regulatory elements controlling pituitary-specific expression of the human prolactin gene. *Molecular and Cellular Biology,* 10(9)**,** 4690-4700.

Perks, C. M., Newcomb, P. V., Grohmann, M., Wright, R. J., Mason, H. D. & Holly, J. M. P. (2003) Prolactin acts as a potent survival factor against c2-ceramide-induced apoptosis in human granulosa cells. *Human Reproduction,* 18(12)**,** 2672-2677.

Peters, B. J. & Rillema, J. A. (1992) Effect of prolactin on 2-deoxyglucose uptake in mouse mammary-gland explants. *American Journal of Physiology,* 262(5)**,** E627-E630.

Pettersson, K., Grandien, K., Kuiper, G. & Gustafsson, J. A. (1997) Mouse estrogen receptor beta forms estrogen response element-binding heterodimers with estrogen receptor alpha. *Molecular Endocrinology,* 11(10)**,** 1486-1496.

Quentien, M. H., Barlier, A., Franc, J. L., Pellegrini, I., Brue, T. & Enjalbert, A. (2006) Pituitary transcription factors: From congenital deficiencies to gene therapy. *Journal of Neuroendocrinology,* 18(9)**,** 633-642.

Raj, A., Peskin, C. S., Tranchina, D., Vargas, D. Y. & Tyagi, S. (2006) Stochastic mrna synthesis in mammalian cells. *Plos Biology,* 4(10).

Raj, A. & Van Oudenaarden, A. (2008) Nature, nurture, or chance: Stochastic gene expression and its consequences. *Cell,* 135(2)**,** 216-226.

Raj, A. & Van Oudenaarden, A. (2009) Single-molecule approaches to stochastic gene expression*Annual review of biophysics.* (vol. 38)Palo Alto, Annual Reviews), 255-270.

Rajan, S., Djambazian, H., Dang, H. C. P., Sladek, R. & Hudson, T. J. (2011) The living microarray: A high-throughput platform for measuring transcription dynamics in single cells. *Bmc Genomics,* 12(

Rang, H. P., Dale, M. M., J.M., R. & P.K., M. (2005) *Pharmacology,* (5th edn) (Elsevier Science Limited).

Raser, J. M. & O'shea, E. K. (2004) Control of stochasticity in eukaryotic gene expression. *Science,* 304(5678)**,** 1811-1814.

Saffin, J. M., Venoux, M., Prigent, C., Espeut, J., Poulat, F., Giorgi, D., Abrieu, A. & Rouquier, S. (2005) Asap, a human microtubule-associated protein required for bipolar spindle assembly and cytokinesis. *Proceedings of the National Academy of Sciences of the United States of America,* 102(32)**,** 11302-11307.

Sanchez, A., Choubey, S. & Kondev, J. (2013) Regulation of noise in gene expression. *Annual Review of Biophysics, Vol 42,* 42(469-491.

Schaeffer, M., Hodson, D. J., Meunier, A.-C., Lafont, C., Birkenstock, J., Carmignac, D., Murray, J. F., Gavois, E., Robinson, I. C., Le Tissier, P. & Mollard, P. (2011) Influence of estrogens on gh-cell network dynamics in females: A live in situ imaging approach. *Endocrinology,* 152(12)**,** 4789-4799.

Schneider-Poetsch, T., Ju, J., Eyler, D. E., Dang, Y., Bhat, S., Merrick, W. C., Green, R., Shen, B. & Liu, J. O. (2010) Inhibition of eukaryotic translation elongation by cycloheximide and lactimidomycin. *Nature Chemical Biology,* 6(3)**,** 209-217.

Schwarzler, P., Untergasser, G., Hermann, M., Dirnhofer, S., Abendstein, B. & Berger, P. (1997) Prolactin gene expression and prolactin protein in premenopausal and postmenopausal human ovaries. *Fertility and Sterility,* 68(4)**,** 696-701.

Scully, K. M., Gleiberman, A. S., Lindzey, J., Lubahn, D. B., Korach, K. S. & Rosenfeld, M. G. (1997) Role of estrogen receptor-alpha in the anterior pituitary gland. *Molecular Endocrinology,* 11(6)**,** 674-681.

Scully, K. M. & Rosenfeld, M. G. (2002) Development - pituitary development: Regulatory codes in mammalian organogenesis. *Science,* 295(5563)**,** 2231-2235.

Seamon, K. B., Padgett, W. & Daly, J. W. (1981) Forskolin - unique diterpene activator of adenylate-cyclase in membranes and in intact-cells. *Proceedings of the National Academy of Sciences of the United States of America-Biological Sciences,* 78(6)**,** 3363-3367.

Segal, E. & Widom, J. (2009) From dna sequence to transcriptional behaviour: A quantitative approach. *Nature Reviews Genetics,* 10(7)**,** 443-456.

Semprini, S., Friedrichsen, S., Harper, C. V., Mcneilly, J. R., Adamson, A. D., Spiller, D. G., Kotelevtseva, N., Brooker, G., Brownstein, D. G., Mcneilly, A. S., White, M. R. H., Davis, J. R. E. & Mullins, J. J. (2009) Real-time visualization of human prolactin alternate promoter usage in vivo using a double-transgenic rat model. *Molecular Endocrinology,* 23(4)**,** 529-538.

Semwogerere, D. & Weeks, E. (2005) Confocal miscroscopy*Encyclopedia of biomaterials and biomedical engineering.* Taylow & Francis).

Shaikh, A. A. (1971) Estrone and estradiol levels in ovarian venous blood from rats during estrous cycle and pregnancy. *Biology of Reproduction,* 5(3)**,** 297-&.

Sharp, Z. D., Mancini, M. G., Hinojos, C. A., Dai, F., Berno, V., Szafran, A. T., Smith, K. P., Lele, T. T., Ingber, D. E. & Mancini, M. A. (2006) Estrogen-receptor-alpha exchange and chromatin dynamics are ligand- and domain-dependent. *Journal of Cell Science,* 119(19)**,** 4101-4116.

Shen, H., Nelson, G., Nelson, D. E., Kennedy, S., Spiller, D. G., Griffiths, T., Paton, N., Oliver, S. G., White, M. R. H. & Kell, D. B. (2006) Automated tracking of gene expression in individual cells and cell compartments. *Journal of the Royal Society Interface,* 3(11)**,** 787-794.

Shimomura, O. (2009) Discovery of green fluorescent protein (gfp) (nobel lecture). *Angewandte Chemie-International Edition,* 48(31)**,** 5590-5602.

Shimomura, O., Johnson, F. H. & Saiga, Y. (1962) Extraction, purification and properties of aequorin, a bioluminescent protein from luminous hydromedusan, aequorea. *Journal of Cellular and Comparative Physiology,* 59(3)**,** 223-&.

Shorte, S. L., Leclerc, G. M., Vazquez-Martinez, R., Leaumont, D. C., Faught, W. J., Frawley, L. S. & Boockfor, F. R. (2002) Prl gene expression in individual living mammotropes displays distinct functional pulses that oscillate in a noncircadian temporal pattern. *Endocrinology,* 143(3)**,** 1126-1133.

Shupnik, M. A. (2002) Oestrogen receptors, receptor variants and oestrogen actions in the hypothalamic-pituitary axis. *Journal of Neuroendocrinology,* 14(2)**,** 85-94.

Shupnik, M. A., Baxter, L. A., French, L. R. & Gorski, J. (1979) Invivo effects of estrogen on ovine pituitaries - prolactin and growth-hormone biosynthesis and messenger ribonucleic-acid translation. *Endocrinology,* 104(3)**,** 729-735.

Simoncini, T., Hafezl-Moghadam, A., Brazil, D. P., Ley, K., Chin, W. W. & Liao, J. K. (2000) Interaction of oestrogen receptor with the regulatory subunit of phosphatidylinositol-3-oh kinase. *Nature,* 407(6803).

Smith, E. P., Boyd, J., Frank, G. R., Takahashi, H., Cohen, R. M., Specker, B., Williams, T. C., Lubahn, D. B. & Korach, K. S. (1994) Estrogen resistance caused by a mutation in the estrogen-receptor gene in a man. *New England Journal of Medicine,* 331(16)**,** 1056-1061.

Soares, M. J. (2004) The prolactin and growth hormone families: Pregnancy-specific hormones/cytokines at the maternal-fetal interface. *Reproductive biology and endocrinology : RB&E,* 2(51-51.

Sobell, H. M. (1985) Actinomycin and dna-transcription. *Proceedings of the National Academy of Sciences of the United States of America,* 82(16)**,** 5328-5331.

Sosa, L. D. V., Gutierrez, S., Petiti, J. P., Palmeri, C. M., Mascanfroni, I. D., Soaje, M., De Paul, A. L. & Torres, A. I. (2012) 17 beta-estradiol modulates the prolactin secretion induced by trh through membrane estrogen receptors via pi3k/akt in female rat anterior pituitary cell culture. *American Journal of Physiology-Endocrinology and Metabolism,* 302(10)**,** E1189-E1197.

Spiller, D. G., Wood, C. D., Rand, D. A. & White, M. R. H. (2010) Measurement of single-cell dynamics. *Nature,* 465(7299)**,** 736-745.

Stirland, J. A., Seymour, Z. C., Windeatt, S., Norris, A. J., Stanley, P., Castro, M. G., Loudon, A. S. I., White, M. R. H. & Davis, J. R. E. (2003) Real-time imaging of gene promoter activity using an adenoviral reporter construct demonstrates transcriptional dynamics in normal anterior pituitary cells. *Journal of Endocrinology,* 178(1)**,** 61-69.

Suter, D. M., Molina, N., Gatfield, D., Schneider, K., Schibler, U. & Naef, F. (2011a) Mammalian genes are transcribed with widely different bursting kinetics. *Science,* 332(6028)**,** 472-474.

Suter, D. M., Molina, N., Naef, F. & Schibler, U. (2011b) Origins and consequences of transcriptional discontinuity. *Current Opinion in Cell Biology,* 23(6)**,** 657-662.

Takahashi, S. & Miyatake, M. (1991) Immunoelectron microscopic study of prolactin cells in the rat - postnatal-development and effects of estrogen and bromocryptine. *Zoological Science,* 8(3)**,** 549-559.

Takasuka, N., White, M. R. H., Wood, C. D., Robertson, W. R. & Davis, J. R. E. (1998) Dynamic changes in prolactin promoter activation in individual living lactotrophic cells. *Endocrinology,* 139(3)**,** 1361-1368.

Tashjian, A. H., Yasumura, Y., Levine, L., Sato, G. H. & Parker, M. L. (1968) Establishment of clonal strains of rat pituitary tumor cells that secrete growth hormone. *Endocrinology,* 82(2)**,** 342-&.

Teilum, K., Hoch, J. C., Goffin, V., Kinet, S., Martial, J. A. & Kragelund, B. B. (2005) Solution structure of human prolactin. *Journal of Molecular Biology,* 351(4)**,** 810-823.

Treier, M., Gleiberman, A. S., O'connell, S. M., Szeto, D. P., Mcmahon, J. A., Mcmahon, A. P. & Rosenfeld, M. G. (1998) Multistep signaling requirements for pituitary organogenesis in vivo. *Genes & Development,* 12(11)**,** 1691-1704.

Van De Weerdt, C., Peers, B., Belayew, A., Martial, J. A. & Muller, M. (2000) Far upstream sequences regulate the human prolactin promoter transcription. *Neuroendocrinology,* 71(2)**,** 124-137.

Van Steensel, B. (2011) Chromatin: Constructing the big picture. *Embo Journal,* 30(10)**,** 1885-1895.

Veldhuis, J. D. (1996) New modalities for understanding dynamic regulation of the somatotropic (gh) axis: Explication of gender differences in gh neuroregulation in the human. *Journal of Pediatric Endocrinology & Metabolism,* 9(237-253.

Veldhuis, J. D. & Johnson, M. L. (1986) Cluster-analysis - a simple, versatile, and robust algorithm for endocrine pulse detection. *American Journal of Physiology,* 250(4)**,** E486-E493.

Villalobos, C., Faught, W. J. & Frawley, L. S. (1999) Dynamics of stimulus-expression coupling as revealed by monitoring of prolactin promoter-driven reporter activity in individual, living mammotropes. *Molecular Endocrinology,* 13(10)**,** 1718-1727.

Vinuelas, J., Kaneko, G., Coulon, A., Vallin, E., Morin, V., Mejia-Pous, C., Kupiec, J. J., Beslon, G. & Gandrillon, O. (2013) Quantifying the contribution of chromatin dynamics to stochastic gene expression reveals long, locus-dependent periods between transcriptional bursts. *Bmc Biology,* 11(19.

Vlahos, N. P., Bugg, E. M., Shamblott, M. J., Phelps, J. Y., Gearhart, J. D. & Zacur, H. A. (2001) Prolactin receptor gene expression and immunolocalization of the prolactin receptor in human luteinized granulosa cells. *Molecular Human Reproduction,* 7(11)**,** 1033-1038.

Walker, J. J., Terry, J. R., Tsaneva-Atanasova, K., Armstrong, S. P., Mcardle, C. A. & Lightman, S. L. (2010) Encoding and decoding mechanisms of pulsatile hormone secretion. *Journal of Neuroendocrinology,* 22(12)**,** 1226-1238.

Walker, P., Germond, J. E., Brownluedi, M., Givel, F. & Wahli, W. (1984) Sequence homologies in the region preceding the transcription initiation site of the liver estrogen-responsive vitellogenin and apo-vldlii genes. *Nucleic Acids Research,* 12(22)**,** 8611-8626.

Walters, K., Wegorzewska, I. N., Chin, Y. P., Parikh, M. G. & Wu, T. J. (2008) Luteinizing hormone-releasing hormone i (lhrh-i) and its metabolite in peripheral tissues. *Experimental Biology and Medicine,* 233(2)**,** 123-130.

Wang, Y. L., Liu, F. & Wang, W. (2013) Dynamic mechanism for the transcription when responses to activators. *Biophysical Journal,* 104(2)**,** 160A-160A.

White, M. R. H., Morse, J., Boniszewski, Z. A. M., Mundy, C. R., Brady, M. A. W. & Chiswell, D. J. (1990) Imaging of firefly luciferase expression in single mammalian cells using high sensitivity charge-coupled device cameras. *Technique (Philadelphia),* 2(4)**,** 194-201.

White, M. R. H., Wood, C. D. & Millar, A. J. (1996) Real-time imaging of transcription in living cells and tissues. *Biochemical Society Transactions,* 24(3)**,** S411-S411.

Woodcock, D. J., Vance, K. W., Komorowski, M., Koentges, G., Finkenstadt, B. & Rand, D. A. (2013) A hierarchical model of transcriptional dynamics allows robust estimation of transcription rates in populations of single cells with variable gene copy number. *Bioinformatics,* 29(12)**,** 1519-1525.

Xu, L., Lavinsky, R. M., Dasen, J. S., Flynn, S. E., Mcinerney, E. M., Mullen, T. M., Heinzel, T., Szeto, D., Korzus, E., Kurokawa, R., Aggarwal, A. K., Rose, D. W., Glass, C. K. & Rosenfeld, M. G. (1998) Signal-specific co-activator domain requirements for pit-1 activation. *Nature,* 395(6699)**,** 301-306.

Zabavnik, J., Wu, W. X., Eidne, K. A. & Mcneilly, A. S. (1993) Dopamine-d(2) receptor messenger-rna in the pituitary during the estrous-cycle, pregnancy and lactation in the rat. *Molecular and Cellular Endocrinology,* 95(1-2)**,** 121-128.

Zhu, X. Y., Gleiberman, A. S. & Rosenfeld, M. G. (2007) Molecular physiology of pituitary development: Signaling and transcriptional networks. *Physiological Reviews,* 87(3)**,** 933-963.

Zlatanova, J., Bishop, T. C., Victor, J.-M., Jackson, V. & Van Holde, K. (2009) The nucleosome family: Dynamic and growing. *Structure,* 17(2)**,** 160-171.

Zluvova, J., Janousek, B. & Vyskot, B. (2001) Immunohistochemical study of dna methylation dynamics during plant development. *Journal of Experimental Botany,* 52(365)**,** 2265-2273.

Zwart, W., Theodorou, V., Kok, M., Canisius, S., Linn, S. & Carroll, J. S. (2011) Oestrogen receptor-co-factor-chromatin specificity in the transcriptional regulation of breast cancer (vol 30, pg 4764, 2011). *Embo Journal,* 30(23)**,** 4850-4850.

Zyzek, E., Dufybarbe, L., Dufy, B. & Vincent, J. D. (1981) Short-term effect of estrogen on release of prolactin by pituitary-cells in culture. *Biochemical and Biophysical Research Communications,* 102(4)**,** 1151-1157.

Appendix A

Transcriptional priming by E2

Appendix A

Transcriptional priming by oestradiol

To test the idea of the endocrine history of a cell priming transcriptional activation, a series of experiments was devised in D44 cells, which express luciferase under the control of a 5 kbp fragment of the human prolactin promoter. These studies were based on the Norris *et al. (2003)* study, which showed an augmented transcriptional response when cells were treated with two stimuli consecutively.

Population studies were carried out D44 cells using live cell luminometry. In this experiment 1.5 x 10^4 cells per well, were treated with a primary stimulus of 0.1% DMSO (control), 10nM oestradiol (E_2) or 5μM forskolin (FSK) for 24 hours. A second round of 24 hours stimulation was carried out, in which each set of cells simulated with one of the first stimuli, was then restimulated with one of the three stimuli, DMSO, E_2 or FSK (See Figure 2.1.) During both 24 hours stimulations, the light intensity of the reporter was collected every 15 minutes.

Several problems were encountered with this experiment. The primary problem was the viability of the cells, which did not survive the culture conditions sufficiently. D44 cells showed the highest degree of transcriptional activity at time 0h, followed by a sharp decrease in expression. Possible explanations for this finding include loss of cell viability or destabilisation of luciferase enzyme in the presence of luciferin substrate (as has been found previously by Takasuka *et al.* (1998). After cell transcription rate stabilized at a lower level (Figure 1. a. and b., respectively), responses to primary and secondary stimuli were more comparable. Control cells treated with DMSO showed a higher transcriptional response than cells treated with FSK. This is surprising, as DMSO, which is used as a solvent for various stimuli, should not induce a transcriptional response, while FSK should, as it has been shown to activate transcription through the upregulation of cAMP (Seamon *et al.*, 1981).

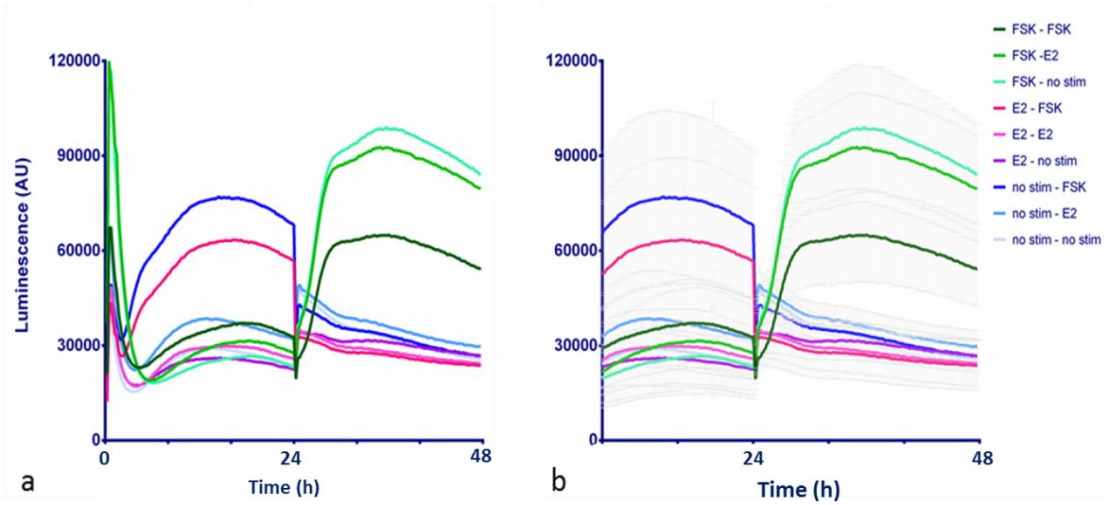

Figure 1. Live cell luminometry re-stimulation experiment

*In **a**. the full raw data from live cell luminescence and in **b.** the same data with the first 8 hours removed to clarify responses to the first and second stimulation protocols. The x axis denotes the time and the y axis denotes luminescence in arbitrary units. Stimulus protocols are shown in the legend on the right.*

Single cell expression studies were carried out using live cell luminescence microscopy. $2x10^5$ BAC 2 cells were plated in a 35mm glass-bottomed dish. Cells were treated with either 10nM E_2 or 0.1% DMSO as a control and imaged for 24 hours. 5μM FSK was then added to each dish and imaged for a further 24 hours. We had hypothesised that cells treated with E_2 in the primary stimulation, would show a greater transcriptional response than controls, if there was a 'priming' effect of prior transcriptional stimulation on subsequent transcriptional response, as had been suggested by previous data for the human growth hormone gene (Norris *et al.,* 2003). The luminescence of single cells was tracked using AQM imaging software (Figure 2 c. and d.).

Similar culture problems were experienced compared to the earlier luminometry studies. An initial transcriptional surge was seen, which interfered with assessment of responses to stimuli. One problem identified was cooling of the culture dishes during transfer to the microscope stage, which can substantially affect the kinetics of

the luciferase enzyme. This was counteracted by transferring culture dishes on a heated block, but, lack of time prevented more than preliminary experiments.

Two different microscopes were available to carry out this experiment (for details see methods section 2.10.2.) meaning that results were not directly comparable. The difference in transcriptional activity between cells pretreated with DMSO and those with E_2 was thus calculated as a fold-change (Figure 3.), and these data indicated that prior stimulation with E_2 did not appear to induce a larger transcriptional response to a second transcriptional activation.

The stimulatory effects of E_2 on prolactin promoter activity in D44 and BAC2 cells have been documented. In GH3 cells transiently transfected to express luciferase under the control of a 5 kbp fragment of the human prolactin promoter, or in stable transfected D44 cells, E_2 induced a 1.8-fold increase in reporter activity (Adamson *et al.,* 2008 and PhD thesis). This induction of transcription was not reproduced in my preliminary experiments described here, with in some cases, cells treated with a DMSO control, showing higher transcriptional activity than E_2. Looking into the effects of previous oestrogen state of a cell and the effects of this on prolactin transcription cycle patterns would complement the *in vivo* work done in this project, providing clues on the mechanisms of increased prolactin transcription in our models of high oestrogen state, oestrus and in males treated with chronic E_2. This would require further optimisation of cell culture conditions and microscopy, and was not pursued further, in order to focus on completion of the physiological studies reported in the thesis.

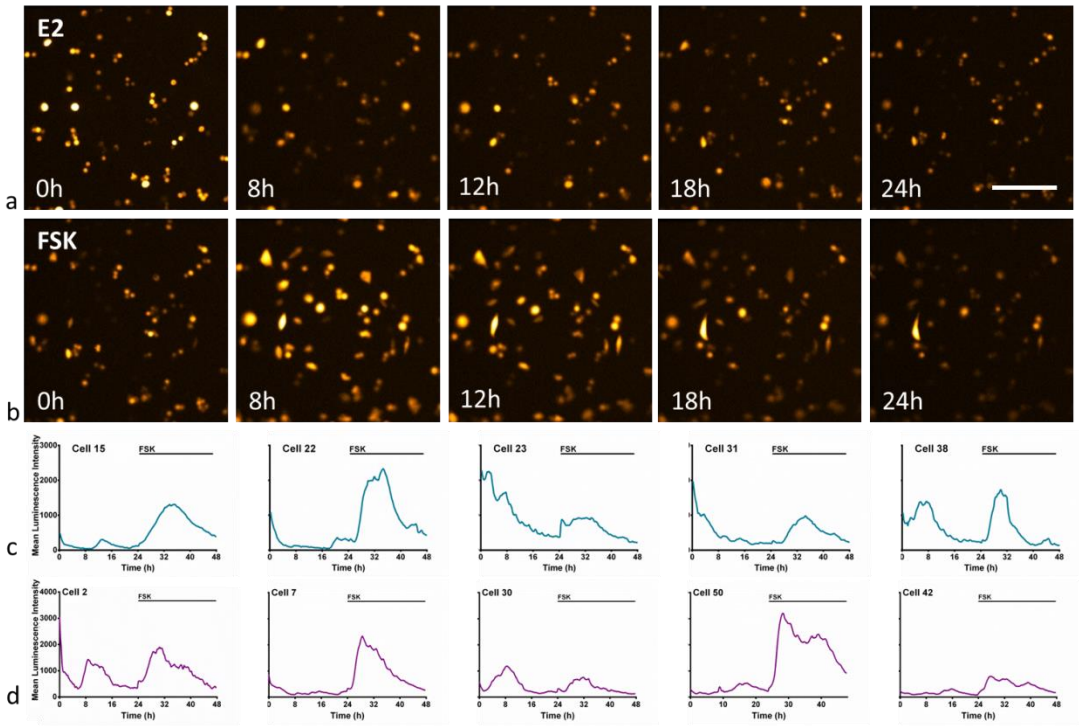

Figure 2. Single cell time lapse luminescence microscopy

Still from single cell luminescence microscopy of BAC2 cells expressing luciferase under the control of a human prolactin genomic fragment. In ***a.*** *24 hours of cells stimulated with 10 nM* E_2 *and in* ***b.*** *the same cells with 5μM added and imaged for a further 24 hours. Scale bar indicates 50 μm. Below, in* ***c.*** *and* ***d.*** *examples of single cells tracked from experiments of controls and cells treated with* E_2 *and then FSK, respectively. The black line indicates addition of FSK.*

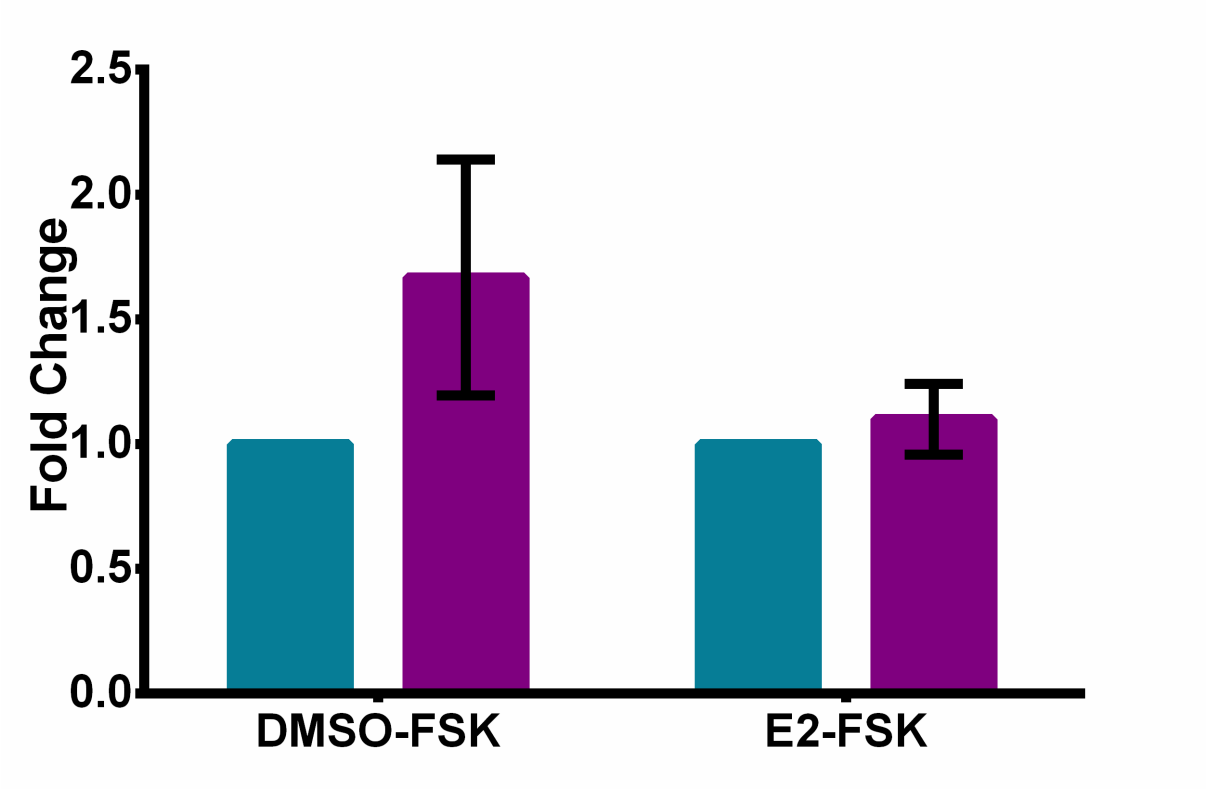

Figure 3. Average fold change in transcription with the addition of FSK after pre-treatment with DMSO and E_2.

Fold changes in transcriptional response were calculated on the average luminescence of the pre-treatment as compared to the average luminescence with 5μM FSK treatment.

Appendix B

Tabulation of animal experiments

Appendix B – Tabulation of animal experiments

Animal no.	Sex	Date culled	Experiment	Oestrogen status	Serum Prolactin (ng/ml)	Tracked	Pit weight	Testis weight
114	F	27.1.10	Flow/IHC	E				
115	F	27.1.10	Flow/IHC	E				
130	F	27.1.10	Flow/IHC	Pro-E				
132	F	27.1.10	Flow/IHC	E				
143	F	27.1.10	Flow/IHC	Pro-E				
124	F	27.1.10	Flow/IHC	Met-DiE				
125	F	27.1.10	Flow/IHC	Met-DiE				
129	F	27.1.10	Flow/IHC	Met-DiE				
133	F	27.1.10	Flow/IHC	Met-DiE				
134	F	27.1.10	Flow/IHC	Met-DiE				
147	F	17.5.10	Flow/IHC	E				
148	F	17.5.10	Flow/IHC	infection?				
160	F	17.5.10	Flow/IHC	E				
161	F	17.5.10	Flow/IHC	v. late ProE				
159	F	17.5.10	Flow/IHC	E				
149	F	17.5.10	Flow/IHC	DiE				
151	F	17.5.10	Flow/IHC	DiE				
152	M	27.9.10	Implant/Flow	E2	935.7		26.6	1.12
153	M	27.9.10	Implant/Flow	E2	724.6		23.8	1.15
154	M	27.9.10	Implant/Flow	E2	1061.2		25.1	1.35
156	M	27.9.10	Implant/Flow	Control	244.6		15.7	3.3
157	M	27.9.10	Implant/Flow	Control	226.7		15.8	3.2
158	M	27.9.10	Implant/Flow	Control	280.9		23	3.29
166	M	17.11.10	qPCR/IHC	E2	1020.8		32.6	1.34
167	M	17.11.10	qPCR/IHC	E2	1656.7		36.4	2.03
168	M	17.11.10	qPCR/IHC	E2	1079		32.2	1.23
182	M	17.11.10	qPCR/IHC	Control	301.2		16	3.49
185	M	17.11.10	qPCR/IHC	Control	340		14	3.54
187	M	17.11.10	qPCR/IHC	Control	295.8		16.1	3.83
177	F	6.6.11	Imaging	E	274.7			
179	F	10.6.11	Imaging	DiE	165.6			
180	F	20.6.11	qPCR/IHC	Late ProE	328.4			

199	F	20.6.11	qPCR/IHC	E				
202	F	20.6.11	qPCR/IHC	ProE?	287.1			
190	F	20.6.11	qPCR/IHC	DiE				
191	F	20.6.11	qPCR/IHC	DiE	121.4			
193	F	20.6.11	qPCR/IHC	DiE				
215	F	26.10.11	Imaging	E	409.9			
216	F	6.12.11	Imaging	E	482.3			
222	F	12.12.11	Imaging	E	709.9			
228	M	14.3.12	Imaging	Control	545.8		38.6	3.69
229	M	12.3.12	Imaging	E2	510			2.23
219	M	22.2.12	Imaging	E2			39.1	3.24
220	M	24.2.12	Imaging	Control			34.2	3.58
223	F	17.5.12	Imaging	ProE	370.8			
235	F	18.6.12	Imaging	DiE	32.8			
240	F	13.8.12	Imaging	E	225.1			
242	F	10.9.12	Imaging DS 13	E (ProE) DS 13	254	x		
249	F	19.10.12	Imaging DS 14	DiE		x		
259	F	21.11.12	Imaging DS 15	DiE				
239	M	15.12.12	Imaging DS 16	Control	56.1	x	15	3.26
245	M	12.12.12	Imaging DS 16	E2	285.4	x	30	1.09
261	F	14.1.13	Imaging DS 17	DiE	79.7	x		
260	F	2.2.13	Imaging DS 18	E	69.2	x		
256	M	9.3.13	Imaging DS 19	Control	61.2	x	20	3.36
258	M	6.3.13	Imaging DS 19	E2	1802.4	x	70	1.14

Appendix C

Abstracts and publications

Appendix C

Abstracts accepted for presentation

British Endocrine Society Meeting (BES) 2012, Harrogate, UK

Poster presentation

Transcriptional regulation of prolactin in the rat oestrous cycle

Amanda L. Patist, Karen Featherstone, David G. Spiller, Sabrina Semprini, Judith R. McNeilly, Alan S. McNeilly, John J. Mullins, Michael R.H. White & Julian R.E. Davis

Endocrine Abstracts (2012) **28** P240

International/European Congress for Endocrinology (ICE/ECE) 2012, Florence, Italy

Oral presentation

Transcriptional regulation of prolactin by oestrogen in vivo

Amanda L. Patist, Karen Featherstone, David G. Spiller, Sabrina Semprini, Judith R. McNeilly, Alan S. McNeilly, John J. Mullins, Michael R.H. White & Julian R.E. Davis

Endocrine Abstracts (2012) **29** OC4.2

Endocrine Society Meeting (ENDO) 2013, San Francisco, USA

Oral presentation

Characterisation of Dynamic Prolactin Transcription Patterns in Living Tissue in Response to Changes in Rat Oestrogen Status

Amanda L. Patist, Karen Featherstone, David G. Spiller, Anne McNamara, Sabrina Semprini, Judith R. McNeilly, Alan S. McNeilly, John J. Mullins, Michael R.H. White & Julian R.E. Davis

Publications contributed to

Peritonitis activates transcription of the human prolactin locus in myeloid cells in a humanized transgenic rat model.

Semprini S, McNamara AV, Awais R, Featherstone K, Harper CV, McNeilly JR, **Patist A,** Rossi AG, Dransfield I, McNeilly AS, Davis JR, White MR, Mullins JJ. Endocrinology. 2012 153(6):2724-34.

Appendix D

CD of time-lapse microscopy

Appendix D

CD of time-lapse microscopy

CD containing the following AVI files:

Diestrus DS 14

Diestrus DS 17

Male control DS 16

Male control DS 19

Male E_2 DS 16

Male E_2 DS 19

Oestrus DS 13

Oestrus DS 18

Each file contains a time-lapse of 48 hours of confocal imaging of a 250µm coronal pituitary tissue slice preparation from either a female Fischer 344 (d2eGFP-hPRL 455) rat in oestrus or diestrus, or a male rat treated a high dose of oestradiol over a period of 21 days or control.